Development of specific electrodes of an electronic tongue for detection of important chemical compounds present in tea

Thesis submitted

By

Trisita Nandy Chatterjee

Doctor of Philosophy (Engineering)

Department of Instrumentation and Electronics Engineering
Faculty Council of Engineering & Technology
Jadavpur University
Kolkata, India

2018

Jadavpur University

Kolkata-700 032

INDEX NO. 72/17/E

1. Title of the thesis

Development of specific electrodes of an electronic tongue for detection of important chemical compounds present in tea

2. Name, Designation and Institution of the Supervisors

Dr. Runu Banerjee Roy
Professor,
Dept. of Instrumentation and Electronics Engineering,
Jadavpur University, Salt Lake Campus,
Sector-III, Block-LB, Plot-8, Kolkata-700098, India.

Dr. Rajib Bandyopadhyay
Professor,
Dept. of Instrumentation and Electronics Engineering,
Jadavpur University, Salt Lake Campus,
Sector-III, Block-LB, Plot-8, Kolkata-700098, India.

3. List of Publications

Papers published in International Journals

[1] Trisita Nandy Chatterjee, Runu Banerjee Roy, Bipan Tudu, Panchanan Pramanik, Himangshu Deka, Pradip Tamuly, Rajib Bandyopadhyay **"**Detection of theaflavins in black tea using a molecular imprinted polyacrylamide-graphite nanocomposite electrode**,"** *Sensors and Actuators B:Chemical*, vol.246, pp. 840-847, 2017.

[2] Trisita Nandy Chatterjee, Debangana Das, Runu Banerjee Roy, Bipan Tudu, Santanu Sabhapondit, Pradip Tamuly, Panchanan Pramanik, Rajib Bandyopadhyay, "Molecular imprinted polymer based electrode for sensing catechin (+C) in green tea," *IEEE Sensors Journal*, vol. 18, no. 6, pp.2236-2244, 2018.

[3] Trisita Nandy Chatterjee, Debangana Das, Runu Banerjee Roy, Bipan Tudu, Ajanto K Hazarika, Santanu Sabhapondit, Pradip Tamuly, Rajib Bandyopadhyay, "Development of a nickel hydroxide

nanopetal decorated molecular imprinted polymer based electrode for sensitive detection of epigallocatechin-3-gallate in green tea," *Sensors and Actuators B:Chemical,* vol.283, pp. 69-78, 2019.

[4] Debangana Das, Trisita Nandy Chatterjee, Runu Banerjee Roy, Bipan Tudu, Santanu Sabhapondit, Ajanto K Hazarika, Panchanan Pramanik, Rajib Bandyopadhyay, "Discrimination of green tea using an epigallocatechin-3-gallate (EGCG) sensitive molecular imprinted polymer (MIP) based electrode," *Carbon-Science and Technology*, 2018.

Papers published in International Conference Proceedings

[1] Trisita Nandy Chatterjee, Runu Banerjee Roy, Bipan Tudu, Sudip Biswas, Rajib Bandyopadhyay, Panchanan Pramanik, Nabarun Bhattacharyya, *"*Discrimination of black tea grades by means of cyclic voltammetry using polyacrylamide/exfoliated graphite composite electrode," International Conference on *Control, Instrumentation, energy and communication (CIEC*) 2016, January 28-30, 2016, Kolkata, India.

[2] Trisita Nandy Chatterjee, Runu Banerjee Roy, Bipan Tudu, Rajib Bandyopadhyay, Panchanan Pramanik, Nabarun Bhattacharyya**,** "Voltammetric determination of catechins in green tea using stainless steel electrode," *International Conference on Intelligent Control, Power and Instrumentation (ICICPI) 2016,* October 21 - 23, 2016, Kolkata, India.

4. List of Patents

A process for forming a molecular imprinted polymer (MIP) based electrode for accurate quantitative detection of total theaflavin (TF) in black tea, Nabarun Bhattacharyya, Trisita Nandy Chatterjee, Runu Banerjee Roy, Bipan Tudu, Panchanan Pramanik, Rajib Bandyopadhyay, Devdulal Ghosh, Patent filed *vide Application Number: 201731011451*

5. List of Presentations in National/International/ Conferences/Workshops

[1] International conference on Perception and Machine Intelligence (PERMIN 2015), February 26-27, 2015, Kolkata, India.

[2] International conference on Control, Instrumentation, Energy and Communication (CIEC) 2016, January 28-30, 2016, Kolkata, India.

[3] International Conference on Intelligent Control, Power and Instrumentation, (ICICPI) 2016, October 21-23, 2016, Kolkata, India.

CERTIFICATE FROM THE SUPERVISORS

This is to certify that the thesis entitled "***Development of specific electrodes of an electronic tongue for detection of important chemical compounds present in tea***" submitted by Smt. Trisita Nandy Chatterjee, who got her name registered on 3rd of January, 2017 for the award of Ph.D (Engg.) degree of Jadavpur University is absolutely based upon her own work under the supervision of Dr. Runu Banerjee Roy and Dr. Rajib Bandyopadhyay and neither her thesis nor any part of the thesis has been submitted for any degree/diploma or any other academic award anywhere before.

Dr. Runu Banerjee Roy
Department of Instrumentation and Electronics Engineering
Jadavpur University, Salt Lake Campus
Kolkata-700098, India

Dr. Rajib Bandyopadhyay
Department of Instrumentation and Electronics Engineering
Jadavpur University, Salt Lake Campus
Kolkata-700098, India

Acknowledgements

The journey of attaining the Doctorate degree was not simple; never did it seem so. However, the path was eased up by a lot many individuals and I am highly grateful to them for their valuable contributions. Firstly, I would like to thank the Almighty for enabling me to pursue my research in the renowned Jadavpur University, Kolkata. I am highly indebted to the facilities and infrastructure provided to me by the Department of Instrumentation and Electronics Engineering (IEE) of this university. I would also like to thank Department of Science and Technology (DST), Government of India, for providing me financial support.

I hereby express a deep sense of gratitude to my supervisors, Dr. Runu Banerjee Roy and Dr. Rajib Bandyopadhyay, Professor, IEE department, for the constant motivation, support and encouragement they provided me throughout the course of research. Apart from adequate guidance, they also taught me to be kind, compassionate and rational towards every aspect of life. My heartfelt thanks go to Dr. Bipan Tudu, Professor, IEE department, for being there every time I needed him. His clear insight towards my work helped me to achieve more perfection in my research. I am also grateful to Dr. Prolay Sharma and other departmental faculties for making the journey smooth and knowledgeable.

I am highly indebted to Dr. Panchanan Pramanik, retired Professor of department of Chemistry, IIT Kharagpur for guiding me about the chemistry related works involved in my thesis. I would also like to mention about Dr. Anutosh Chatterjee, retired scientist, Bose Institute and Dr. Nabarun Bhattacharyya, Director, Centre for Development of Advanced Computing (C-DAC), Kolkata for their valuable contributions in assisting my thesis work.

The research works pursued in this thesis is based on tea and its different attributes. In this regard, I would like to extend a heartfelt thanks to the tea scientists of Tocklai Tea Research Institute, Jorhat, Assam, India. Especially, I would like to thank Dr. Pradip Tamuly, Dr. Santanu Sabhapondit and Mr. Ajanto Kumar Hazarika, who helped me with every minute details related to tea. They also provided me the tea samples for analysis and their standard quantified data. This thesis would not have been complete without their support and cooperation.

The technical and non-technical staffs of the IEE department helped me profoundly to carry out my research work. My heartfelt gratitude goes especially, to Mr. Gautam Majumder and Ms. Ruma De, who were always by my side when I needed them. My seniors, contemporary labmates and juniors played a very important role in this due course of time by providing me guidance, support and cooperating in each and every possible ways. I am highly grateful to Dr. Arunangshu Ghosh, Dr. Rashmita Das, Dr. Sudip Biswas, Ms. Kamalika Tiwari, Mr. Somdeb Chanda, Ms. Susmita Pradhan, Ms. Saumita Kar, Mr. Hemanta Naskar, Mr. Sukanta Ghosh, Mr. Ujjwal Manikya Nath, Ms. Barnali Ghatak, Ms. Mahua Bhattacharyya Banerjee, Ms. Samhita Dasgupta, Ms. Debangana Das, Mr. Dilip Sing, Mr. Nilabha Debabhuti for making a cheerful ambience and helping me to overcome my frustrations.

It is indeed a very correct saying that a supportive family is important for achieving great heights. I am really thankful to God for having such an encouraging family. I would like to thank my in-laws, especially my mother-in-law and my father-in-law for believing in my abilities and constantly being beside me in all the tough times. It is highly gratifying that they understood the level of stress during my research work and relieved me from many household chores. I would also like to thank my parents and my family for letting their daughter pursue her choice of career and supporting in every possible ways they could.

My husband, Mr. Souvanik Nandy has been one of the best things happened to my life. He taught me that not only his, my work is equally important and motivated me to pursue the same. He has helped me to be punctual and regular in the laboratory and also acted as a source of enthusiasm whenever I got frustrated. He was always by my side and also burnt midnight oil during write up of this dissertation helping me in a number of ways he could. I, therefore, take this opportunity to dedicate this thesis to him for his constant support and encouragement.

November, 2018 **Trisita Nandy Chatterjee**

Dedicated to

my parents; my in-laws and my husband

CONTENTS

List of figures

List of tables

ABBREVIATIONS

AA	Acrylic acid
AAT	Acetic acid thiophene
AEP	P-acryloylaminophenyl-{(4-aminophenyl)-diethyl ammonium}-ethylphosphate
AIBN	2,2'-Azobisisobutyronitrile
AIVN	2,2'-Azobis (2, 4-dimethylvaleronitrile)
AMAM	Amidoamine
AMP	2,2'- Azobis(2-methylpropionitrile)
APTES	3-aminopropyltriethoxysilane
APM	Acoustic plate mode
Ag/AgCl	Silver/Silver chloride
Au	Gold
BA	Butyl acrylate
CA	Control amplifier
CAT	Catechin
CD	Carbon dots
CE	Ceramic electrode
CNT	Carbon nanotube
CV	Cyclic voltammetry
CHEMFET	Chemical field effect transistor
CPE	Carbon paste electrode
CuO	Copper oxide
DAEth	3, 6-Diamino-9-ethylcarbazole
DAU	1, 3-Diacryloyl urea
DPV	Differential pulse voltammetry

ABBREVIATIONS

DPASV	Differential pulse anodic stripping voltammetry
DVB	Di-vinyl benzene
Diffamp	Differential amplifier
EBA	N,N'-Ethylenebisacrylamide
EDOT	3, 4- Ethylenedioxythiophene
EGCG	Epigallocatechin-3-gallate
EGDMA	Ethylene glycol dimethacrylate
EGMRA	Ethylene glycol maleic rosinate acrylate
EIS	Electrochemical impedance spectroscopy
GCE	Glassy carbon electrode
GO	Graphene oxide
Gr	Graphene
GUI	Graphical user interface
HEMA	2-hydroxyethyl methacrylate
HCl	Hydrochloric acid
IL	Ionic liquid
ISFET	Ion sensitive field effect transistor
Inverse miniEP	Inverse mini emulsion polymerization
LSV	Linear sweep voltammetry
LOD	Limit of detection
MAA	Methacrylic acid
MAAsp	Methacrylamidoaspartic acid

ABBREVIATIONS

MA-Ade	Methaacryloylamidoadenine
MAAP-Fe(III)	Methacrylamidoantipyrine-iron (III)
MAGA	Methacryloylamidoglutamic acid
MAH-Cu(II)	Methacryloylamidohistidine-copper (II)
MDA	N,N'-methylene diacrylamide
MIP	Molecular imprinted polymer
MWCNT	Multiwalled carbon nanotube
MnO_2	Manganese oxide
mPD	Meta-phenylenediamine
MWNT	Multiwalled carbon nanotube
NAEMA	N-(2-aminoethyl)methacrylamide hydrochloride
NMGA	N-methacryloyl glutamic acid
NP	Nanoparticle
N-GS	Nitrogen doped graphene sheets
NaOH	Sodium hydroxide
***o*-AT**	*o*-aminothiophenol
***o*-PD**	*o*-phenylenediamine
PCA	Principal component analysis
PLSR	Partial least square regression
PVA	Poly vinyl acetate
py-PBA	Pyrrole phenylboronic acid
QCM	Quartz crystal microbalance

ABBREVIATIONS

QD	Quantum dot
RIfS	Reflectometric interference spectroscopy
rGO	Reduced graphene oxide
SAW	Surface acoustic wave
SCE	Saturated calomel reference electrode
SERS	Surface-enhanced Raman scattering
SPR	Surface plasmon resonance
SWV	Square wave voltammetry
TEGMPA	Tetraethylene glycol 3-morpholin propionate acrylate
TEOS	Tetra ethyl orthosilane
TF	Theaflavin
TMPTM	Trimethylolpropane trimethacrylate
VBA	*p*-vinylbenzoic acid
WD-20	Vinyltriethoxysilane
3-APBA	3-amino phenyl boronic acid

Chapter 1

Introduction and scope of the thesis

This chapter gives an overview of black tea and the current scenario of tea tasting methods pursued in the tea industries. Further it highlights the cost effective means to estimate the quality of tea and discusses its merits and demerits. Here, different transduction mechanisms are discussed along with the various sensing strategies implemented by the researchers for assessing the quality of tea. The chapter focuses on to the objective of this thesis work and introduces molecular imprinted polymer (MIP) based sensors. A brief literature survey consisting of different types of imprinting processes, implementation of MIP based sensors for the detection of various molecules and biomolecules have also been highlighted here.

List of sections

Chapter 1

Introduction and scope of the thesis

1.1. Introduction

India is one of the largest tea producers in the world owing to its suitable geographical location and it maintains its predominant presence in the global tea market due to high investments in tea processing units, continuous innovation and strategic commercialization. The growing demand for export of finest qualities of tea urges the need for a quick estimation technique for its quality determination. A typical tea garden is presented in Fig.1.1. In India, there are mainly three variants of tea, namely, the Darjeeling tea, Assam tea and Nilgiri tea notable for their export worthiness. The tea obtained from each of these regions possesses some special characteristics. For example, Darjeeling tea is known for strong floral aroma, Assam tea is admired for its astringent and colourful liquor, the Nilgiri tea, on the other hand is famous for their light liquor and delicate aroma [1].

Fig.1.1. Pictorial views of tea garden; inset showing the suitable 'two and a bud' tea leaves for plucking

The quality of tea is largely dependent on the various processing stages, which in turn also gives a fair idea regarding the formation of green tea and its subsequent conversion processes [2]. The various stages of tea processing are depicted in Fig.1.2. The first and foremost step is *leaf plucking*, where the tea leaves and the flushes are plucked such that they constitute a terminal bud and two young leaves (also known as 'two and a bud'). The plucking of the leaves occurs twice a year, during early spring and early summer or late spring. The second step, *withering* is used to extract the excess amount of water by keeping it into a sunny

environment or in a cool breezy room. As a result, more than a quarter of weight is lost from the tea leaves and the breakdown of free protein into amino acids takes place. It also increases the free caffeine content simultaneously. In order to speed up the withering process, machine based physical and chemical withering are also practised by the tea industries. Consequently, the withering time can be reduced from about 12 hours to approximately less than 6 hours depending on the variety of the tea. After withering, the tea leaves are kept in a climate controlled atmosphere to undergo *fermentation* or *oxidation*. For oxidation of tea, the leaves are left in a climate-controlled room where they turn progressively into coppery red colour. This is followed by agitation in some cases. Consequently, the chlorophyll in the leaves is broken down, and its tannins are released or transformed. It depends on the tea producer to choose the oxidation time depending on the desired qualities in the final tea as well as the weather conditions (heat and humidity). For light oolong teas this may be anywhere from 5-40% oxidation, 60-70% in case of darker oolong teas, whereas, black tea requires 100% oxidation. Oxidation imparts tea its liquor colour, strength, and briskness. Depending on the type of tea desired, under or over-oxidation/fermentation can result in grassy flavours, or overly thick winey flavours. The percentages of oxidation decide the appropriate variant of tea (for example, green or oolong or black) and also have a significant influence on the quality, taste and flavour of the liquor. It is interesting to note that the black tea manufacturing process involves additional processes of withering, a cycle of crushing-tearing-curling (CTC) and oxidation in comparison to the other variants of tea. As a result, some difference in the chemical composition and to some extent difference in health benefits of green and black tea is observed.

Further, in the *rolling* step, the damp tea leaves are wrinkled into strips either by a rolling machine or manually, such that important essential oils and juices of the leaves are oozed out thereby enhancing the taste of the tea. The strips of tea can then be formed into other shapes, such as being rolled into spirals, kneaded and rolled into pellets, or tied into balls, cones and other elaborate shapes. Rolling is an important step for the production of orthodox tea. The cell wall of the tea ruptures on passing the withered and conditioned tea through the rolling table. The cell contents are then exposed to the atmospheric oxygen and oxidation starts. For giving the leaves a desired shape, rolling machine twists the leaves and also cut down the bigger twisted leaves into smaller sizes. The pressure and the twist exerted by the machine among the leaves and also between the leaf and the surface of the rolling table enhance the chemical reactions. However the process should be monitored and controlled in such a way

that the heat generated due to friction does not affect adversely by forming undesirable constituents that may have an effect on the quality of the tea. In many types of oolong tea, the rolled strips of tea leaf are then rolled to spheres or half spheres by placing the damp leaves in large cloth bags, followed by kneading them by hand or machine in a specific manner. For CTC (cut-tear-curl) variant of tea, as the withered leaves after the rotor vane are passed through the CTC machine, the machine performs all the crushing, tearing and curling operations simultaneously. The robust machine continuously processes steady stream of leaf and produce the granular constituents of CTC tea. The cut achieved in the CTC machine have a deep impact on the make, appearance, grade percentage, fiber content, liquor and brew of the made tea.

After the completion of these preliminary processing steps, the tea leaves undergoes *drying* and *grading*, in order to make the finished product ready for final sale. Drying can be done in a number of ways like panning, sunning, air drying, or baking. The drying of the produced tea is responsible for many new flavour compounds particularly important in green teas. The tea leaves are packed after sorting, consisting of extracting the fibres with the aid of winnowing machines and grading the tea by volumetric weight and size. This is the final stage before longer leaves, such as orange pekoes, are used for loose tea. The left-over fanning and dust leaves are used for tea bags.

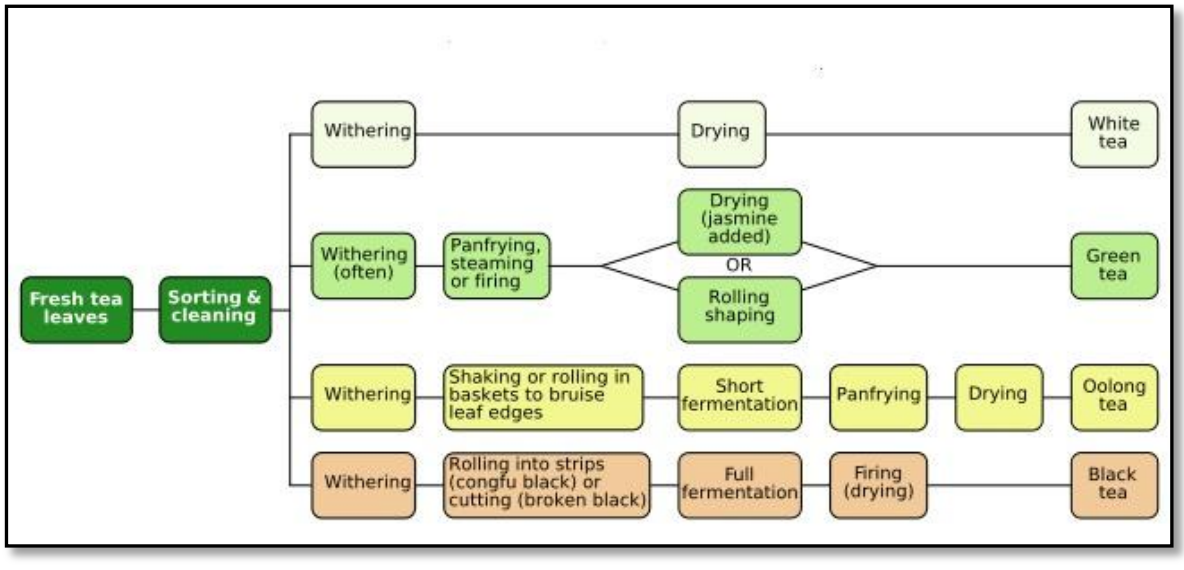

Fig.1.2. Steps of tea processing

Depending on the varieties of tea, produced as a result of the different processing stages, some of the important biochemical markers as identified by the tea scientists [3] that are responsible for the taste of tea are depicted in Table 1.1.

Table 1.1 Important taste determining constituents of tea

Sl. No.	***Compounds***	***Taste***
1	Theaflavins	Astringent
2	Thearubigins	Ashy and slightly astringent
3	Catechin	Astringent
4	Epigallocatechin-3-gallate	Astringent and bitter
5	Caffeine	Bitter
6	Amino acids	Brothy

For the purpose of qualitative discrimination in relation to the taste of tea, tea industries normally employ a group of human panellists, known as 'tea tasters'. These experts assign individual scores in the scale of 1-10 to different variants of tea on the basis of its colour, aroma and taste [4]. But these gradations are influenced by different human psychological, physiological and emotional attributes and as a result, are highly subjective and suffer from various inconsistencies [5]. On the contrary, though high end instrumental techniques like high performance liquid chromatography (HPLC) [6], capillary electrophoresis [7], spectrophotometry [8] provide valuable and reproducible quantitative information about the different constituents of tea, but these are expensive, time consuming and also require skilled personnel. Therefore, such techniques cannot be afforded on regular basis by the tea parlons located in the remote areas.

Towards this direction, electronic tongue (E-tongue) has been proposed for more cost effective and objective quality evaluation of tea. The term 'E-tongue' has been derived from the natural taste sensor of human beings, i.e. tongue. The sensation of taste in a human tongue is operated by the tissue papillae distributed on its surface. The anatomy of human tongue [9] is depicted in Fig.1.3. The taste buds are mainly responsible for the perception of tastes in human beings. These are cluster of cells present in the goblet shaped structures known as papillae and are connected by a small pore to the mouth cavity.

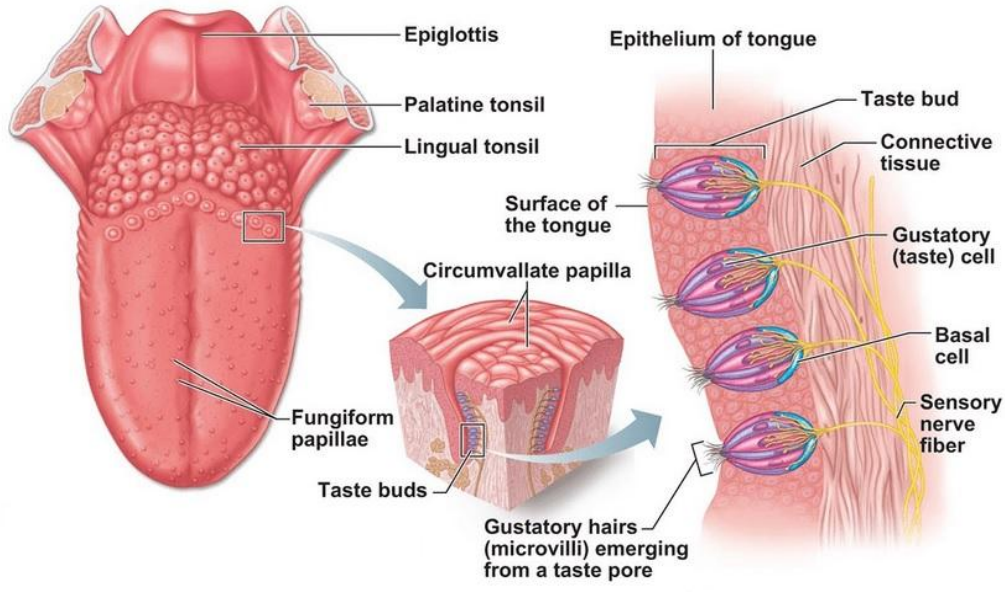

Fig.1.3. Anatomy of human tongue

A single taste bud, on the other hand, consists of about 50 to 75 taste receptor cells arranged in a banana like cluster fashion pointing towards the gustatory cell. The human tongue contains around 2,000-8,000 taste buds in an average basis and the taste sensation produced in a particular taste bud also varies from one another. The gustatory receptors in small papillae on the soft palate and the back roof of the mouth in adults are sensitive to sour and bitter tastes, whereas, the tongue receptors are relatively more sensitive to sweet and salty tastes. The fifth taste umami is detected by oropharynx which is located at the back of the mouth. The combination of these basic sensations of a human tongue represents the overall taste of a food product [9].

The physiological basis of different taste perceptions of a human being mainly occur due to the following classes of the chemical compounds.

- ***Sour:*** The hydrogen ions of the acids, for e.g. from hydrochloric acid, acetic acid, citric acid, etc. are largely responsible for the sour taste [10].
- ***Salt:*** The taste of saltiness is mainly produced by sodium chloride (NaCl) or related compounds [11]**.**
- ***Bitter:*** This sensation of taste is produced by quinine, caffeine, L-tryptophan and magnesium sulphate ($MgSO_4$) [11].
- ***Sweet:*** Sucrose, glucose, L-alanine, etc., are mainly responsible for sweet tastes [12].

- ***Umami:*** The sense of 'delicious' taste called umami is primarily caused by monosodium glutamate (MSG), present in seaweeds, disodium inosinate (IMP), contained in meat and fish and disodium guanilate (GMP), present in mushrooms [13].

In a similar manner, E-tongue also consists of an array of electrodes; each of which is an individual sensor, sensitive to a group of analytes. Here, the response profile of all the electrodes undergoes soft computing and are intelligently processed so as to discriminate the important parameters of tea. The functional block diagram of an E-tongue [14], as used in our laboratory has been described in Fig.1.4. It consists of four modules, namely, (i) an array of electrodes in the electronic tongue test cell; (ii) PC-based signal generation with software controlled level shifter, amplifier and switching circuit; (iii) PC-based data acquisition; and (iv) a taste characterizing software. The process of signal generation and data acquisition are performed using a LabVIEW-based virtual instrumentation system and a low cost multifunctional data acquisition card USB 6008, as supplied by National Instruments. The data acquisition card digitizes the analog signal with a resolution of 12 bits at a sampling rate of 10 kS/s. The customized LabVIEW software interacts with the user by means of a graphical user interface (GUI). The analysis using an E-tongue is rapid and objective and does not require any complicated sample preparation or synthetic steps. Moreover, it can generate a large amount of information characterized by the constitution of a complex multi-component sample.

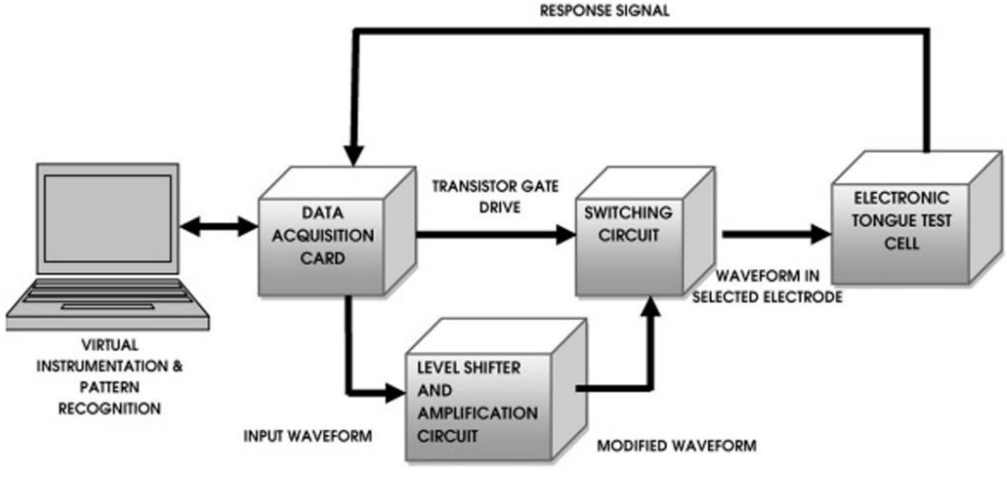

Fig.1.4. Functional block diagram of an E-tongue

Though the task of discrimination by an E-tongue is rapid and can be easily tunable, but the sensing materials used here normally consists of noble metals which have low selectivity and are also not specific to the target analyte. Moreover, the data obtained from an E-tongue generally contains a pattern of waveforms that is processed by means of appropriate recognition algorithms. In regard to the above limitations, it is believed that the performance of an E-tongue could be enhanced if functionalized electrodes are used instead of noble metal electrodes.

Therefore, to overcome certain limitations of an E-tongue, i.e., to decrease the number of individual sensors and enhance the sensitivity of them simultaneously, molecularly imprinted polymer (MIP) based technique have been proposed in this thesis work. In order to primarily ensure the suitability of the monomers regarding effective sensing of the overall quality of tea, some background studies have been carried out by preparing electrodes made up of polyacrylamide-graphite (without template imprinting) composite. Cyclic voltammetry analysis (CV) combined with multivariate statistical methods ensured that the electrode can suitably discriminate different grades of black tea liquor. In another work, a stainless steel (SS) electrode has been used towards determination of catechin (+C). The performance of the electrode has been compared with that of the carbon paste electrode (CPE) and the noble metal Pt electrode in regard to the sensory evaluation by means of cyclic voltammetry (CV). Not only the SS electrode displayed a higher peak current compared to the other ones, but also it was found effective in discriminating different commercially available green tea samples. These preliminary results led to the development of more specific and selective electrodes for assessing the different chemical constituents of tea.

The present thesis titled "***Development of specific electrodes of an electronic tongue for detection of important chemical compounds present in tea***" explores the possibility of the development of the electrodes, each specific for an individual taste attributing agent of tea. Here three different electrodes have been synthesized using the principle of MIP for the selective detection of total theaflavins (TF), catechin (+C), and epigallocatechin-3-gallate (EGCG), respectively. The particle size, structural variations and the morphological changes of the imprinted electrodes were characterized using powder X-ray diffraction (PXRD) technique, fourier transform infra-red (FTIR) spectroscope and field emission scanning electron microscope (FESEM), respectively. The analytical characteristics of all the electrodes have been detailed in this work. Furthermore, in order to have an insight to the performance of the electrodes towards quantification of the different analytes in tea samples

for real time applications, partial least square regression models have been executed and its different parameters have been calculated.

1.2. Different transduction mechanisms

A transduction process is generally involved with the transformation of one form of energy into another. This transformation mainly takes place by means of two elements. Firstly, sensing the input energy specifically from the measurand using a sensing element and then transforming it into another form of energy by means of a transduction element.

The most common types of transduction mechanisms are presented in Table 1.2 followed by a brief overview of each of them [15].

Table 1.2 Different transduction mechanisms for sensors

Sl. No.	Transduction mechanisms	Subdivisions
1	Optical	Fluorescence
		Luminescence
		Reflection
		Absorption
		Surface Plasmon resonance
		Scattering evanescent waves
2	Thermal	Calorimetry
		Enzyme thermistor
3	Piezoelectric	QCM
		SAW
		APM
		Lamb wave
		Love wave
4	Electrochemical	Potentiometry
		Amperometry
		Voltammetry
		ISFET/CHEMFET

1.2.1. Optical

In this type of transduction, interaction between the analyte and the receptor occurs by means of optical phenomenon. These include various properties of light such as, absorption of light, fluorescence/phosphorescence, bio/chemi luminescence, reflectance, Raman scattering and refractive index [15]. These are advantageous because of their high speed, robustness, sensitivity, permissibility for miniaturization of the components and capability of detection of a multiple number of analytes.

1.2.2. Thermal

This technique employs the principle of absorption or evolution of heat to mediate the interaction between the analyte and the receptor. The sensors, also called calorimetric sensors, convert the heat generated or lost during a reaction into an electrical signal. The heat generated due to the chemical reactions is recorded using a thermistor or a platinum thermometer.

1.2.3. Piezoelectric

Piezoelectric transduction is based on the principle that when a force is applied onto a quartz crystal, an electric charge is generated on the surface of the crystal [16]. The charge produced consequently, is known as piezoelectricity. Since, the charge produced is very small, a charge amplifier is required in order to obtain high output voltage. In these types of sensors, the quartz crystal vibrates at a specific frequency on application of an electrical signal. Further, on addition of the sample, a specific binding occurs between the bio-capture molecules on the sensors and the analyte thereby resulting into a change of mass. As a result, the oscillation frequency changes and electrical signal is generated thereby leading to the detection of the analyte.

1.2.4. Electrochemical

Electrochemical transduction technique is used to quantify different types of analyte in gas phase or liquid phase. For the purpose of detection, these sensors employ redox reactions, where the current flowing through the sample or the potential difference between the electrodes as a result of oxidation and reduction process of the target analyte are being used to obtain information regarding the quantification of the sample. Among the different transduction techniques discussed previously, electrochemical sensors provide outputs which are highly stable, highly sensitive, yields quick response and suffer from lesser interferences [17]. Moreover, the cost of fabricating these types of sensors is also relatively less.

1.2.4.1. Types of electrochemical techniques

The most important parameters or the controlling factors of an electrochemical reaction are potential, current, charge and time. Interestingly, any electrochemical reaction possesses the following five characteristics:

i) the potential of the electrode determines the form of the analyte at its surface,

ii) the analyte may be involved in other reactions along with the conventional oxidation and the reduction processes,

iii) current is a measure of the analyte's oxidation and reduction rate,

iv) current and potential across an electrode cannot be controlled simultaneously,

v) the concentration of the analyte present at the electrode's surface is not necessarily similar to that in the bulk solution.

The corresponding response of the system is dependent on the selection of one of these parameters as the excitation signal. Based on the excitation signal and the obtained response, the electrochemical techniques can be categorized in the following manner.

a) Coulometry

This type of electroanalytical method measures the amount of electricity (coulomb), required for an analyte to get converted into a different oxidation state. Coulometric analysis method is based on the application of Faraday's first law of electrolysis [18], i.e., the extent of chemical reaction at an electrode is directly proportional to the quantity of electricity through the electrode. If the charge transferred is *Q* coulomb and *w* is the weight of the substance produced or consumed in an electrolysis, then

$$w = \frac{MQ}{96487n} \tag{1.1}$$

here, *M* is the molecular mass of the substance liberated or consumed and *n* is the number of electrons involved in the reaction.

For coulometric analysis, two generalized techniques are normally used. They are namely, controlled potential (potentiostatic) coulometry and controlled current (amperostatic) coulometry. In case of controlled potential type, the potential of the working electrode is kept at a constant level so that the oxidation or the reduction of the analyte can be performed without the involvement of less reactive species in the sample or the solvent. On the other hand, in controlled current type coulometry, a constant current passes through the cell until the completion of the analytical reaction is indicated by a signal. Further, the quantity of the required charge to reach the end point is measured from the magnitude of the current and the time during which the current passes. This method is also known as coulometric titration.

b) Potentiometry

The potentiometry method is concerned with the measurement of potential of an electrochemical cell without drawing appreciable amount of current. The set up consists of a two electrode system, the first one being the measuring electrode, also called indicator electrode and the other one is the reference electrode. On placing the electrode in a solution, a certain potential is produced and the potential across the indicator electrode is measured with respect to the reference electrode. Potentiometry technique can also be subdivided into direct potentiometry and potentiometric titrations. Direct potentiometry determines the cell potential and relates it to the concentration of the active chemical species; whereas, in potentiometric titrations the cell potential is measured as a function of the volume of reagent added [18].

c) Voltammetry

In voltammetry, the current is measured across the electrode while varying the potential values [18, 19]. The potential is varied to cause the redox reactions of the electroactive chemical species at the surface of the electrode. The current produced consequently, is proportional to the concentration of these electrochemical species.

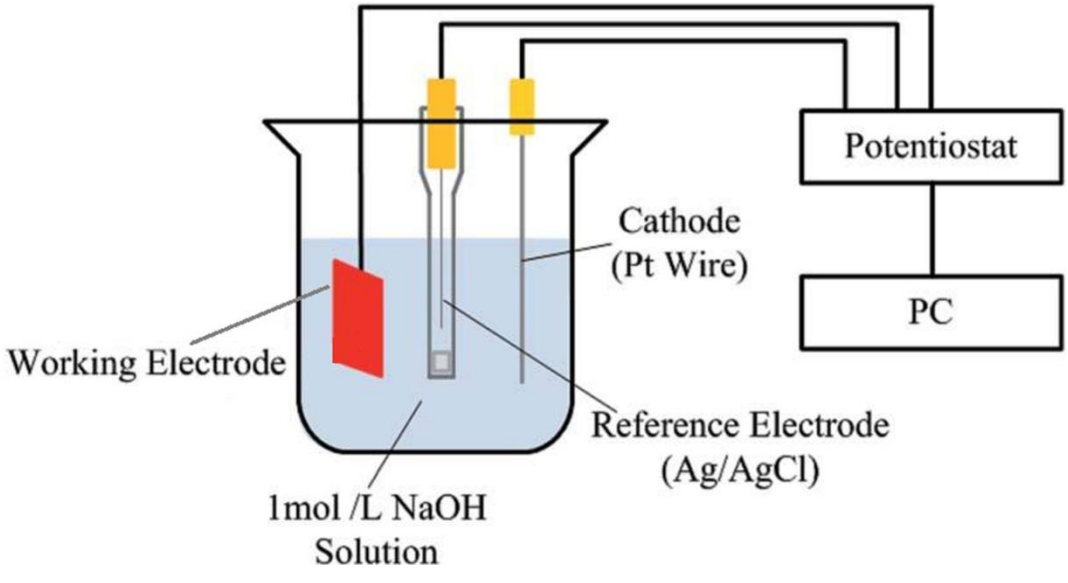

Fig.1.5. Voltammetric arrangements for three electrode configuration

In this procedure, a three electrode set up is used unlike the potentiometric method as shown in Fig.1.5 [20]. These are namely, the reference electrode, such as the saturated calomel reference electrode (SCE) or Ag/AgCl electrode, an auxillary or the counter electrode, and a working or the measuring electrode. These three electrodes are connected to the power source

known as potentiostat, responsible for maintaining a constant potential difference between the reference electrode and the working electrode. The potentiostat bears an analogy with the controlled voltage source in an electrical system. It controls and measures the voltage applied across the working electrode; which in turn induces redox reactions at the electrode interface and a current is produced. The current so generated flows between the counter electrode and the working electrode; and also contains useful information about the electrochemical characteristics and the reaction kinetics of the system.

The corresponding electrochemical connections and the three electrode setup are shown in Fig.1.6 (a) and (b), respectively [19]. The three electrode configuration as used in this work consists of the current electrode (CE), reference electrode (RE) and a working electrode (WE), respectively. Here, the current flows between the CE and WE. The potential difference, on the other hand, is controlled between the WE and CE and is measured between the RE and sense (S) connections. In this regard, it is to be mentioned that the RE is placed in close proximity to WE inorder to reduce the solution resistance. Since the WE is connected to S and WE is kept at a fixed stable potential by controlling the polarization of the CE, the potential created between the RE and WE is controlled all the time.

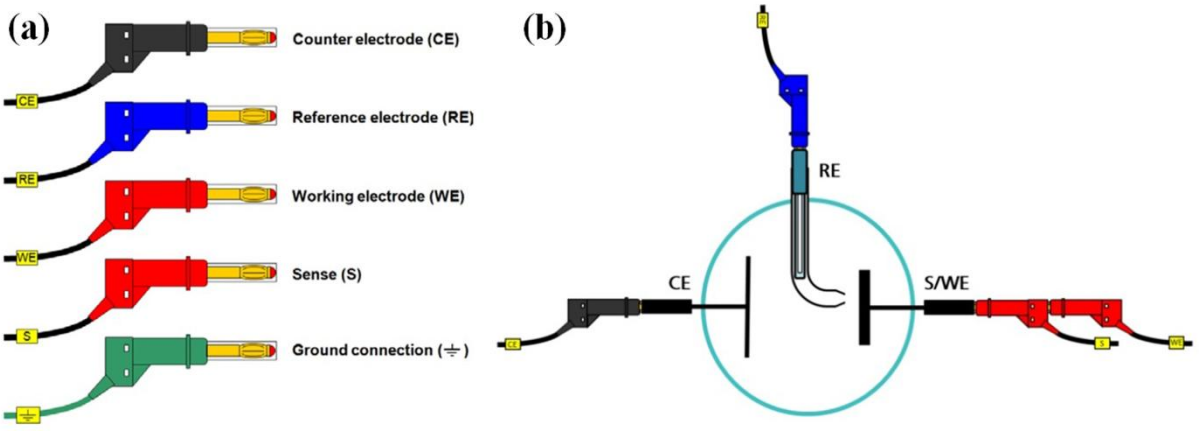

Fig.1.6. (a) Connections available on the cell cables of Autolab PGSTAT101 with the corresponding colour codes; (b) Schematic view of the three electrode setup

The basic electrical circuitry of potentiostat has been depicted in Fig.1.7 [19]. From the diagram, it may be observed that CE is connected to the control amplifier (CA) block, which forces the current to flow through the cell. On the other hand, WE is connected to the current follower (Low CF) circuit. The corresponding value of the current is measured using a low CF or a shunt (high CR), for low and high currents, respectively. The potential difference is measured between RE and S, using a differential amplifier (DiffAmp). The resultant signal is

fed to the summation point (Σ), which along with the waveform set by the digital to analog converter (E_{in}) will be used as an input to CA. E_{out} and I_{out} are the output potential and the output current, respectively.

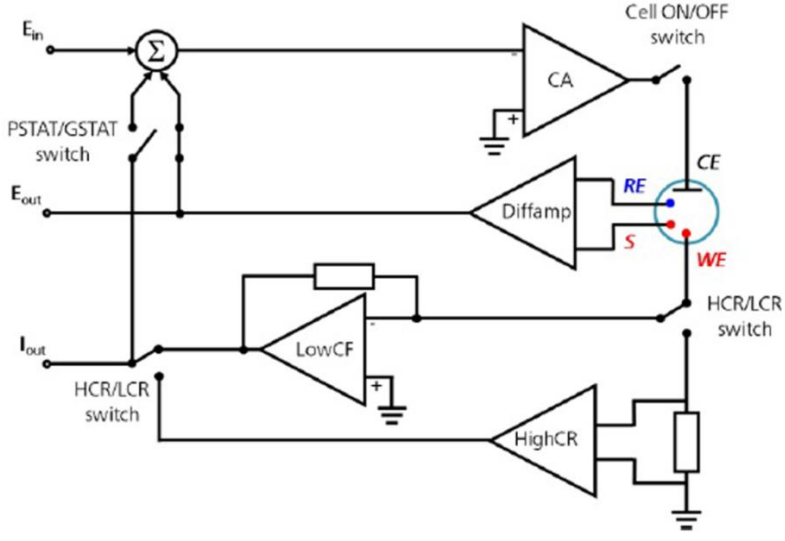

Fig.1.7. Basic electrical circuitry of a potentiostat

The most common forms of voltammetric measurements are as follows:

i) Linear sweep voltammetry (LSV)

It is a voltammetric technique where the current across an electrochemical cell is measured as a function of time and potential between the working and the reference electrodes. Here the potential is varied linearly with respect to time and stops at the end point. The characteristics of a linear sweep voltammogram mainly depend upon the following three factors [18]:

- The rate of electron transfer reactions taking place
- The chemical reactivity of the electroactive species
- The voltage scan rate

On increasing the scan rate in a LSV, the capacitive current increases and cannot be electronically compensated. Therefore, the sensitivity of this method is low and the detection limits are of the order of mg/l.

ii) Cyclic voltammetry (CV)

CV is a type of potentiodynamic electrochemical measurement where the potential of the working electrode is ramped linearly versus time [18]. Here, unlike LSV, after reaching the set potential, the working electrode's potential ramps in the opposite direction to return to the initial potential value. Fig.1.8 (a) and (b) depicts the typical cyclic voltammogram thereby showing the cathodic (i_{pc}) and the anodic currents (i_{pa}) corresponding to the oxidation and the reduction processes, respectively, in response to different time intervals. As shown in Fig. 1.8 (a) and 1.8 (b) [21], during the forward scan from time t_0 to t_1, on application of an increasing potential, the current increases until the anodic peak is reached. At this point, the process of oxidation takes place in a fastest possible rate due to the abundance of reactants. During further increase of the voltage, the supply of these reactants become diffusion limited and the current drops to a lower or sometimes to a constant value. On reversal of the sweep (during the reverse scan from t_1 to t_2), the reduction of the oxidized species takes place and the cathodic peak is recorded.

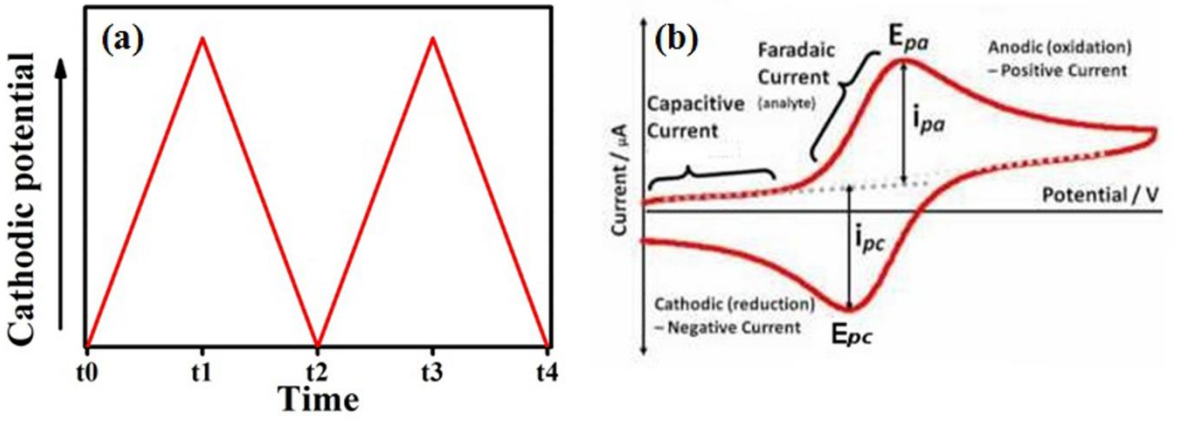

Fig.1.8. (a) Cyclic voltammetry waveform; (b) Typical cyclic voltammogram showing the different parameters for a reversible reaction

iii) Pulse voltammetry

Pulse voltammetry technique relies on the difference in the rate of the decay of the charging and the faradaic currents following a potential step or pulse. The charging current decays exponentially; whereas the faradaic current decays at a much slower rate, being the function of $1/(\text{time})^{1/2}$. This technique was developed by Barker and Jenkin [22] and by means of it; detection of an analyte upto 10^{-8} M concentration level is possible. It may be noted that various pulse voltammetric techniques differ by the applied potential waveform and the corresponding current profile.

- **Normal pulse voltammetry (NPV)**

Here, a series of potential pulses of monotonically increasing amplitude is applied and the corresponding current is measured at the end of each pulse thereby allowing some time for the decay of the charging current. The duration of the pulse time (t) in response to the potential (E_i) ranges from 1 to 100 ms with the corresponding interval being 0.1 to 5 s. In the voltammogram, the sampled current is displayed on the vertical axis, whereas, the pulse is stepped on the horizontal axis.

- **Differential pulse voltammetry (DPV)**

A typical representation of the differential pulse voltammetry (DPV) method is shown in Fig.1.9 [23]. This technique is similar to the NPV method discussed previously, but here the potential is scanned with a series of pulses. Here the baseline potential is held for a certain duration for the application of the next pulse and the corresponding sequential current is sampled twice; one before the pulse and other at the end of the pulse. The resulting difference between these two values of sampled current are recorded for analysis.

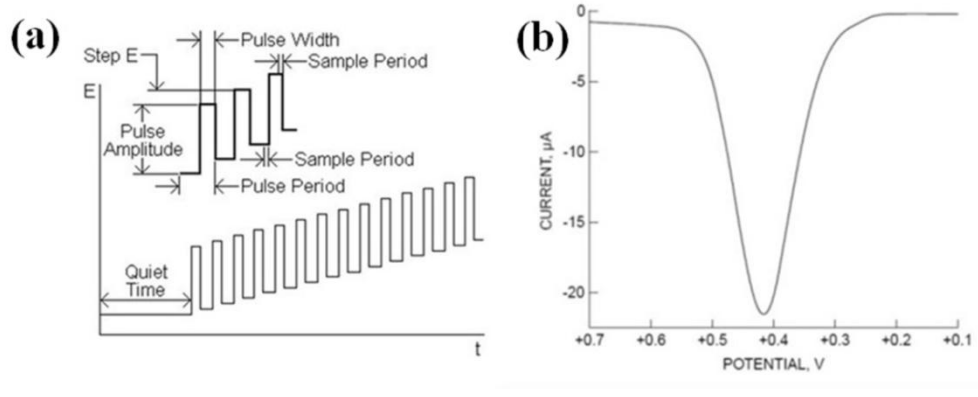

Fig.1.9. (a) Excitation potential waveform for differential pulse voltammetry; (b) A typical differential pulse voltammogram

Consequently, the effect of charging current on the sensitivity gets nullified, and detection limits up to a very low order can be achieved by this technique.

- **Square wave voltammetry (SWV)**

In square wave voltammetry (SWV), the applied potential consists of a series of symmetrical square-wave pulse of amplitude of E_{sw} superimposed on a staircase waveform, such that the forward pulse of the square wave coincides with the step of the staircase [18]. The resultant current is calculated on the basis of the difference between the forward and the reverse currents and is centred on the redox potential. Here the peak heights and the concentration of

the electroactive species are linearly dependent on each other and detection limit up to the order of 10^{-8} M is possible.

iv) Stripping voltammetry

Stripping voltammetry is mainly performed for sensitive electrochemical determination of trace amounts of metals in a solution [18]. The methodology may be categorized in to the following three steps.

In the first step, a certain potential is applied onto the electrode thereby enabling the deposition of the target metal ions on its surface. The solution undergoes constant stirring inorder to maximize the number of metal ions for deposition.

The second step allows the solution to reach a steady state and the stirring process is discontinued.

In the 3rd step, also known as the stripping step, the deposited metal ions are stripped from the electrode by scanning the potential. The current produced as a result, is proportional to the amount of the metal present in the solution.

There are two different types of stripping voltammetry depending upon the positive potential scan or negative potential scan of the stripping process. These are known as Anodic Stripping Voltammetry (ASV) and Cathodic Stripping Voltammetry (CSV), respectively.

1.3. Different sensing strategies implemented to ascertain the quality of tea

Over the years, scientists have employed different techniques for the detection of the chemical constituents of tea. These are depicted in Table 1.3.

Table 1.3 Different sensing techniques used to identify various constituents of tea

Sl No.	Target analyte	Electrode	Technique used	References
1	TF	Array of noble metal electrodes viz., Au, Ir, Pt, Pd, and Rh	Large amplitude pulse voltammetry (LAPV)	[24]
		Array of noble metal electrodes viz., Au, Ir, Pt, Pd, and Rh	Multi-frequency large amplitude pulse voltammetry (MLAPV)	[25]
2	CAT	Hydroxypropyl-betacyclodextrin modified carbon paste electrode (CPE)	Osteryoung square wave anodic voltammetry (OSWAV) and Differential pulse cathodic voltammetry (DPCV)	[26]

Sl No.	Target analyte	Electrode	Technique used	References
		Poly(methylene blue) modified CPE	CV and DPV	[27]
		MnO_2-CNT/Pt NP composite modified GCE	CV and DPV	[28]
		Polyaspartic acid modified GCE	CV and DPV	[29]
		MWCNT modified CPE	DPV	[30]
		Nickel complex and thiol on gold electrode	SWV	[31]
		$(Ru(bpy)_3^{3+})$ modified BDD	CV	[32]
3	EGCG	Glassy carbon electrode (GCE)	SWV	[33]

In regard to the detection of TF, though there are no such reports indicating the development of individual sensors, Ghosh et al. [24], have successfully quantified the amount of TF using an E-tongue made up of noble metal (Au, Ir, Pt, Pd and Rh) electrodes by means of LAPV method. In this work, they have used different neural networks and algorithms in order to develop a model. The prediction model so obtained delivered the prediction performance accuracy of over 95 %, correlation factor of over 0.95 and the worst case prediction of more than 76 %. In another work, Ghosh et al. [25] have used the MLAPV technique in order to quantify the TF-digallate (commonly assumed as the briskness indicator) in black tea by means of a PLS model using an E-tongue comprising of noble metal (namely, Au, Ir, Pt, Pd and Rh) electrodes.

For the detection of catechin (+C), El-Hady et al. [26] modified the CPE using hydroxypropyl-beta-cyclodextrin and implemented the OSWAV and DPCV, respectively, for determination of catechin. The corresponding linear range achieved was upto 7.20 and 4.20 µg/ml for both the voltammetric processes, respectively. The limits of detections (LOD) were calculated as 0.12 ng/ml and 0.30 ng/ml using both the anodic and cathodic voltammetry, respectively. Also, the developed sensor was successfully used to determine the catechin content in urine, commercial cocoa, coffee and tea samples, respectively. Due to the presence of electron rich sulphur and nitrogen heteroatom in its structure, Methylene blue (MB) is a water soluble cationic dye and an excellent redox mediator. Also, MB can get strongly

adhered on to the surface of graphite by means of π-π electrostatic interactions owing to its planar aromatic structure. Towards this direction, Manasa et al. [27] electropolymerized MB and modified the CPE by Poly(MB) for successful detection of catechin. DPV response profile indicated two linear ranges, viz., 1.0 x 10^{-3} to 1.0 x 10^{-6} M and 1.0 x 10^{-7} to 0.1 x 10^{-8} M, respectively for the synthesized electrode. The LOD value was calculated to be 4.9 nM. Moreover, satisfactory recovery values were also obtained by subjecting the electrode to green tea and spiked fruit juice samples. Vilian et al. [28] modified the MWCNT with MnO_2 and Pt nanoparticles and deposited them on to the glassy carbon electrode (GCE) inorder to detect catechin. The CV and the DPV results revealed excellent electrocatalytic characteristics and larger effective surface area, greater porosity and more reactive sites were visible on the surface of the electrode. The authors achieved a linear range of 2-950 µM and an LOD of 0.02 µM. The real time application of the sensor was also tested in red wine, black tea and green tea samples and it delivered satisfactory results. A fast and convenient analytical approach was presented by Wang et al. [29] by immobilizing an electropolymerized film of polyaspartic acid on the surface of GCE followed by its use towards the determination of catechin in phosphate buffer solution of pH 6.8. The modified electrode demonstrated a linear range from 2.5 x 10^{-7} to 3.0 x 10^{-5} mol/l and the LOD of 7.2 x 10^{-8} mol/l, respectively. In another study, Masoum et al. [30] investigated the use of a chemometric method for the determination of catechin in presence of gallic acid (GA). The electrode was prepared by modification of the CPE with MWCNT in order to achieve an enhanced conductivity. Multivariate curve resolution-alternating least squares (MCR-ALS) algorithm have been proposed by the researchers for identification of catechin from green tea samples. The change of pulses in the DPV response profile was selected as a feature to generate electrochemical second order data. Further, the MCR-ALS technique was applied on these corrected sets of data to quantitatively analyse the catechin content. The linear range of the concentration profile was between 0.10-2.69 µM for catechin and the corresponding value of LOD was 0.017 µM. The studies by Moccelini et al. [31] indicates the synthesis of a novel mononuclear nickel(II) complex, where the phenolate groups are capped by the bulky substituents (*tert*-butyl) in the *ortho* and *para* positions of the pentadentate H_2L ligand. The synthesized Ni(II) complex was immobilized on to a self assembled monolayer (SAM) gold electrode for effective detection of catechin. The modified electrode offered a linear range from 3.31 x 10^{-6} to 2.53 x 10^{-5} mol/l with an LOD of 8.26 x 10^{-7} mol/l. Wu et al. [32] have proposed an electrochemical method using ruthenium tris (2, 2') bipyridyl (Ru $(bpy)_3^{3+}$) modified boron doped diamond (BDD) electrode based on its electrochemical autoxidation.

They have monitored the reduction characteristics by studying the interactions between the Ru $(bpy)_3^{3+}$ modified oxidized BDD electrode and the intermediates produced as a result of autoxidation of catechin. The amperometric readings indicated a linear range from 0.3268 µM to 0.1591 mM. On application of the methodology towards determination of catechin in commercial samples, the results were found to be in good correlation with the traditional HPLC data.

Detection of EGCG has been investigated by Novak et al. [33] using GCE and SWV over a wide range of solution conditions. The linear response of EGCG was obtained with the concentration values from 1×10^{-7} M to 1×10^{-6} M having LOD of 6.59×10^{-8} M. The authors validated the performance of their electrode in green tea samples using standard addition method. The EGCG content was found to be in same order of magnitude as obtained from the HPLC data.

It may be noted from the above mentioned literature survey that for the quantification of theaflavin and its different fractions, the noble metal based E-tongue has been considered for obtaining the response profile. In this regard, a number of chemometric techniques have been explored in order to achieve the performance index of the E-tongue. On the other hand, the methodologies applied for the detection of catechin are either costly or involves tedious sample preparation and storage. For example, HP-β-CD/CPE electrode is needed to be stored in Britton-Robinson buffer at pH 3 in order to ensure effective performance. During preparation of some of the electrodes, researchers have also used expensive modifying agents. The preparations of these agents are extremely complex and time consuming. Some reports indicated the use of GCE where GCE was polished with alumina powder and further activated by performing 20 cycles of CV in 0.5 M H_2SO_4. All in all, it may be inferred from the literature survey that the electrodes used for the detection of catechin went through tedious experimental cycles. As a result, the overall process of fabrication of electrodes becomes costly and also difficult to replicate. There is only one report related to the electrochemical detection of EGCG. The study indicates the use of GCE for the determination of EGCG. The electrochemical studies were carried out in acidic pH and also the electrode lacks selectivity.

Therefore, as documented earlier, in order to overcome the above disadvantages and prepare sensors in a cost effective and simple manner, MIP based methodology has been proposed

herein. Moreover, this technique also ensures proper affinity, selectivity and sensitivity of the target molecules and the preparation process is easily reproducible.

1.4. Molecular imprinted polymer (MIP) based technique

Molecular imprinting is referred to as the arrangement of one or more of various types of polymer-forming components (functional monomers) in a complementary fashion to the template, either by the formation of covalent bonds, or by self-association. The matrix-forming material or cross-linker and a porogenic solvent are also added and the whole mixture is cured to give a porous material containing cavities that perfectly matches with the shape and orientation of the template molecule. Template removal is done by washing with solvent or a combination of chemical treatment. The washing process is believed to remove some, or all, of the template from the polymer. As a result, the vacant imprinted sites become available for rebinding of the template or its structural analogues. The experiments related to molecular imprinting was first performed by Dickey in the 1940s and 1950s [34, 35] in which the affinity for dye molecules in silica gel was established in combination with a theory of Linus Pauling [36]. The basic schematic of an MIP process [37] is depicted in Fig.1.10.

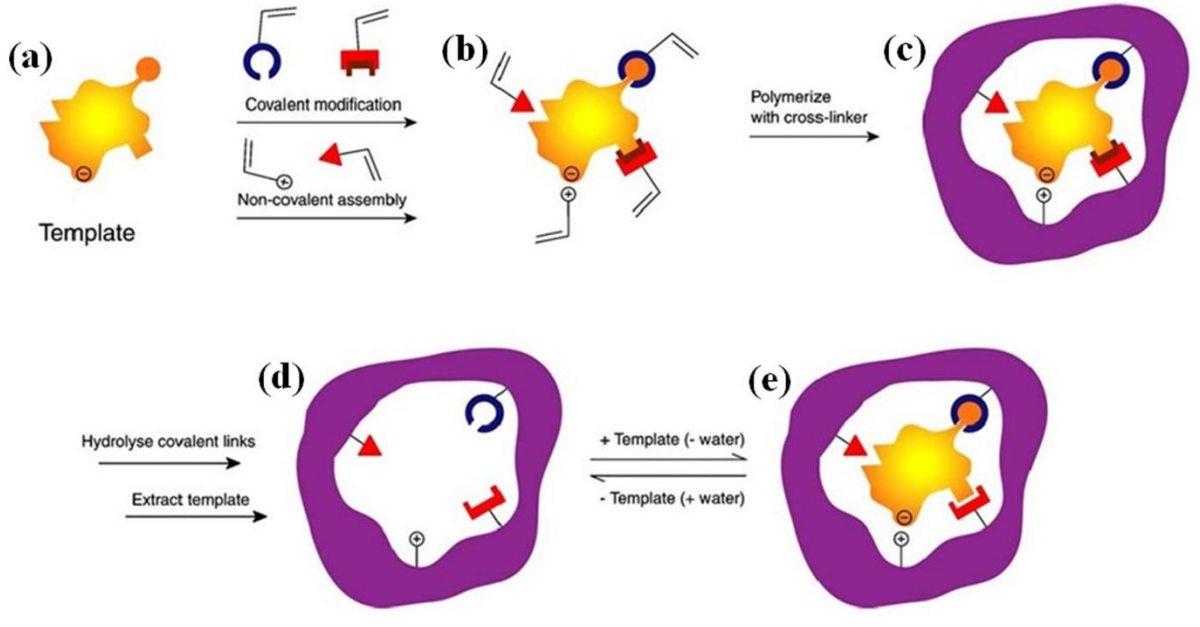

Fig.1.10. Schematic representation of the imprinting process showing (a) the template; (b) template monomer complex by means of covalent and non-covalent interactions; (c) subsequent polymerization; (d) extraction of the template; (e) rebinding of the template on interaction of the MIP with the analyte.

Therefore, the method of forming a MIP can be distinguished in terms of the following three steps [38]:

a) **Association:** The target analyte, suitable functional monomer and crosslinkers are selected to form the complex by covalent or non covalent binding.

b) **Polymerization:** Different types of polymerization techniques are performed, as a result of which crosslinked copolymers entrapped with the template molecules are obtained.

c) **Elution:** Template molecules entrapped within the polymer matrix are extracted by using appropriate elution agent. Consequently, cavities similar in size and shape of the template molecule are formed for specific recognition purposes.

Essentially, there are two factors that contribute to the underlying mechanisms by virtue of which the molecular recognition takes place [39]. These are namely;

- Pre-organization of the complementary functional groups in the polymer by the template.
- Formation of a shape-selective cavity that is complementary to the template.

Therefore, the imprinting effect can be perceived as a three dimensional effect. This is because it regulates the three dimensional interactions by the template with the surrounding functional monomers and the crosslinked matrix.

MIPs are advantageous due to the fact that they are highly rigid, flexible and offer great mechanical stability. Moreover, due to the wide availability of the functional monomers, MIP sensors suitable to any target analyte can be designed successfully. Further, MIP technique can also be used as a replacement of unstable biological molecules like antibodies and enzymes in biosensors. The merits of MIP sensors over sensors based on natural biomolecules [38] have been listed in Table 1.4.

Table 1.4 Comparison of sensors based on natural biomolecules and MIP sensors

Sl. No.	Sensor based on natural biomolecules	MIP sensors
1	Poor stability	Highly stable even at low/high pH values, pressure, and temperature (<140 °C)
2	Enzymes and receptors are expensive	Inexpensive and easy to prepare
3	Perform poorly in non aqueous media	They can respond in organic solvents
4	Different natural biomolecules have different operational requirements (pH, ionic strength, temperature, substrate)	Polymers for different targets can respond in the same specific environment
5	For some important analytes, natural receptors and enzymes do not exist and antibodies cannot be prepared	Polymers could be prepared for practically any compound
6	Poor compatibility with micromachining technology and miniaturization	Polymers are fully compatible with micromachining technology

There are various chemical routes by means of which binding sites can be formed between the polymer matrix and the template. These are viz., covalent imprinting, non covalent imprinting, semicovalent imprinting and imprinting with sacrificial spacers. The different types of imprinting processes are elaborated in the subsequent sections.

1.4.1. Types of imprinting techniques

1.4.1.1 Covalent imprinting

Covalent imprinting is an imprinting strategy where the template and one or more polymerizable units are attached by covalent bonds to form a template–monomer complex by means of a chemical step independent of polymer formation. Here in this method, at first a pre-polymerization derivative is formed from the functional monomer and the template, followed by the subsequent polymerization process. On removal of the template from the polymer post polymerization, the covalent linkage between the polymer and the template is cleaved. The same linkage is again established on rebinding of the template molecule within MIP [40]. The typical feature of this methodology is that the removal of the template and subsequent rebinding steps will both involve chemical reactions and the rebound template will be indistinguishable from template immediately after polymerization. The covalent imprinting process is described in the form of a schematic shown in Fig.1.11 [41].

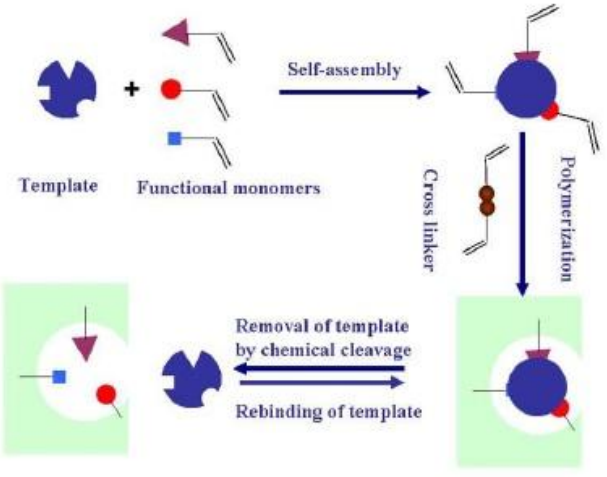

Fig.1.11. Schematic explaining the covalent imprinting process

a) Imprinting with readily reversible covalent bonds

This type of covalent imprinting promotes the preparation of the template-monomer complexes by means of readily reversible condensation reactions such as boronate ester, ketal/acetal and Schiff's base formation, respectively. The formation of these assemblies necessitates mild aqueous conditions to hydrolyse the template molecule from the polymer. The specific structural requirements of covalent methods certainly limits the number of templates that can be imprinted in this way, namely, 1,2- and 1,3-diols (boronate ester and ketal/acetal), aldehyde (acetal and Schiff's base), ketone (ketal) and amine (Schiff's base).

One of the distinct advantages of this method is that the rebound state is identical to the as prepared polymer in which all binding sites more or less bear a resemblance to one another. Moreover, as there is no excess of functional monomer present, non-specific binding may be greatly reduced. However, the need for synthesis of the template–monomer is perceived as the limitation of any covalent imprinting technique and also the template monomers of this type may be very sensitive to the presence of water, thus preventing the use of emulsion and suspension polymerization methods. Further, the reactions occurring in the imprinted polymer sites impose additional steric requirements, which in turn hinder the process of the exchange of the template molecule.

b) Covalent imprinting with boronate esters

The boronate ester approach is believed to be the most successful reversible covalent methods, because it is applicable to the imprinting of carbohydrate derivatives. This method, being first implemented by Gunter Wulff et al., includes the templates, namely, glyceric acid, derivatives of mannose, galactose and fructose, sialic acid, castasterone, l-DOPA and nucleotides [42-46] for the imprinting process. A number of researches have indicated the incorporation of boronate esters in MIPs for fluorescent sensing [47-49], in imprinted polyelectrolyte hydrogels [50], functionalised polyaniline coatings for microtitre plates [51] and also for the enantioselective synthesis of amino acids. Moreover, the use of boronophthalide-based monomers [52, 53] has extended this technique to the imprinting of monoalcohol templates and those with spatially separated multiple hydroxyl groups. Also, selective derivatization of sterols by polymeric protecting groups has been achieved by the polymers prepared using this strategy [54].

c) Covalent imprinting with Schiff's bases

Schiff's base (imine) chemistry involves the condensation of a primary amine and a carbonyl compound (usually an aldehyde). It is therefore a potentially useful method for the imprinting of either amine or aldehyde-bearing templates. Amino acid derivatives have been successfully imprinted by this method [55] but exchange with the resultant enantioselective polymers is generally too slow for use in chromatographic separations.

d) Covalent imprinting with acetals and ketals

Mono and di-ketone templates have been extensively studied by Shea et al [56-58] where a polymerizable diol has been employed as the binding group for the preparation of the MIP. A series of cyclic hemi-acetals has also been investigated for their potential as binding groups for monoalcohols [59].

1.4.1.2. Noncovalent imprinting

Noncovalent imprinting on the other hand overcomes the limitations as is seen in the case of covalent imprinting. The use of non-covalent interactions dates back to the earliest reports of imprinting in the silica matrices, but it has been popularised by the work of Mosbach's group in the 1980s, where it was established as a viable method for producing imprinted receptors in synthetic polymers [60]. A schematic of the noncovalent imprinting process is shown in Fig.1.12 [41]. Here, in this method, template-monomer complexes are formed in an appropriate solvent based on various interactive forces. The template is removed from the polymerized sample and can rebound to it by means of the same interactive force. The typical force of attraction between molecules includes hydrogen bonds, ion-pairs, dipole–dipole interactions and Van der Waals forces to generate adducts of template and functional monomers in solution.

Non covalent imprinting is one of the most practised strategies as it offers flexibility in terms of the functionalities on a template that can be targeted. It is generally assumed that in this process, after the formation of a pre-polymerisation complex between the template and functional monomers, small sections of polymer structure having multiple functional groups begins to wrap around the template molecule. Consequently, a cooperative effect is produced due to the multiple interactions than that would have occurred in case of single monomer–template interactions. As polymerisation proceeds, these structures further develop and change their shape with the addition of more functional monomer. This leads to higher affinity of the template molecule in the receptor site until it matures to completion in the fully polymerised system.

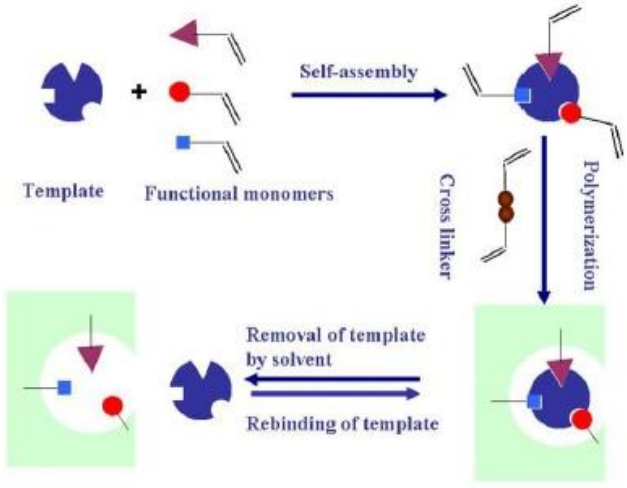

Fig.1.12. Schematic explaining the mechanism of non covalent imprinting

Non covalent imprinting process can be carried out either with a single monomer or combination of monomers.

a) Non-covalent imprinting with a single functional monomer

This is the simplest approach to non-covalent imprinting. It is the first method that was demonstrated to work and is also most widespread in the literature. However, here also the nature of the polymerization complex present and the probable interactions between the template and the monomer with the crosslinkers must be taken into account. This is because the former may play an important role in defining or refining functional receptor sites, whereas the latter can shift the equilibria away from the desired template monomer interactions. Moreover, complications can also arise due to self-association characteristics of some of the functional monomer. For example, carboxylic acids have a strong tendency to dimerise. Further, the possible interactions with the initiator should also be considered as they are normally present (at least initially) at a concentration similar to that of the template. Typical examples of the functional monomers tested during the years for non covalent imprinting are summarised in Table 1.5, where they are classified according to whether they are acidic, basic or neutral in nature. Despite the apparent drawback of strong dimerisation under the conditions generally employed in noncovalent imprinting (high concentration, low solvent polarity), carboxylic acid-based monomers, principally methacrylic acid have been by far the most successful. This may be attributed to the presence of relatively few bonds with rotational degrees of freedom and their ability to interact in various ways with template, namely as, H-bond donors, H-bond acceptors and through formal ion-pair formation, and also as weaker dipole–dipole interactions, etc. Vinylbenzoic acid can also be considered an

attractive option, due to the bulk and k electron system of the aromatic ring, but it possesses relatively poor reactivity ratios with typical (meth)acrylate cross-linkers and hence results into unfavourable interactions with template molecules. Phosphonates and phosphates, on the other hand, are also utilized in imprinting based on their metal ion complexation. In their basic form, the monomer, vinyl pyridine represents electron rich k-electron ring systems, and interacts strongly with electron deficient aromatic rings through acid–base interactions and H-bond acceptance or donation. These monomers are found to often interact strongly with templates and thus they are believed to be highly efficient in imprinting. They have been proved useful in many cases, but their use can also have significant drawbacks. These monomers yield very strong *k–k* interactions that occur during template rebinding in aqueous conditions, thereby causing a significant disadvantage. It generally leads to extremely high levels of nonspecific binding of analytes to the polymer, so that both the imprinted and the non imprinted polymers often displays identical binding abilities. Other basic monomers include the family of tertiary amino monomers. Though they are effective in a few cases, but in general yield less satisfactory results than acidic monomers. This is possibly due to their much greater chain flexibility and the fact that the amine functionality is more remote from the polymer backbone.

Table 1.5 List of some monomers and combination of monomers used in non covalent molecular imprinting

Sl. No.	Monomers	Application areas
1	**Monomers bearing acidic residues**	a) Imprinting of amino acid derivatives, peptides, theophylline, morphine, etc.
	Methacrylic acid (MAA)	
	Acrylic acid	
2	**Monomers bearing basic residues**	a) Imprinting of S-Naproxen, amino acid derivatives. b) Imprinting of atrazine
	4-Vinylpyridine	
	Diethylaminoethyl methacrylate	
3	**Neutral monomers**	a) Imprinting of amino acid derivatives b) Imprinting of ephedrine, cholesterol
	Acrylamide	
	2-Hydroxyethyl methacrylate (HEMA)	
4	**Electrostatically charged monomers**	a) Imprinting of sialic acid b) Fluorescent monomer used in the imprinting of cAMP.
	N,N,N-trimethylaminoethyl methacrylate chloride	
	trans-4-[p-(N,N-Dimethylamino)styryl]-N-vinylbenzylpyridinium chloride	
5	**Monomer combinations**	a) The combination of monomers is superior to either monomer alone in the imprinting of some amino acid derivatives.
	Methacrylic acid and 2-vinylpyridine	
	Acrylamide and 2-vinylpyridine	

b) Non-covalent imprinting with combination of monomers

Superficially, it seems highly attractive to combine the specific interaction potential of a variety of different monomers. In reality, it is dependent on the consideration of all the equilibria present in a pre-polymerisation mixture. Although it often contains no strongly interacting functional groups, it will surely also interact with both template and monomers, since it is generally present in significant molar excess. Interesting recent work by Spivak has shown that if the crosslinker is appropriately functionalised, no further functional monomers are required to achieve effective imprinting [61]. In order to be successful, the bonds formed between the template and the functional monomers need to be stronger than any interactions between the functional monomers. This is often very difficult to predict intuitively. Interestingly, computational virtual imprinting has predicted combination imprinting recipes that have worked well in practice, though the analysis may not have been extensive enough to definitively show that the monomer mixture performed better than any optimised single monomer formulation. While this would be detrimental to template monomer adduct formation (due to equilibrium shifting) it might also be argued that it could reduce nonspecific binding in such polymers since it would reduce the incidence of isolated carboxylic acid or pyridine groups in the final polymer forming low affinity binding sites. This gives them more opportunity to interact with the template, leading to functional receptor sites.

1.4.1.3. Semicovalent imprinting

In the previous sections it has been observed that in case of covalent imprinting, the template molecule has to be chemically modified with the functional monomer and can only be removed by the cleavage of the covalent bonds, so formed. On the other hand, a comparatively lenient approach is the non covalent technique where relatively weak forces of attraction, namely, electrostatic interactions, hydrogen bonding, π-π bonding, hydrophobic interactions, etc., can serve the purpose of attachment of the template to the monomer. This method involves the covalent attachment during the polymerization and hydrogen bond formation during recognition, thus overcoming the disadvantages of covalent imprinting.

Semicovalent imprinting is the hybrid form of both the covalent and the non covalent imprinting process, in which the template is covalently bounded to the functional monomer during polymerization and uses the non covalent interactions only during the rebinding process. For example, a (meth)acrylate ester of the template is copolymerised with the matrix-forming monomer mixture. The template is subsequently removed by hydrolysis, with

rebinding of the unesterified template to the polymer, as a result of the interaction of the template hydroxyl(s) with (meth)acrylic acid residues introduced into the imprinted site. But this type of imprinting is compromised to a certain extent due to the lack of straightforward template hydrolysis and difference in steric requirements of an acid and an alcohol in hydrogen bonding contact from the corresponding ester.

1.4.1.4. Imprinting with sacrificial spacers

Some of the limitations of the semi-covalent imprinting approach can be mitigated by the utilization of a linker group between the template part and the functional molecule, which is lost as a result of template removal. The linker group performs the dual role of attaching the template to the functional monomer during formation of the polymer and also acts as a spacer between the template and polymer-bound functionality inorder to prevent the steric crowding in the non-covalent rebinding step. The spacer must be easily removed with the template; hence it can be termed a sacrificial spacer.

For example, the carbonyl group of a carbonate ester was the first sacrificial spacer group used in the imprinting of cholesterol [62]. Here the monomer, cholesterol (4- vinyl) phenyl carbonate was copolymerised with EGDMA. Hydrolysis of the resultant polymers with NaOH in methanol released the template (cholesterol) with simultaneous loss of the spacer group as CO_2. Rebinding of cholesterol in non-polar solvents was shown to occur by hydrogen-bonding between the 4-vinylphenol residue of the polymer sites and the hydroxyl group of cholesterol. Other MIP syntheses have employed carbonyl spacers in template monomers linked through urea [63] and carbamate (urethane) [64, 65] linkages, and also with carbonate esters [66, 67].

Salicylate (2-hydroxybenzoate) has also been used as a spacer group between a polymerizable methacrylic acid residue and primary amine of the template [68]. The method is effective because a close proximity was maintained by intramolecular hydrogen-bonding between the amide hydrogen and ester oxygen in the non-covalent binding step and the phenyl methacrylate ester is cleaved easily than the corresponding amide.

1.4.2. Literature survey on MIP based sensors

The recent developments in MIP based detection related to different domains of application have been detailed in this section based on the transduction technique used. This is because the transduction technique has a major impact on the selection of the monomers and

optimization of the polymerization process. Table 1.6 depicts some of the recent researches pursued in relation to the MIP method using electrochemical transduction followed by a detailed description of some of the highly cited works.

Table 1.6 Literature survey indicating the development of MIP method using electrochemical transduction

Sl. No.	Target analyte	Components of MIP	Polymerization method	Principle of operation	References
1	Atrazine	a) Monomer: MAA b) Crosslinker: EGDMA c) Initiator: AIBN	Polymerization by means of UV light irradiation on the surface of Au electrode	CV	[69]
2	Atrazine	a) Monomer: AAT b) Crosslinker: EDOT	Electrodeposition on Pt electrode	CV	[70]
3	Insulin	a) Monomer: AEP b) Crosslinker: EGDMA c) Initiator: AIBN	Bulk polymerization onto the surface of vinyl group functionalized MWCNT	CV, DPASV	[71]
4	Caffeine	a) Monomer: MAA b) Crosslinker: EGDMA c) Initiator: AIBN	Bulk polymerization followed by modification of CPE	CV, DPV	[72]
5	Cadmium (II)	a) Monomer: MAA b) Crosslinker: EGDMA c) Initiator: AIBN	Bulk polymerization	DPASV	[73]
6	Tobramycin	Monomer: Pyrrole	Electropolymerization on GCE	CV and SWV	[74]
7	Bovine serum albumin	a) Monomer: TEGPMA b) Crosslinker: DAU	Free radical polymerization on the MWCNTs-CE surface	CV and DPV	[75]
8	Lamotrigine	a) Monomer: MAA b) Crosslinker: EGDMA c) Initiator: AIBN	Bulk polymerization followed by modification of CPE	CV, DPV	[76]
9	L-cysteine	a) Monomer: MAA b) Crosslinker: EGDMA c) Initiator: AIBN	Bulk polymerization followed by modification of CPE	CV, DPV and EIS	[77]
10	Methyl parathion	Monomer: Phenol	Electropolymerization on the surface of nitrogen doped	CV	[78]

Sl. No.	Target analyte	Components of MIP	Polymerization method	Principle of operation	References
			graphene sheet modified Au electrode		
11	Trimethoprim	Monomer: Pyrrole	Electropolymerization on the surface of GCE	EIS,CV	[79]
12	Carbofuran	a) Monomer: MAA b) Crosslinker: EGMRA	Electropolymerization after modification of GCE by rGO@Au	CV and EIS	[80]
13	Ochratoxin A	Monomer: Pyrrole	Electropolymerization on the surface of MWCNT modified GCE	CV and DPV	[81]
14	Norfloxacin	Monomer: Pyrrole	Electropolymerization on the surface of MWCNT modified GCE	CV and SWV	[82]
15	Melamine	Monomer: Pyrrole	Bulk polymerization using CNT-IL as carrier	CV and SWV	[83]
16	Dopamine	Monomer: py-PBA	Electropolymerization on the surface of GCE	CV and DPV	[84]
17	Theophylline	a) Monomer: MAA b) Crosslinker: EGDMA, TEOS c) Initiator: AIVN	Precipitation polymerization followed by combination with graphite microparticles and deposition of the composite on the surface of epoxy-graphite electrode	DPV	[85]
18	Isoniazid	a) Monomer: Acrylamide b) Crosslinker: MDA c) Initiator: Ammonium persulfate	Electropolymerization on the surface of Au NP modified MWCNT/GCE	CV, LSV	[86]
19	Glucose	Monomer: PVA	Bulk polymerization followed by modification with MnO_2@GO/CuO nanocomposite	CV	[87]
20	Procaine	a) Monomer: AA, WD-20, BA b) Initiator: AIBN	Bulk polymerization on the surface of GCE	DPV	[88]
21	Gallic acid	a) Monomer: MAA b) Crosslinker: EGDMA c) Initiator: AMP	Precipitation polymerization followed by deposition of the MIP on the MWCNT modified CPE	DPV	[89]
22	Thiamethoxam	a) Monomer: *p*-vinylbenzoic acid b) Crosslinker: EGDMA c) Initiator: AIBN	Gr modified MIP prepared by bulk polymerization and dropcasted on GCE	CV, EIS, LSV	[90]
23	EGCG	Monomer: β-cyclodextrin	Electropolymerization on GO modified GCE	CV, DPV	[91]
24	Testosterone	Monomer: o-	Electropolymerization on the	CV, EIS	[92]

Sl. No.	Target analyte	Components of MIP	Polymerization method	Principle of operation	References
		PD	surface of GO modified electrode		
25	Imidacloprid	a) Monomer: VBA b) Crosslinker: EGDMA c) Initiator: AIBN	Bulk polymerization followed by the deposition of MIP/Gr on GCE	LSV	[93]
26	Thiamine	a) Monomer: NMGA b) Initiator: AIBN	Free radical polymerization on the surface of Ni nanomer modified pencil graphite electrode	DPASV, CV	[94]
27	Simazine	Monomer: *o*-AT	Electropolymerization after modification with Au NPs	CV, EIS	[95]
28	Sulfanilamide	a) Monomer: MAA b) Crosslinker: DVB c) Initiator: AIBN	Bulk polymerization followed by modification with GO and deposition on GCE	CV, EIS	[96]
29	17-β-estradiol	Monomer: DAEth	Electropolymerization	CV and EIS	[97]
30	Salbutamol	Monomer: o-PD, 3-APBA	Electrocopolymerization on the surface of a grapheme nanocomposite modified screen printed carbon electrode	CV, DPV	[98]

For example, in a report by Pardieu et al. [70], the authors have employed the MIP technique for the detection of atrazine. Here in this work acetic acid thiophene (AAT) has been selected as the monomer owing to its ability of hydrogen bond formation with the target molecule. Though 3, 4-ethylenedioxythiophene (EDOT) cannot form hydrogen bonding, it is selected as the crosslinker here due to its hydrophilic properties, very well suitable to counteract with the hydrophobic characteristics of the AAT molecule thus ensuring electroactivity in the aqueous media. The copolymer has been synthesized electrochemically on to the Pt electrode based on the principle of association of the template molecule to AAT by hydrogen bonding and subsequent removal of atrazine from the polymer thereby creating enough reactive sites for binding with atrazine. In this work, the successful detection of atrazine was carried out from the concentration range of 10^{-9} mol/L to 1.5 x 10^{-2} mol/L and the corresponding LOD was found to be 10^{-7} mol/L.

Prasad et al. [71] developed an MIP sensing element for the detection of insulin over the surface of vinyl group functionalized MWCNTs. The MWCNTs went through various treatments, viz., acidification to generate COOH groups, acylation to obtain MWCNT-COCl

structure followed by functionalization with the vinyl group. The authors have synthesized the monomer p-acryloylaminophenyl-{(4-aminophenyl)- diethyl ammonium}-ethylphosphate (AEP) and employed free radical polymerization on the surface of functionalized MWCNTs using EDGMA as the crosslinker. The sensor was fabricated on the surface of pencil graphite rods by means of spin coating. The CV and the DPASV results demonstrated a linear range from 0.068-5.682 nmol/L with the LOD being 0.0183 nmol/L.

In another such work [78], Xue et al. synthesized an MIP by means of electropolymerization on to Au electrode for the detection of methyl parathion, a kind of organophosphate pesticide. The Au electrode was further modified with nitrogen doped graphene sheets (N-GS) in order to enhance the band gap and modulate the conductivity by the substitution of carbon atoms with foreign atoms. The monomer phenol was electropolymerized on the surface of Au electrode and CV was employed for the electrochemical characterizations. The results revealed a linear range from 0.1 to 10 µg/mL and LOD of 0.01 µg/mL.

Carbofuran belongs to the carbamate group of pesticides and is responsible for reducing the growth period of crops thereby increasing its yield. Tan et al. [80] fabricated an electrochemical based MIP sensor and deposited it onto modified GCE. The MIP sample was synthesized using methacrylic acid (MAA) as the monomer and ethylene glycol maleic rosinate acrylate (EGMRA) as the crosslinking agent. The GCE, on the other hand was modified with reduced graphene oxide and gold nanoparticles followed by deposition of the MIP by means of electropolymerization. Hexacyanoferrate has been used as a probe molecule and the electrochemical properties of the sensor have been studied by CV and EIS. The results indicated a linear range of the concentration profile from 5.0×10^{-8} to 2.0×10^{-5} mol/L with LOD of 2.0×10^{-8} mol/L.

Liu et al. [83] designed a MIP sensor using carbon nanotube-ionic liquid composite for the selective and sensitive determination of melamine. Melamine contains a considerably high proportion of nitrogen and thus added by unscrupulous manufactures in various milk products in order to enhance their protein content. Due to its unique property of large specific surface area, good mechanical stability and high electronic conductivity, CNTs have been preferred in this work. Moreover, ionic liquids are also advantageous due to good ionic conductivity, high viscosity and high chemical and thermal stabilities. Therefore, the composite of CNT and ionic liquid acted as a carrier material towards increase of sensitivity of MIP. The authors prepared the MIP using pyrrole as the monomer by means of bulk polymerization. CV and

SWV technique revealed linearity in the concentration of melamine from 0.4 to 9.2 µM with the corresponding LOD being 0.11 µM.

Dopamine is an important neurotransmitter and plays a pivotal role towards the regulation of various cognitive functions, like, stress, behaviour, attention, etc [99]. In pursuit of its detection using the MIP technique, Zhong et al. [84] synthesized a novel monomer py-PBA such that it can enable cyclic boronic ester formation with dopamine. The resultant boronic ester in combination with the imprinted cavities endowed double recognition capacities towards the detection of dopamine. The electrochemical properties of the fabricated electrode were studied using CV and DPV technique. A linear range of concentration was observed between the values of 5×10^{-8} mol/L to 1×10^{-5} mol/L. The results also indicated an LOD of 3.3×10^{-8} mol/L.

An enzyme free novel MIP sensor was developed by Farid et al. [87] for the selective detection of glucose. Here, the sensor was prepared using poly vinyl acetate (PVA) as the monomer and subsequently modified by MnO_2/CuO loaded graphene oxide (GO) nanoparticles. The electrochemical properties of the electrode were studied using CV. The results indicated a linear range for concentration values from 0.5 to 4.4 mM. The corresponding LOD was calculated as 53 µM.

In another study [92], Liu et al. designed an ultrasensitive sensor for the detection of testosterone, an anabolic androgenic steroid. The regulation of testosterone levels is essential, as it is associated with prostate cancer and is also used by athletes as dopants for improvement of their performance. In pursuit of the development of the sensor, the authors have used o-PD as the monomer and electropolymerized it on the surface of GO modified electrode. The electrochemical characterizations were performed using CV and EIS techniques. A linear range from 1 fM to 1 µM of concentration was observed under optimized experimental conditions with the LOD being 0.4 fM.

Quartz crystal microbalance (QCM) is a well known transduction element for chemical sensors due to certain advantages namely, portable, rapid and sensitive. It can detect up to the nanogram level of mass change loaded on to the surface of the QCM resonator. A number of works concerning the development of MIP sensors employing QCM based detection have been pursued by the researchers. These are illustrated in Table 1.7.

Table 1.7 Literature survey indicating the development of MIP method using QCM based transduction

Sl. No.	Target analyte	Components of MIP	Polymerization method	References
1	Terpenes	a) Monomer: MAA b) Crosslinker: EGDMA, TMPTM c) Initiator: AIBN	UV light irradiation using a 125-W medium pressure mercury lamp	[100]
2	Cu(II) ions	a) Monomer: MAA b) Crosslinker: TMPTM c) Initiator: AIBN	UV induced polymerization on the surface of QCM	[101]
3	Thymine	a) Monomer: MA-Ade b) Crosslinker: EGDMA c) Initiator: AIBN	UV induced polymerization for 4h	[102]
4	Folic acid	a) Monomer: N-vinyl 2-pyrrolidone b) Crosslinker: EGDMA c) Initiator: AIBN	UV mediated polymerization	[103]
5	Caffeic acid	a) Monomer: MAAP-Fe(III) b) Crosslinker: EGDMA c) Initiator: AIBN	UV light irradiated polymerization on the surface of QCM	[104]
6	Ractopamine	Monomer: *o*-AT	Electropolymerization on the surface of Au NP modified QCM	[105]
7	Cholic acid	a) Monomer: MAH-Cu(II) b) Crosslinker: EGDMA c) Initiator: AIBN	UV light irradiated polymerization for 4 h	[106]
8	Kaempferol	a) Monomer: MAAsp b) Crosslinker: EGDMA, HEMA c) Initiator: AIBN	UV irradiated polymerization for 1 h	[107]
9	Lovastatin	a) Monomer: MAA b) Crosslinker: EGDMA, HEMA c) Initiator: AIBN	UV light irradiated polymerization on the surface of QCM chip	[108]
10	Atrazine	a) Monomer: HEMA-phenol b) Crosslinker: EGDMA c) Initiator: AIBN	UV induced polymerization for 1 h	[109]
11	Methimazole	a) Monomer: AMAM b) Crosslinker: EGDMA c) Initiator: AIBN	Bulk polymerization	[110]
12	Epitope of human serum albumin	a) Monomer: Zinc acrylate b) Crosslinker: EGDMA	Bulk polymerization	[111]

Sl. No.	Target analyte	Components of MIP	Polymerization method	References
		c) Initiator: AIBN		
13	Amantadine	Monomer: *o*-AT	Electropolymerization on the QCM surface modified by rGO-AuNPs	[112]
14	Enrofloxacin	a) Monomer: APTES b) Crosslinker: TEOS	Bulk polymerization	[113]
15	Amoxicillin	Monomer: mPD	Electropolymerization	[114]

A MIP based QCM sensor has been designed by Gültekin et al. [104] for the sensitive detection of caffeic acid in plant materials. For the purpose of sensor development, Methacrylamidoantipyrine-iron (III) (MAAP-Fe(III)), ethylene glycol dimethacrylate (EGDMA) and 2,2'-azobisisobutyronitrile (AIBN) has been selected as the monomer, crosslinker and initiator, respectively. The polymerization process was carried out in UV irradiated conditions for 4 h. The sensor performed linearly over a concentration range from 0.01-1000 µM and the LOD was calculated as 7.8 nM. Quantitative estimations of caffeic acids in plant materials were carried out by correlating the response of the synthesized electrode with the HPLC data. The results indicated good accuracy at 95 % confidence level.

Gupta et al. [107], employed QCM based MIP technique for the determination of kaempferol. Here in, the authors have used Methacrylamidoaspartic acid (MAAsp) as the monomer. 2-hydroxyethyl methacrylate (HEMA), EGDMA and AIBN have been used as the crosslinker and initiator, respectively. Here also, polymerization occurred by means of UV irradiation for 1 h. The concentration profile of kaempferol varied linearly from 2.0×10^{-10} M to 1.5×10^{-9} M with the LOD being 6.0×10^{-11} M. The performance of the electrode was validated by taking the response profile of apple and orange juices. The corresponding recovery values were obtained from 90.6 % to 96.0 % and 91.4 % to 95.9 %, respectively.

In a report by Eren et al. [108], a QCM based MIP sensor has been developed for selective determination of lovastatin in red yeast rice. Here, MAA, EGDMA, HEMA and AIBN were used as the monomer, crosslinker and initiator, respectively. The polymerization occurred by means of UV radiation on the surface of the Au coated QCM for 1 h. The linear range of the concentration of lovastatin varied from 0.10-1.25 nM. The corresponding detection limit was calculated as 0.030 nM.

In another research by Gupta et al. [109], QCM based MIP technique have been implemented for selective detection of atrazine in waste water. UV induced polymerization reaction took

place on the surface of the QCM chip. HEMA-phenol has been selected as the monomer for this work with EGDMA and AIBN acting as the crosslinker and initiator, respectively. The sensor offered the linear range of the concentration from 0.08-1.5 nM and an LOD of 0.028 nM.

Apart from the electrochemical and QCM based MIP sensors, host of other transduction strategies have been implemented over the years for the detection of various important molecules. Among them, surface plasmon resonance (SPR) based MIP sensors have been used widely for the determination of target analytes having low molecular weight. When a p-polarized light passes through a prism, it hits the prism at a particular angle and SPR phenomenon is said to take place. These types of sensors have found important applications in regard to the determination of affinity binding constants and analyzing genotypes. Further, in some of the works, the property of fluorescence of a material has been explored and utilized to generate MIP based sensors. This is due to the fact that the fluorescence exhibiting materials possesses good biocompatibility, excellent photostability and size dependent photoluminescence characteristics [115]. Surface-enhanced Raman scattering (SERS), on the other hand, is a widely used technique, thereby finding its application over a vast area from biological analysis to environmental monitoring, food safety, clinical diagnosis and therapy [116]. Thus, obviously the combination of SERS and MIP methodology can result into sensors for diverse fields of applications. Another interesting method of transduction is reflectometric interference spectroscopy (RIfS), an optical detection method based on the interference caused by white light on thin layers. The change in optical thickness controls the interaction of the molecules with the sensitive layer. RIfS is considered advantageous over SPR method as it is relatively cheaper, independent of temperature and permits the use of glass or polymer transducers instead of metal. Some of the MIP sensors on the basis of these transduction techniques are summarized in Table 1.8.

Table 1.8 Literature survey indicating the development of MIP method using other transduction strategies

Sl. No.	Transduction technique	Target analyte	Components of MIP	Polymerization method	References
1	SPR	Sudan dyes	a) Monomer: MAA b) Crosslinker: EGDMA c) Initiator: AIBN	Thermal polymerization and photo polymerization	[117]
		Citrinin	a) Monomer: MAGA b) Crosslinker: EGDMA, HEMA	UV irradiated polymerization for 1h	[118]

Sl. No.	Transduction technique	Target analyte	Components of MIP	Polymerization method	References
			c) Initiator: AIBN		
2	Fluorescence	Trinitrotoluene	Monomer: Amino-CDs	Bulk polymerization	[119]
		Dibutyl phthalate	a) Monomer: Acrylamide b) Crosslinker: EGDMA	Precipitation polymerization on the surface of SiO_2@QD	[120]
3	SERS	Pyrethroids	a) Monomer: Acrylamide b) Crosslinker: EGDMA c) Initiator: AIBN	Precipitation polymerization using Ag particles as SERS substrate	[121]
		Bisphenol A	a) Monomer: TEOS b) Crosslinker: APTES	Bulk polymerization on SiO_2@Ag NPs	[122]
4	Optical RIfS	Penicilin G	a) Monomer: NAEMA b) Crosslinker: EBA	Inverse miniEP	[123]

1.5. Objectives and scope

The lower selectivity and non specificity of the E-tongue sensors have paved the way for the demand of an alternative technique in order to detect the major taste attributing agents of tea. MIP based methodologies, on the other hand, are relatively simple, easy to prepare and the precursors involved here are less costly. Therefore, the present work focuses on the implementation of the MIP technique for the development of specific electrodes for some of the taste contributing analytes of tea viz., theaflavin, catechin and epigallocatechin-3-gallate, respectively. In regard to the development of the sensors, various experimental parameters like, effect of pH, effect of buffer and effect of scan rate have been studied in detail. The typical characteristics of a sensor namely, selectivity, repeatability, reusability and reproducibility have been analyzed thoroughly. Furthermore, the present work also intended to ascertain the performance of the fabricated electrodes for detection of respective analytes in tea samples.

Therefore, the objectives of this thesis work can be summed up as follows:

- Development of MIP electrodes for respective target analytes.
- Characterization of the samples in terms of their dimensions, structural and morphological variations.

- Investigation of the electrocatalytic properties of the electrodes and optimization of the experimental conditions.
- Study of various analytical characteristics of the electrode.
- Evaluation of the performance of the electrode for field trials by subjecting them to tea samples and comparing the results obtained from HPLC.

In view of the aforesaid objectives, the entire work has been organized in terms of the following distinct chapters.

Chapter 1 elucidated the origin of the problem and outlined the objectives of this thesis work. In the first phase, this chapter described the different transduction techniques that are normally used for the purpose of detection. Further, it focused on to the different methodologies used until now for quality estimation of tea along with their advantages and disadvantages. Followed by it, the applications of MIP based detection techniques have been discussed as an approach to mitigate the limitations caused by normal electrochemical detection techniques. Here, an introduction of the MIP technique is given along with its types and advantages followed by a brief literature survey indicating the works done on this principle in the recent years using different transduction principles.

Chapter 2 focuses on the synthesis of the polymer-graphite nanocomposites imprinted with TF for the determination of TF in black tea. Here two types of monomer and crosslinker have been used to fabricate the TF sensors and a comparative analysis has been presented. The electrochemical characteristics of the developed electrode and the experimental parameters for detection of TF are discussed here in detail followed by analysis of black tea samples using PLSR technique.

Chapter 3 is devoted to the development of a MIP based electrode for sensitive detection of catechin (+C) in green tea. Here, in this chapter, the MIP is prepared by using acrylonitrile as the monomer and graphite as the conducting material. The electrochemical properties of the electrode have been detailed in this chapter along with a vivid study of the electron kinetics in the reaction system. Additionally, also in this chapter, the performance of the developed electrode has been assayed by subjecting them to the green tea samples followed by correlation with the HPLC data using PLSR modelling technique.

Chapter 4 proposes a slight modification of the MIP technique and highlights its corresponding implementation for the detection of EGCG in green tea. In this chapter,

different metal oxide/hydroxide nanoparticles, for example, TiO_2, CuO and $Ni(OH)_2$ have been synthesized and homogenously mixed with the MIP sample consisting of acrylonitrile and graphite as the monomer and the conducting material, respectively. On comparison of the CV results, the MIP modified with $Ni(OH)_2$ nanopetals have been found to yield best results. The influence of the $Ni(OH)_2$ nanopetals on the imprinted polymer sample has been also investigated in detail in this chapter towards the selective detection of EGCG. Moreover, the experimental parameters concerning the efficient detection of EGCG and the kinetics of the system are also studied and a prediction model has been developed for quantification of EGCG from green tea samples.

Chapter 5 finally presents an overall summary of the work done and highlights the concluding remarks. The advantages and disadvantages of the proposed system have been discussed here in this chapter followed by some recommendations and possible modifications that can be performed.

1.6. Conclusion

In this chapter, firstly the important chemical constituents that are responsible for the quality of tea are focussed followed by the techniques used by the tea industries in order to discriminate them. E-tongue has been tried and tested by researchers over the past years as a promising alternative to subjective human experts and costly analytical instruments. But as the sensors contained in an E-tongue are made up of noble metals, they lack complete specificity to the different taste contributing agents of tea. The limitations discussed herein introduced the origin of the problem followed by the objectives of the proposed thesis to develop specific functionalized sensors of an E-tongue such that a qualitative and quantitative analysis of tea can be performed. Different transduction mechanisms are also discussed in this chapter and a brief survey on the different sensing techniques used till date to detect the compounds, namely, TF, CAT and EGCG in tea has been focussed along with their merits and demerits. Further, the principle of MIP used for the purpose of fabrication of sensors in this work has been elucidated here in detail thereby briefing the past works pursued by the researchers for the detection of other biomolecules.

References

[1] N. Arya, Indian tea scenario, Int. J. Sci. Res. Pub. 3 (2013) 1-10.

[2] S. Sarkar, A. Chowdhury, P. Mandal, M. Chowdhury, Major tea processing practices in India, Int. J. Bioassays 5 (2016) 5071-5083.

[3] P. K. Mahanta, Colour and flavour characteristics of made tea, In: H. F. Linskens, J. F. Jackson (Eds.), Modern method of plant analysis, Springer-Verlag, Berlin, Germany, 221-295.

[4] N. Bhattacharyya, R. Bandyopadhyay, M. Bhuyan, B. Tudu, D. Ghosh, A. Jana, Electronic nose for black tea classification and correlation of measurements with 'tea taster' marks, IEEE Trans. Instrum. Meas. 57 (2008) 1313–1321.

[5] C. A. Blanco, R. Fuente, I. Caballero, M. L. Rodriguez-Méndez, Beer discrimination using a portable electronic tongue based on screen printed electrodes, J. Food Eng. 157 (2015) 57-62.

[6] Y. Zuo, H. Chen, Y. Deng, Simultaneous determination of catechins, caffeine and gallic acids in green, Oolong, black and pu-erh teas using HPLC with a photodiode array detector, Talanta 57 (2002) 307– 316.

[7] H. Horie, T. Mukai, K. Kohata, Simultaneous determination of qualitatively important components in green tea infusions using capillary electrophoresis, J. Chromatogr. A 758 (1997) 332–335.

[8] E. A. H. Roberts, R. Smith, Phenolic substances of manufactured tea. IX. Spectrophotometric evaluation of tea liquors, J. Sci. Food Agric. 14 (1963) 689–700.

[9] T. Huynh, W. Kutner, Molecularly imprinted polymers as recognition materials for electronic tongues, Biosen. Bioelec. 74 (2015) 856-864.

[10] A. L. Huang, X. Chen, M. A. Hoon, J. Chandrashekar, W. Guo, D. Tränkner, N. J. P. Ryba, C. S. Zuker, The cells and logic for mammalian sour taste detection, Nature 442 (2006) 934-938.

[11] Y. Zhang, M. A. Hoon, J. Chandrashekar, K. L. Mueller, B. Cook, D. Wu, C. S. Zuker, N. J. P. Ryba, Coding of sweet, bitter and umami tastes different receptor cells sharing similar signalling pathways, Cell 112 (2003) 293-301.

[12] G. Nelson, M. A. Hoon, J. Chandrashekar, Y. Zhang, N. J. P. Ryba, C. S. Zuker, Mammalian sweet taste receptor, Cell 106 (2001) 381-390.

[13] N. Chaudhuri, H. Yang, C. Lamp, E. Delay, C. Cartford, T. Than, S. Roper, The taste of monosodium glutamate: membrane receptor in taste buds, J. Neurosci. 16 (1996) 3817-3826.

[14] M. Palit, B. Tudu, P. K. Dutta, A. Dutta, A. Jana, J. K. Roy, N. Bhattacharyya, R. Bandyopadhyay, A. Chatterjee, Classification of black tea taste and correlation with tea taster's mark using voltammetric electronic tongue, IEEE Trans. Instrum. Meas. 59 (2010) 2230-2239.

[15] A. F. Collings, F. Caruso, Biosensors: recent advances, Rep. Prog. Phys. 60 (1997) 1397-1445.

[16] M. Pohanka, Overview of piezoelectric biosensors, immunosensors and DNA sensors and their applications, Materials (Basel) 11 (2018) 1-13.

[17] B. J. Privett, J. H. Shin, M. H. Schoenfisch, Electrochemical sensors, Anal. Chem. 80 (2008) 4499-4517.

[18] F. Scholz, Voltammetric techniques of analysis: the essentials, ChemTexts 1 (2015) 1-24.

[19] Autolab application note EC08, Basic overview of the working principle of a potentiostat/galvanostat (PGSTAT)-Electrochemical cell setup, (2011) 1-3.

[20] Y. Xie, Y. Ju, Y. Toku, Y. Morita, Fabrication of Fe_2O_3 nanowire arrays based on oxidation-assisted stress-induced atomic-diffusion and their photovoltaic properties for solar water splitting, RSC Adv. 7 (2017) 30548-30553.

[21] https://www.zimmerpeacocktech.com/knowledge-base/faq/cyclic-voltammetry/

[22] H. H. Willard, Jr. L. L. Merrit, J. A. Dean, Jr. F. A. Settle, Instrumental Methods of Analysis, 6th Edn. D. Van Nostrand, Princeton, 1981.

[23] https://www.basinc.com/manuals/EC_epsilon/Techniques/Pulse/pulse

[24] A. Ghosh, P. Tamuly, N. Bhattacharyya, B. Tudu, N. Gogoi, R. Bandyopadhyay, Estimation of theaflavin content in black tea using electronic tongue, J. Food Eng. 110 (2012) 71-79.

[25] A. Ghosh, T. N. Chatterjee, D. Sing, B. Tudu, P. Tamuly, N. Bhattacharya, R. Bandyopadhyay, Assessment of theaflavin-digallate in black tea by multi-frequency large amplitude pulse voltammetric electronic tongue in: Proceedings Of International Symposium for Electronic nose (ISOEN 2015), June 28 to July 1st, 2015, Dijon, France.

[26] D. A. El-Hady, Selective and sensitive hydroxypropyl-betacyclodextrin based sensor for simple monitoring of (+)-catechin in some commercial drinks and biological fluids, Anal. Chim. Acta 593 (2007) 178–187.

[27] G. Manasa, R. J. Mascarenhas, A. K. Satpati, O. J. D'Souza, A. Dhason, Facile preparation of poly(methylene blue) modified carbon paste electrode for the detection and quantification of catechin, Mater. Sci. Eng. C 73 (2017) 552–561.

[28] A. T. E. Vilian, R. Madhu, S. Chen, V. Veeramani, M. Sivakumar, Y. S. Huh, Y. Han, Facile synthesis of MnO_2/carbon nanotubes decorated with a nanocomposite of Pt nanoparticles as a new platform for the electrochemical detection of catechin in red wine and green tea samples, J. Mater. Chem. B 3 (2015) 6285-6292.

[29] X. Wang, J. Li, Y. Fan, Fast detection of catechin in tea beverage using a poly-aspartic acid film based sensor, Microchim. Acta 169 (2010) 173-179.

[30] S. Masoum, M. Behpour, F. Azimi, M. H. Motaghedifard, Potentiality of chemometric approaches for the determination of (+)-catechin in green tea leaves at the surface of multiwalled carbon nanotube paste electrode, Sens. Actuators B Chem. 193 (2014) 582-591.

[31] S. K. Moccelini, S. C. Fernandes, T. P. Camargo, Self-assembled monolayer of nickel (II) complex and thiol on gold electrode for the determination of catechin, Talanta 78 (2009) 1063-1068.

[32] J. Wu, H. Wang, L. Fu, Z. Chen, J. Jiang, G. Shen, R. Yu, Detection of catechin based on its electrochemical oxidation, Talanta 65 (2005) 511-517.

[33] I. Novak, M. Šeruga, Š. Komorsky-Lovrić, Electrochemical characterization of epigallocatechin-gallate using square-wave voltammetry, Electroanalysis 21 (2009) 1019-1025.

[34] F. H. Dickey, The preparation of specific adsorbents, Proc. Natl. Acad. Sci. U.S.A. 35 (1949) 227-229.

[35] F. H. Dickey, Specific adsorption, J. Phys. Chem. 59 (1955) 695-707.

[36] L. Pauling, A theory of the structure and process of formation of antibodies, J. Am. Chem. Soc. 62 (1940) 2643-2657.

[37] A. G. Mayes, M. J. Whitcombe, Synthetic strategies for the generation of molecularly imprinted organic polymers, Adv. Drug. Del. Rev. 57 (2005) 1742-1778.

[38] S. Piletsky, S. Piletsky, I. Chianella, MIP-based sensors in Molecularly imprinted sensors: Overview and applications, Elsevier (2012) ISBN No. 978-0-444-56331-6.

[39] D. A. Spivak, Optimization, evaluation and characterization of molecularly imprinted polymers, Adv. Drug Del. Rev. 57 (2005) 1779-1794.

[40] L. Chen, S. Xu, J. Li, Recent advances in molecular imprinting technology: current status, challenges and highlighted applications, Chem. Soc. Rev. 40 (2011) 2922-2942.

[41] P. Wang, X. Sun, X. Su, T. Wang, Advancement on molecularly imprinted polymers in food safety field, Analyst 141 (2016) 3540-3553.

[42] G. Wulff, S. Schauhoff, Enzyme-analog-built-polymers: 27 Racemic-resolution of free sugars with macroporous polymers prepared by molecular imprinting-selectivity dependence on the arrangement of functional group versus requirements, J. Org. Chem. 56 (1991) 395-400.

[43] A. Kugimiya, J. Matsui, T. Takeuchi, K. Yano, H. Muguruma, A. V. Elgersma, I. Karube, Recognition of sialic-acid using molecularly imprinted polymer, Anal. Lett. 28 (1995) 2317-2323.

[44] A. Kugimiya, J. Matsui, H. Abe, M. Abrutani, T. Takeuchi, Synthesis of castasterone selective polymers prepared by molecular imprinting, Anal. Chim. Acta 365 (1998) 75-79.

[45] G. Wulff, J. Vietmeier, Enzyme-analogue built polymers: 26. Enantioselective synthesis of amino acids using polymers possessing chiral cavities obtained by an imprinting procedure with template molecules, Makromol. Chem. 190 (1989) 1727-1735.

[46] N. Sallacan, M. Zayats, T. Bourenko, A. B. Kharitonov, I. Wilner, Imprinting of nucleotide and monosaccharide recognition sites in acrylamide phenylboronic acid-acrylamide copolymer membranes associated with electronic transducers, Anal. Chem. 74 (2002) 702-712.

[47] S. H. Gao, W. Wang, B. H. Wang, Building fluorescent sensors for carbohydrates using template-directed polymerizations, Bioorg. Chem. 29 (2001) 308-320.

[48] S. A. Piletsky, K. Piletskaya, E. V. Piletskaya, K. Yano, A. Kugimiya, A. V. Elgersma, R. Levi, U. Kahlow, T. Takeuchi, I. Karube, T. I. Panasyuk, A. V. Elskaya, A biomimetic receptor system for sialic acid based on molecular imprinting, Anal. Lett. 29 (1996) 157-170.

[49] W. Wang, S. H. Gao, B. H. Wang, Building fluorescent sensors by template polymerization: the preparation of a fluorescent sensors for D-fructose, Org. Lett. 1 (1999) 1209-1212.

[50] Y. Kanekiyo, M. Sano, R. Iguchi, S. Shinkai, Novel nucleotide-responsive hydrogels designed from copolymers of boronic acid and cationic units and their application as a QCM resonator system to nucleotide sensing, J. Polym. Sci. A. Polym. Chem. 38 (2000) 1302-1310.

[51] A. Bossi, S. A. Piletsky, E. V. Piletska, P. G. Righetti, A.P.F. Turner, Surface-grafted molecularly imprinted polymers for protein recognition, Anal. Chem. 73 (2001) 5281-5286.

[52] G. Wulff, R. Dederichs, R. Grotstollen, C. Jupe, On the chemistry of binding sites: II. Specific binding of substances to polymers by fast and reversible covalent interactions in: T.C.J. Gribnau, J. Visser, R.J.F. Nivard (Eds.), Affinity Chromatography and Related Techniques, Elsevier, Amsterdam, 1982, PP. 207-216.

[53] G. Wulff, Selective binding to polymers via covalent bonds-the construction of chiral cavities as specific receptor sites, Pure Appl. Chem. 54 (1982) 2093-2102.

[54] C. Alexander, C. R. Smith, M. J. Whitecombe, E. N. Vulfson, Imprinted polymers as protecting groups for regioselective modification of polyfunctional substrates, J. Am. Chem. Soc. 121 (1999) 6640-6651.

[55] G. Wulff, W. Best, A. Akelah, Enzyme-analogue built polymers, 17 Investigations on the racemic resolution of amino acids, React. Polym. 2 (1984) 167-174.

[56] K. J. Shea, T. K. Dougherty, Molecular recognition on synthetic amorphous surfaces-the influence of functional group positioning on the effectiveness of molecular recognition, J. Am. Chem. Soc. 108 (1986) 1091-1093.

[57] K. J. Shea, D. Y. Sasaki, On the control of microenvironment shape of functionalized network polymers prepared by template polymerization, J. Am. Chem. Soc. 111 (1989) 3442-3444.

[58] K. J. Shea, D. Y. Sasaki, An analysis of small-molecule binding to functionalized synthetic polymers by C-13 CP/MAS NMR and FT-IR spectroscopy, J. Am. Chem. Soc. 113 (1991) 4109-4120.

[59] G. Wulff, G. Wolf, On the chemistry of binding sites: Part 6. On the suitability of various aldehydes and ketones as binding sites of monoalcohols, Chem. Ber. 119 (1986) 1876-1889.

[60] R. Arshady, K. Mosbach, Synthesis of substrate-selective polymers by host-guest polymerization, Makromol. Chem. 182 (1981) 687-692.

[61] M. Sibrian-Vazquez, D. A. Spivak, Molecular imprinting made easy, J. Am. Chem. Soc. 126 (2004) 7827-7833.

[62] M. J. Whitcombe, M. E. Rodriguez, P. Villar, E. N. Vulfson, A new method for the introduction of recognition site functionality into polymers prepared by molecular imprinting-synthesis and characterization of polymeric receptors for cholesterol, J. Am. Chem. Soc. 117 (1995) 7105-7111.

[63] M. Lübke, M. J. Whitecombe, E. N. Vulfson, A novel approach to the molecular imprinting of polychlorinated aromatic compounds, J. A. Chem. Soc. 120 (1998) 13342-13348.

[64] A. Katz, M. E. Davis, Molecular imprinting of bulk, microporous silica, Nature 403 (2000) 286-289.

[65] A. L. Graham, C. A. Carlson, P. L. Edmiston, Development and characterization of molecularly imprinted sol-gel materials for the selective detection of DDT, Anal. Chem. 74 (2002) 458-467.

[66] C. J. Percival, S. Stanley, A. Braithwaite, M. I. Newton, G. McHale, Molecular imprinted polymer coated QCM for the detection of nadrolone, Analyst 127 (2002) 1024-1026.

[67] M. Petcu, J. Cooney, C. Cook, D. Lauren, P. Schaare, P. Holland, Molecular imprinting of a small substituted phenol of biological importance, Anal. Chim. Acta 435 (2001) 49-55.

[68] J. U. Klein, M. J. Whitecombe, F. Mulholland, E. N. Vulfson, Template-mediated synthesis of apolymeric receptor specific to amino acid sequences, Angew. Chem. Int. Ed. 38 (1999) 2057-2060.

[69] R. Shoji, T. Takeuchi, I. Kubo, Atrazine sensor based on molecularly imprinted polymer-modified gold electrode, Anal. Chem. 75 (2003) 4882-4886.

[70] E. Pardieu, H. Cheap, C. Vedrine, M. Lazerges, Y. Lattach, F. Garnier, S. Remita, C. Pernelle, Molecularly imprinted conducting polymer based electrochemical sensor for detection of atrazine, Anal. Chim. Acta 649 (2009) 236-245.

[71] B. B. Prasad, R. Madhuri, M. P. Tiwari, P. S. Sharma, Imprinting molecular recognition sites on multiwalled carbon nanotubes surface for electrochemical detection of insulin in real samples, Electrochim. Acta 55 (2010) 9146-9156.

[72] T. Alizadeh, M. R. Ganjali, M. Zare, P. Norouzi, Development of a voltammetric sensor based on a molecularly imprinted polymer (MIP) for caffeine measurement, Electrochim. Acta 55 (2010) 1568-1574.

[73] H. Ashkenani, M. A. Taher, Determination of cadmium (II) using carbon paste electrode modified with a Cd-ion imprinted polymer, Microchim. Acta 178 (2012) 53-60.

[74] V. K. Gupta, M. L. Yola, N. Özaltin, N. Atar, Z. Üstündağ, L. Uzun, Molecular imprinted polypyrrole modified glassy carbon electrode for the determination of tobramycin, Electrochim. Acta 112 (2013) 37-43.

[75] B. B. Prasad, A. Prasad, M. P. Tiwari, Multiwalled carbon nanotubes-ceramic electrode modified with susbtrate-selective imprinted polymer for ultra-trace detection of bovine serum albumin, Biosens. Bioelec. 39 (2013) 236-243.

[76] M. B. Gholivand, G. Malekzadeh, M. Torkashvand, Determination of lamotrigine by using molecularly imprinted polymer carbon paste electrode, J. Electroanal. Chem. 692 (2013) 9-16.

[77] K. K. Aswini, A. M. V. Mohan, V. M. Biju, Molecularly imprinted polymer based electrochemical detection of L-cysteine at carbon paste electrode, Mater. Sci. Eng. C 37 (2014) 321-326.

[78] X. Xue, Q. Wei, D. Wu, H. Li, Y. Zhang, R. Feng, B. Du, Determination of methyl parathion by a molecularly imprinted sensor based on nitrogen doped graphene sheets, Electrochim. Acta 116 (2014) 366-371.

[79] H. Da Silva, J. G. Pacheco, J. MCS. Magalhães, S. Viswanathan, C. Delerue-Matos, MIP-graphene modified glassy carbon electrode for the determination of trimethoprim, Biosens. Bioelec. 52 (2014) 56-61.

[80] X. Tan, Q. Hu, J. Wu, X. Li, P. Li, H. Yu, X. Li, F. Lei, Electrochemical sensor based on molecularly imprinted polymer reduced graphene oxide and gold nanoparticles modified electrode for detection of carbofuran, Sens. Actuators B Chem. 220 (2015) 216-221.

[81] J. G. Pacheco, M. Castro, S. Machado, M. F. Barroso, H. P. A. Nouws, C. Delerue-Matos, Molecularly imprinted electrochemical sensor for ochratoxin A detection in food samples, Sens. Actuators B Chem. 215 (2015) 107-112.

[82] H. Da Silva, J. Pacheco, J. Silva, S. Viswanathan, C. Delerue-Matos, Molecularly imprinted sensor for votlammetric detection of norfloxacin, Sens. Actuators B Chem. 219 (2015) 301-307.

[83] B. Liu, B. Xiao, L. Cui, M. Wang, Molecularly imprinted electrochemical sensor for the highly selective and sensitive determination of melamine, Mater. Sci. Eng. C 55 (2015) 457-461.

[84] M. Zhong, Y. Teng, S. Pang, L. Yan, X. Kan, Pyrrole-phenylboronic acid: A novel monomer for dopamine recognition and detection based on imprinted electrochemical sensor, Biosens. Bioelec. 64 (2015) 212-218.

[85] F. Bates, M. Valle, Voltammetric sensor for theophylline using sol-gel immobilized molecularly imprinted polymer particles, Microchim. Acta 182 (2015) 933-942.

[86] B. Wu, L. Hou, T. Zhang, Y. Han, C. Kong, A molecularly imprinted electrochemical sensor based on gold nanoparticle/carbon nanotube hybrid material for sensitive detection of isoniazid, Anal. Methods 7 (2015) 9121-9129.

[87] M. M. Farid, L. Goudini, F. Piri, A. Zamani, F. Saadati, Molecular imprinting method for fabricating novel glucose sensor: Polyvinyl acetate electrode reinforced by MnO_2/CuO loaded on graphene oxide nanoparticles, Food Chem. 194 (2016) 61-67.

[88] X. Guan, X. Li, S. Chai, X. Zhang, Q. Zou, J. Zhang, A sensitive electrochemical sensor based on solution polymerised molecularly imprinted polymers for procaine detection, Electroanalysis 28 (2016) 2007-2015.

[89] S. Shojaei, N. Nasirizadeh, M. Entezam, M. Koosha, M. Azimzadeh, An electrochemical nanosensor based on molecularly imprinted polymer (MIP) for detection of gallic acid in fruit juices, Food Anal. Methods 9 (2016) 2721-2731.

[90] T. Xie, M. Zhang, P. Chen, H. Zhao, X. Yang, L. Yao, H. Zhang, A. Dong, J. Wang, Z. Wang, A facile molecularly imprinted electrochemical sensor based on graphene: application to the selective determination of thiamethoxam in grain, RSC Adv. 7 (2017) 38884-38894.

[91] Y. Liu, L. Zhu, Y. Hu, X. Peng, J. Du, A novel electrochemical sensor based on a molecularly imprinted polymer for the determination of epigallocatehin gallate, Food Chem. 221 (2017) 1128-1134.

[92] W. Liu, Y. Ma, G. Sun, S. Wang, J. Deng, H. Wei, Molecularly imprinted polymers on graphene oxide surface for EIS sensing of testosterone, Biosen. Bioelec. 92 (2017) 305-312.

[93] M. Zhang, H. T. Zhao, T. J. Xie, X. Yang, A. J. Dong, H. Zhang, J. Wang, Molecularly imprinted polymer on graphene surface for selective and sensitive electrochemical sensing imidacloprid, Sens. Actuators B Chem. 252 (2017) 991-1002.

[94] B. B. Prasad, R. Singh, K. Singh, Development of highly electrocatalytic and electroconducting film using Ni nanomer for ultra-trace detection of thiamine, Sens. Actuators B Chem. 246 (2017) 38-45.

[95] J. Zhang, C. Wang, Y. Niu, S. Li, R. Luo, Electrochemical sensor based on molecularly imprinted composite membrane of poly(*o*-aminothiophenol) with gold nanoparticles for sensitive determination of herbicide simazine in environmental samples, Sens. Actuators B Chem. 249 (2017) 747-755.

[96] X. Wei, X. Xu, W. Qi, Y. Wu, L. Wang, Molecularly imprinted polymer/graphene oxide modified glassy carbon electrode for selective detection of sulfanilamide, Pro. Nat. Sci. Mater. Int. 27 (2017) 374-379.

[97] W. Liu, H. Li, S. Yu, J. Zhang, W. Zheng, L. Niu, G. Li, Poly(3,6-diamino-9-ethylcarbazole) based molecularly imprinted polymer sensor for ultra-sensitive and selective detection of 17-β-estradiol in biological fluids, Biosens. Bioelec. 104 (2018) 79-86.

[98] D. Dechtriat, B. Sookcharoenpinyo, P. Pranjogtat, C. Sriprachuabwong, A. Sanguankiat, A. Tuantranont, S. Hannongbua, An electrochemical MIP sensor for selective detection of salbutamol based on a graphene/PEDOT: PSS modified screen printed carbon electrode, RSC Adv. 8 (2018) 206-212.

[99] M. Sajid, M. K. Nazal, M. Mansha, A. Alsharaa, S. M. S. Jillani, C. Basheer, Chemically modified electrodes for electrochemical detection of dopamine in the presence of uric acid and ascorbic acid: A review, Trends Analyt. Chem. 76 (2016) 15-29.

[100] C. J. Percival, S. Stanley, M. Galle, A. Braithwaite, M. I. Newton, G. McHale, W. Hayes, Molecular-imprinted, polymer-coated quartz crystal microbalances for the detection of terpenes, Anal. Chem. 73 (2001) 4225-4228.

[101] Z. Yang, C. Zhang, Designing of MIP-based QCM sensor for the determination of Cu(II) ions in solution, Sens. Actuators B Chem. 142 (2009) 210-215.

[102] S. E. Diltemiz, D. Hür, A. Ersöz, A. Denizli, R. Say, Designing of MIP based QCM sensor having thymine recognition sites based on biomimicking DNA approach, Biosens. Bioelec. 25 (2009) 599-603.

[103] M. Hussain, N. Iqbal, P. A. Lieberzeit, Acidic and basic polymers for molecularly imprinted folic acid sensors-QCM studies with thin films and nanoparticles, Sens. Actuators B Chem. 176 (2013) 1090-1095.

[104] A. Gültekin, G. Karanfil, M. Kuş, S. Sönmezoğlu, R. Say, Preparation of MIP-based QCM nanosensor for detection of caffeic acid, Talanta 119 (2014) 533-537.

[105] L. Kong, M. Pan, G. Fang, X. He, Y. Yang, J. Dai, S. Wang, Molecularly imprinted quartz crystal microbalance sensor based on poly(o-aminothiophenol) membrane and Au nanoparticles for ractopamine determination, Biosens. Bioelec. 51 (2014) 286-292.

[106] A. Gültekin, G. Karanfil, S. Sönmezoğlu, R. Say, Development of a highly sensitive MIP based-QCM nanosensor for selective determination of cholic acid level in body fluids, Mater. Sci. Eng. C 42 (2014) 436-442.

[107] V. K. Gupta, M. L. Yola, N. Atar, A novel molecular imprinted nanosensor based quartz crystal microbalance for determination of kaempferol, Sens. Actuators B Chem. 194 (2014) 79-85.

[108] T. Eren, N. Atar, M. L. Yola, H. Karimi-Maleh, A sensitive molecularly imprinted polymer based quartz crystal microbalance nanosensor for selective determination of lovastatin in red yeast rice, Food Chem. 185 (2015) 430-436.

[109] V. K. Gupta, M. L. Yola, T. Eren, N. Atar, Selective QCM sensor based on atrazine imprinted polymer: Its application to wastewater sample, Sens. Actuators B Chem. 218 (2015) 215-221.

[110] M. Pan, G. Fang, Y. Lu, L. Kong, Y. Yang, S. Wang, Molecularly imprinted biomimetic QCM sensor involving a poly(amidoamine) dendrimer as a functional monomer for the highly selective and sensitive determination of methimazole, Sens. Actuators B Chem. 207 (2015) 588-595.

[111] X. Ma, X. He, W. Li, Y. Zhang, Epitope molecularly imprinted polymer coated quartz crystal microbalance sensor for the determination of human serum albumin, Sens. Actuators B Chem. 246 (2017) 879-886.

[112] Y. Yun, M. Pan, G. Fang, Y. Gu, W. Wen, R. Xue, S. Wang, An electrodeposited molecularly imprinted quartz crystal microbalance sensor sensitized with AuNPs and rGO material for highly selective and sensitive detection of amantadine, RSC Adv. 8 (2018) 6600-6607.

[113] M. Pan, Y. Gu, M. Zhang, J. Wang, Y. Yun, S. Wang, Reproducible molecularly imprinted QCM sensor for accurate, stable, and sensitive detection of enrofloxacin residue in animal-derived foods, Food Anal. Methods 11 (2018) 495-503.

[114] A. G. Ayankojo, J. Reut, R. Boroznjak, A. Öpik, Molecularly imprinted poly(meta-phenylenediamine) based QCM sensor for detecting Amoxicillin, Sens. Actuators B Chem. 258 (2018) 766-774.

[115] J. Y. Kim, O. Voznyy, D. Zhitomirsky, E. H. Sargent, 25th anniversary article: colloidal quantum dot materials and devices: a Quarter-Century of advances, Adv. Mater. 25 (2013) 4986–5010.

[116] P. Wang, L. Wu, Z. Lu, Q. Li, W. Yin, F. Ding, H. Han, Gecko-inspired nanotentacle surface-enhanced Raman spectroscopy substrate for sampling and reliable detection of pesticide residues in fruits and vegetables, Anal.Chem. 89 (2017) 2424–2431.

[117] X. Xu, X. Tian, L. Cai, Z. Xu, H. Lei, H. Wang, Y. Sun, Molecularly imprinted polymer based surface Plasmon resonance sensors for detection of sudan dyes, Anal. Methods 6 (2014) 3751-3757.

[118] N. Atar, T. Eren, M. L. Yola, A molecular imprinted SPR biosensor for sensitive determination of citrinin in red yeast rice, Food Chem. 184 (2015) 7-11.

[119] S. Xu, H. Lu, Mesoporous structured MIPs@CDs fluorescence sensor for highly sensitive detection of TNT, Biosen. Bioelec. 85 (2016) 950-956.

[120] Z. Zhou, T. Li, W. Xu, W. Huang, N. Wang, W. Yang, Synthesis and characterization of fluorescence molecularly imprinted polymers as sensor for highly sensitive detection

of dibutyl phthalate from tap water samples, Sens. Actuators B Chem. 240 (2017) 1114-1122.

[121] H. Li, X. Wang, Z. Wang, J. Jiang, Y. Qiao, M. Wei, Y. Yan, C. Li, A high-performance SERS-imprinted sensor doped with silver particles of different surface morphologies for selective detection of pyrethroids in rivers, New J. Chem. 41 (2017) 14342-14350.

[122] W. Yin, L. Wu, F. Ding, Q. Li, P. Wang, J. Li, Z. Lu, H. Han, Surface-imprinted SiO_2@Ag nanoparticles for the selective detection of BPA using surface enhanced Raman scattering, Sens. Actuators B Chem. 258 (2018) 566-573.

[123] P. Weber, B. R. Riegger, K. Niedergall, G. E. M. Tovar, M. Bach, G. Gauglitz, Nano-MIP based sensor for penicillin G: Sensitive layer and analytical validation, Sens. Actuators B Chem. 267 (2018) 26-33.

Chapter 2

Detection of total theaflavins in black tea using a molecularly imprinted polymer based sensor

This chapter depicts a facile and convenient approach for the synthesis of a molecular imprinted electrode for detecting total theaflavin (TF) in black tea. Here in, the MIP samples have been synthesized by using two different monomers and crosslinkers, respectively. The MIP samples (MIP-TF1 and MIP-TF2) underwent detailed characterization by fourier transform infra-red (FTIR) and field emission scanning electron microscope (FESEM) techniques. It has been observed that there is a substantial effect of the monomer and crosslinker on the analytical characteristics of an electrode. On application of CV and DPV, the MIP-TF1 electrode depicted a detection limit of 14 µM (S/N = 3) and a linear range of 20 to 100 µM. The electrode also showed an excellent selectivity and sensitivity to TF from its structural analogues. On the other hand, the MIP-TF2 electrode yielded a LOD of as low as 50 nM and also found to possess good selectivity, repeatability and reproducibility as well. The proposed electrodes were employed to determine the TF content in black tea samples by correlating with HPLC data and good prediction accuracy has been obtained.

List of sections

Content of this chapter is based on the following publication:

T. Nandy Chatterjee et al., Detection of theaflavins in black tea using a molecular imprinted polyacrylamide-graphite nanocomposite electrode, Sens. Actuators B Chem. 246 (2017) 840-847.

Chapter 2

Detection of total theaflavins in black tea using a molecularly imprinted polymer based technique

2.1. Introduction

The increasing intake of different varieties of tea among mankind urges the development of advanced smart electrode materials for estimation of its quality. Tea leaves, produced from the shoots of the plant *Camelia sinensis*, can be categorized into three major types depending upon different levels of fermentation during the processing from green tea leaves to the end product. They are namely unfermented green tea, partially fermented oolong tea and fully fermented black tea. In the course of fermentation for conversion of green tea to black tea, the monomeric flavon-3-ols of green tea undergo polyphenol oxidase dependent oxidative polymerization leading to the formation of bisflavanols, thearubigins, theaflavins and other oligomers [1]. Theaflavins (TF) are low molecular weight orange-red pigments and includes four derivatives viz. simple theaflavin, theaflavin-3-gallate, theaflavin-3'-gallate and theaflavin-3,3'-digallate. In the tea industries these are referred to as TF-1, TF-2A, TF-2B and TF-3 respectively. The generalized structure of theaflavin is shown in Fig.2.1. It possesses benzotroplone rings with dihydroxy- or trihydroxy substitutions depending on its fractions.

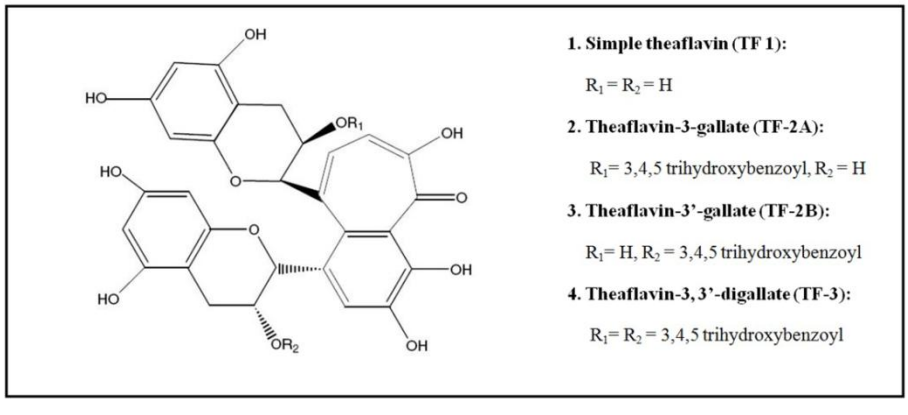

Fig.2.1. Structure of theaflavins showing the variation of hydroxy groups depending upon its fractions.

Total TF weigh upto about 2-6 % of dry black tea and imparts desired level of briskness and astringency on the human palate. The difference in astringency levels in tea liquor caused by TF, contribute to its overall quality [2, 3]. Due to the lower taste threshold of TF than that of thearubigin and other polyphenols, various clones of tea liquor can be distinguished based on

their TF content. TF also accounts for numerous health benefits such as antiallergic, antibacterial, anticarcinogenic, antichlolesterol, antidiabetic, anticardiovascular, antifungal, neuroprotective effects [4-9], etc. due to its antioxidant activity and metal chelating properties [10, 11]. Therefore, the detection and determination of TF plays a very important role not only for organoleptic sensations but also for its biological aspects.

As discussed in Chapter 1, several researches have been pursued in order to quantify the content of TF. These include high performance liquid chromatography (HPLC) [12], high speed counter current chromatography (HSCCC), gel column chromatography (GLC) [13], flavognost method [14], differential pulse polarography (DPP) [15], pulse radiolysis [16] and capillary electrophoresis techniques [17]. These methods are tedious, expensive and require professional experts. Fernando et al., [15] and Roginsky et al., [18] have explored the principle of cyclic voltammetry and linear scan voltammetry by using hanging mercury drop electrode (HMDE) and carbon disk electrode, respectively, for estimating TF and polyphenol contents in different varieties of tea. Also, combinations of various voltammetric and chemometric means have been adopted for evaluating TF content in black tea. These reports demonstrate the use of large amplitude pulse voltammetry (LAPV) and multifrequency large amplitude pulse voltammetry (MLAPV) methods accompanied by different prediction algorithms for assaying the total TF and TF fractions contained in black tea. But as already mentioned, the working electrodes used for these voltammetric measurements constituted an array of noble metals [19-21]. This is a conventional arrangement of electrodes and is used to evaluate the quality of other food stuffs and beverages as well [22, 23].

The research work presented in this chapter is aimed towards implementation of the principle of MIP for detection of total theaflavin content in black tea which consists of a mixture of other compounds with similar chemical characteristics. In this work, detection of total theaflavin is preferred over its individual fractions because the overall quality profiling of tea is best assessed by the total content of theaflavin. The primary components of an MIP are the monomer, crosslinker, template and an initiator. It is interesting to note that the performance of an MIP sensor largely depends upon the selection of the monomer and the crosslinker. One can rationally design a highly sensitive and stable sensor by optimising the suitable combination of the monomer and crosslinker [24]. This in turn may result into a very low limit of detection (LOD) of the target analyte. Towards this direction, here two TF specific electrodes (MIP-TF1 and MIP-TF2) have been synthesized by using two different types of monomer and crosslinker, respectively. Firstly, the monomer acrylamide and crosslinker

divinyl benzene has been opted here as it is non-toxic, less costly and easily available. On the other hand, the second electrode (MIP-TF2) has been developed by using acrylonitrile as the monomer and EGDMA, as the crosslinker, respectively. Graphite is also the most commonly available and inexpensive carbonaceous material with good electrical conductivity and has been chosen as the conducting material for both the cases. Here, an extremely simple and cost effective synthesis route has been employed to develop the electrodes from a composite of graphite and the respective monomers and crosslinkers, for the detection of TF. The electrochemical characterizations of the MIP-TF1 and MIP-TF2 electrodes have been investigated by using CV and DPV, respectively. Analyses of black tea samples were carried out by comparing their total theaflavin content obtained using the proposed electrodes with that from HPLC technique by partial least square (PLS) analysis. A high degree of correlation of analytical data was obtained between the present method and HPLC technique thereby establishing the suitability of the electrodes for industrial applications. Moreover, it may also be witnessed from the results, that the constituents of the MIP framework also have a considerable impact on the analytical characteristics of the electrode.

The protocol adopted for the synthesis of the MIP electrodes and the electrochemical studies followed thereafter, is illustrated in the form of following two flowcharts. The first one (Fig.2.2 (a)) highlights the basic synthesis procedure adopted for MIP-TF1 electrode. It may be mentioned here that the MIP-TF2 electrode and all the other electrodes (MIP-CAT and MIP-EGCG) in the following chapters were prepared following the same methodology; except that there are modifications in terms of the precursors used.

The second flowchart (Fig.2.2 (b)) reveals the electrochemical studies undertaken in order to have an insight to the properties of the synthesized electrodes and their analytical characteristics. The performances of all the electrodes prepared throughout this dissertation were crosschecked by using tea samples and the results were correlated with the HPLC data using PLSR technique.

(a)

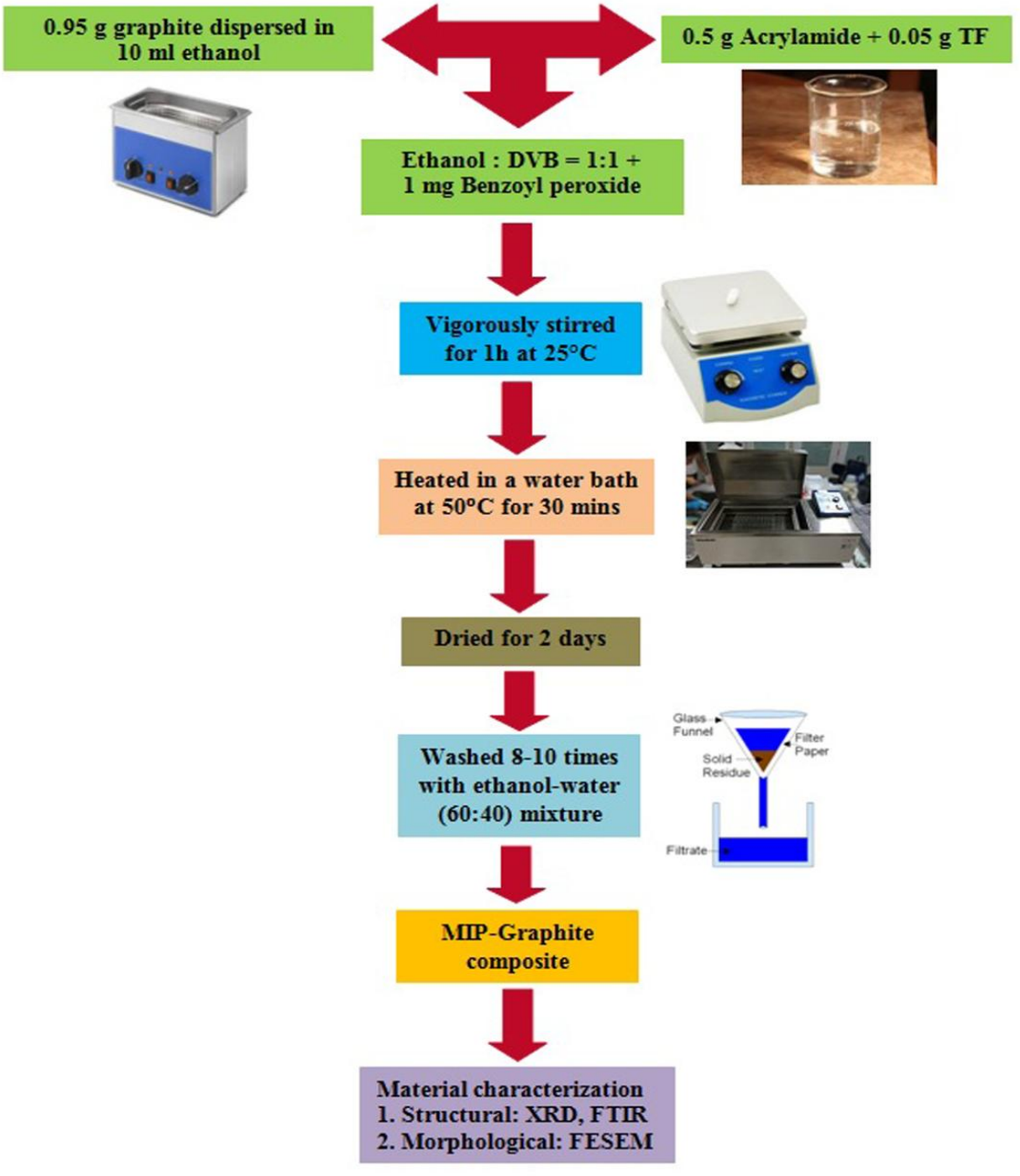
0.95 g graphite dispersed in 10 ml ethanol
0.5 g Acrylamide + 0.05 g TF
Ethanol : DVB = 1:1 + 1 mg Benzoyl peroxide
Vigorously stirred for 1h at 25°C
Heated in a water bath at 50°C for 30 mins
Dried for 2 days
Washed 8-10 times with ethanol-water (60:40) mixture
MIP-Graphite composite
Material characterization
1. Structural: XRD, FTIR
2. Morphological: FESEM
Glass Funnel
Filter Paper
Solid Residue
Filtrate

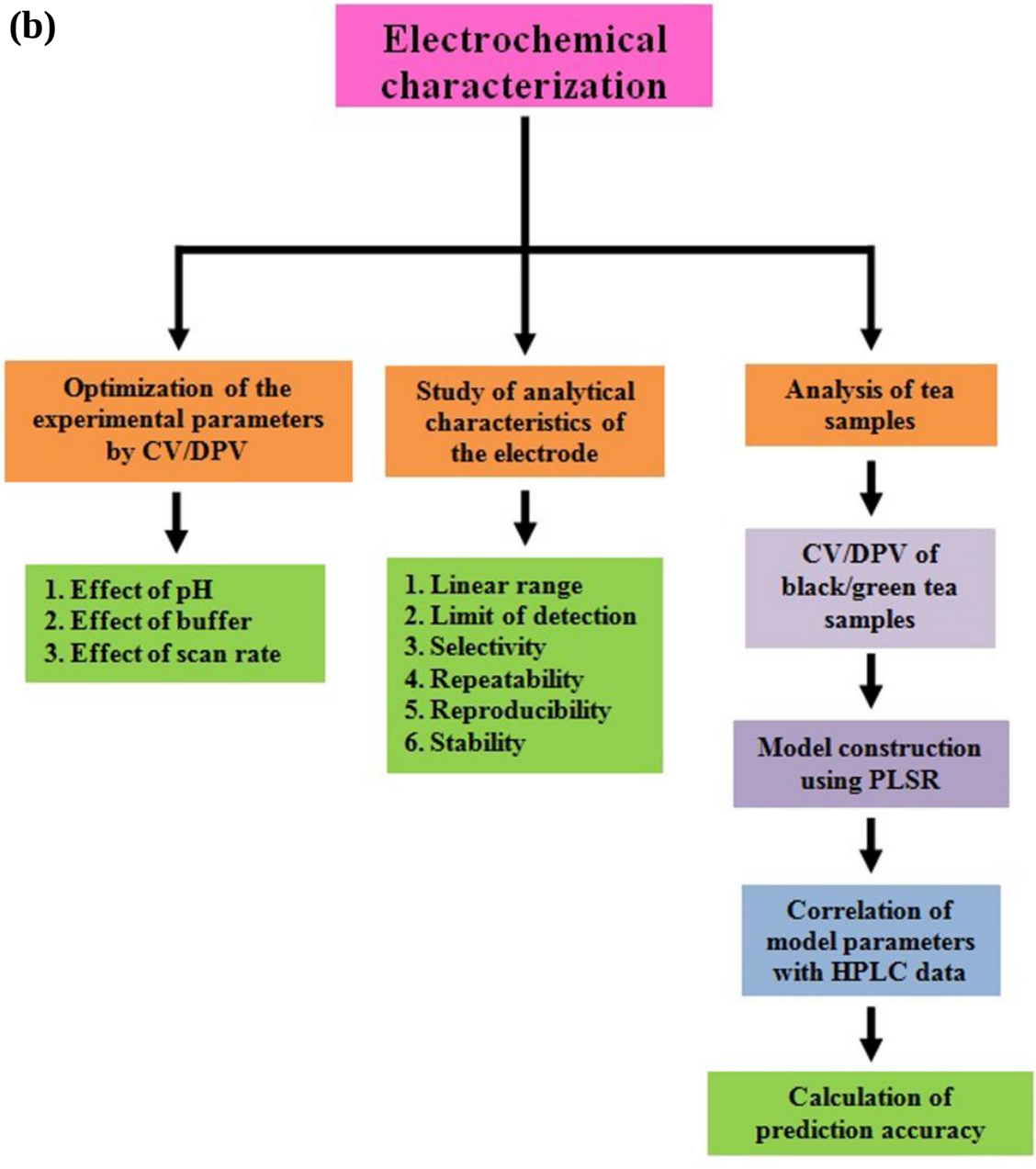

Fig.2.2. Flowchart illustrating the (a) synthesis and material characterization of the MIP samples and (b) electrochemical characterization of the MIP electrode followed throughout the thesis work

2.2. Experimental process

2.2.1. Chemical reagents

Acrylamide and benzoyl peroxide were obtained from Sisco Research Laboratories Pvt. Ltd. and E-Merck, respectively. Acrylonitrile, ethylene glycol dimethacrylate (EGDMA), caffeine (CAF), epigallocatechingallate (EGCG), catechin hydrate (CAT), theaflavin (TF), di-vinyl benzene and graphite powder (99%) were procured from Sigma Aldrich. Sodium acetate,

glacial acetic acid, sodium dihydrogen phosphate, sodium hydrogen phosphate, paraffin oil and ethanol were purchased from Merck. All the reagents were of analytical grade and used without further purification. The required solutions and the electrodes were prepared using Millipore water (Resistance=18 MΩ).

2.2.2. Preparation of the molecular imprinted polymer (MIP)

For the development of MIP-TF1 sample, graphite (0.95 g) was dispersed in 5 ml ethanol for 1 h by ultrasonication. Then 0.05 g of acrylamide and 0.02 g of TF was added to it under constant stirring. In another beaker 10 µl of divinylbenzene and 1 mg of benzoyl peroxide (polymerization initiator) were dispersed in 5 ml ethanol for 30 mins and then added to the acrylamide-TF mixture followed by stirring for 1 h in pure N_2 atmosphere. After that it was heated at 50 ℃ for 2 h. Polymerization took place and the powdered sample was collected. This is the optimized preparative condition for best sensitivity.

For the preparation of the MIP-TF2 sample, 0.95 g of commercial graphite powder was first left to disperse in 15 ml of ethanol for 2 hours. After that, 0.05 g of acrylonitrile and 0.05 g of TF were added to it followed by constant stirring. Further, 1 mg of benzoyl peroxide and 400 µl of EGDMA were added to mixture and it was stirred constantly for 2 hours in pure N_2 atmosphere. The polymerization process was performed by heating the resulting solution in a water bath at 40 °C for 1 h. The final product, so obtained, was then collected and dried.

The MIP was prepared by washing the precipitate repeatedly with 100 ml water and ethanol till no detectable concentration of TF in filtrate as evidenced in its spectral scan in the 400-700 nm range using a UV Vis spectrometer. Finally the filtrate was dried in vacuum desiccators and used for further measurements. The non imprinted polymer (NIP) for both the electrodes were prepared using the same protocols respectively; except that TF was not added during its synthesis.

2.2.3. Preparation of the electrodes

0.25 mg of MIP and NIP samples respectively was added with paraffin oil to make a fine paste. Then the paste was put into a glass tube of inner diameter 2.5 mm and packed tightly into the tube by pressing with a metal rod. Electrical contacts were made by connecting a Pt-wire from the backside of the tube. The entire process is depicted in Fig.2.3. The surface of all the electrodes were smoothed and rinsed carefully with Millipore water prior to each measurement.

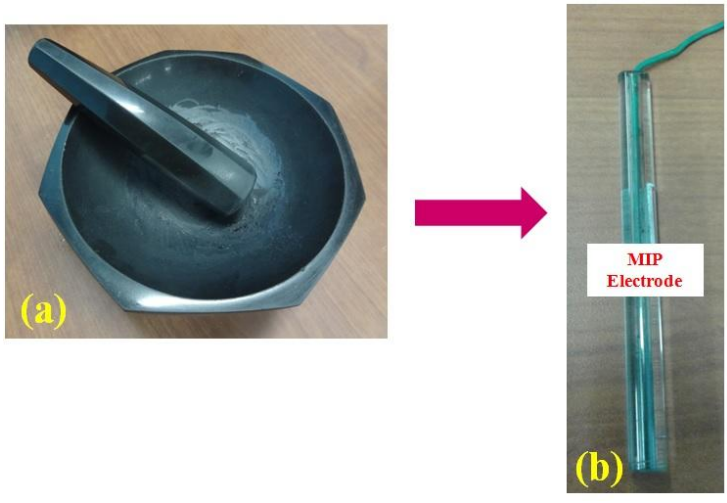

Fig.2.3. Preparation of the electrodes showing the (a) grinding of the sample with paraffin oil using mortar and pestle; (b) the final working electrode formed as a result

The electrodes were dipped in the target solution with one end of them being connected to the potentiostat. The response of the potentiostat was fed into a personal computer (PC) by means of an USB interface from where the voltammetric data points were recorded. The complete arrangement of the measurement setup adopted in our laboratory is depicted in Fig.2.4.

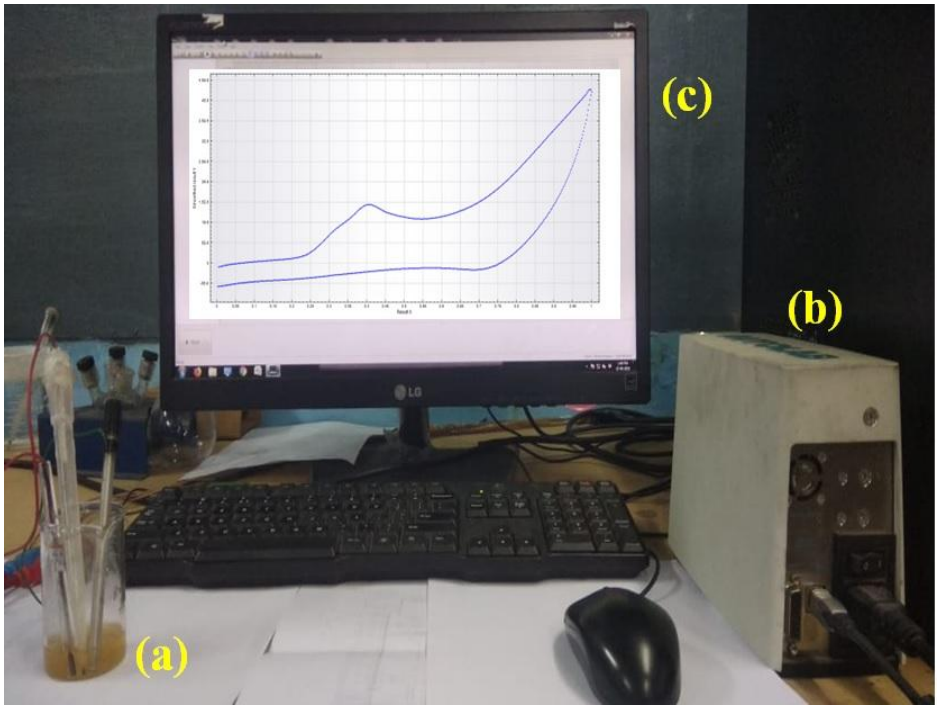

Fig.2.4. Complete measurement setup adopted in our laboratory showing the (a) three electrode system; (b) Autolab potentiostat and (c) corresponding voltammogram from PC

2.2.4. Preparation of the buffer solutions

The electrochemical experiments were carried out using acetate buffer, phosphate buffer, citrate buffer and phthalate buffer as supporting solutions, respectively. It is known that a buffer solution doesnot changes its pH on addition of a small amount of acid or base or the dilution with pure solvent. The pH of a buffer solution is calculated by means of Henderson-Hasselbalch equation [25] shown in equation (2.1) and (2.2).

$$pH = pK_a + \log\left(\frac{[Salt]}{[Acid]}\right) \quad (2.1)$$

$$pOH = pK_b + \log\left(\frac{[Salt]}{[Base]}\right) \quad (2.2)$$

Equation (2.1) has been used for calculating the pH of a solution consisting of a weak acid and its conjugate base (salt). Equation (2.2) on the other hand, can be used in case of the buffer solution containing a mixture of weak base and its salt.

The preparative methods of all of these buffers are discussed in the following section:

i) Preparation of acetate buffer

Acetate buffers of pH values ranging from 4 to 6 was prepared by mixing different volumes of a standard solution of 0.1 M acetic acid and 0.1 M sodium acetate. For the preparation of 0.1 M sodium acetate standard solution, 82.03 g of anhydrous sodium acetate was dissolved in 1000 ml of water. The 0.1 M standard acetic acid solution, on the other hand, was prepared from glacial acetic acid by means of titration followed by dilutions. The amount of reagents required for the preparation of acetate buffer of different pH values are detailed in Table 2.1.

Table 2.1 Preparatory method of acetate buffer of different pH values

Sl. No.	Value of pH	Volume of 0.1 M acetic acid (ml)/l	Volume of 0.1 M sodium acetate (ml)/l
1	4	847	153
2	5	357	643
3	6	52.2	947.8

ii) Preparation of phosphate buffer

The phosphate buffer was prepared by mixing appropriate amounts of 0.1 M sodium dihydrogen phosphate (NaH_2PO_4) and 0.1 M sodium hydrogen phosphate (Na_2HPO_4), respectively in 100 ml double distilled water. The exact quantity of the precursors used for the preparation of phosphate buffer of pH values 5, 6, and 7 are indicated in Table 2.2.

Table 2.2 Preparatory method of phosphate buffer of different pH values

Sl No.	Value of pH	Amount of NaH_2PO_4 (gm)	Amount of Na_2HPO_4 (gm)
1	5	1.3615	0.036
2	6	1.2143	0.3218
3	7	0.5836	1.5466

iii) Preparation of citrate buffer

For the preparation of 1 lit of citrate buffer, 20.1 gm of citric acid was mixed with 8 gm of NaOH. The pH of the solution was adjusted by the addition of dilute HCl till it reached 5.

2.2.5. Preparation of the stock solution of TF

For the preparation of 1mM stock TF solution, 0.0564 gm of TF was first sonicated in 20 ml ethanol till it dissolved fully. Then the remaining volume of the volumetric flask was made up by the addition of water. It was ensured that TF got fully dissolved in the solvents.

2.2.6. Preparation of the black tea liquor for real sample analysis

The performance of the imprinted electrodes was validated using the tea samples, and the results, so obtained, were correlated with that of the HPLC data. For the analysis of TF imprinted electrode, black CTC tea samples were considered. The CTC (crush tear and curl) tea samples were obtained from Tea Research Association, Tocklai, Jorhat, Assam such that the samples under consideration covered the available range of total TF content in black tea. 200 mg of the tea samples were taken in a thermoflask and 30 ml of boiling water was added to it. After infusion for ten minutes, it was filtered through cotton to obtain the liquor. On cooling down to room temperature, 20 ml of the liquor samples were poured into beakers and

five replicated cyclic voltammetric readings were obtained from each of them using the MIP electrode.

2.3. Data analysis using PLSR

In this chapter, partial least square regression (PLSR) technique has been implemented in order to correlate the electrode's response profile with that of the HPLC data of the black tea samples.

PLSR is used to relate two data matrix namely, the predictor matrix **X** and the response matrix **Y**, by means of a linear multivariate model. A traditional multivariate model only relates the response variables with the predictor variables, whereas; the structure of **X** and **Y** can also be modelled by PLSR [26]. PLSR is normally implemented when the datasets of **X** and **Y** consist of noisy, collinear and incomplete variables. The precision of the model parameters depends upon the relevant variables and increases on increasing their number. The central part of the model estimation deals with the calculation of the model parameters as the slopes of bivariate regression of partial components of predictors and the responses in the form of least squares.

The PLSR algorithm is as follows [27]:

a) Given the predictor matrix **X** of *N* observations each of *K* variables and response matrix **Y** of *N* observations each with **M** response elements. Let the number of PLS components be *A*. The index of the response elements can be represented by *m*, such that $m = 1, 2... M$. The corresponding index of PLS components can be represented by a, such that $a = 1, 2... A$.
b) Perform the scaling and centering of **X** and **Y** data.
c) Perform initialization of the processing steps for the first response vector (first column) of **Y**, i.e. y_m with $m = 1$.
d) Perform initialization of the processing steps for the PLS component, i.e., p_1.
e) Obtain the starting vector of $\boldsymbol{u_a}$, such that $\boldsymbol{u_a}$ is one of the columns of Y, i.e. $\boldsymbol{u_a} = \boldsymbol{y_m}$. For univariate **Y**, $\boldsymbol{u_a} = \boldsymbol{y_1}$.
f) Calculate the X-weights $\boldsymbol{w_a}$ such that

$$\boldsymbol{w_a} = \boldsymbol{X}' \boldsymbol{u_a} / \boldsymbol{u_a}' \boldsymbol{u_a}$$

Modify w such that norm of $\boldsymbol{w_a}$ is 1.

g) Calculate X-scores, $\boldsymbol{t_a}$ i.e.,

$$t_a = Xw_a$$

h) Calculate Y-weights, c_a i.e.,

$$c_a = Y' t_a / t_a' t_a'$$

2.4. Results and discussion

2.4.1. Detection principle of TF using MIP electrodes

The proposed detection mechanism of TF using the MIP technique has been illustrated in Fig.2.5. TF molecules have many phenolic groups. Amongst those, three are consecutive in aromatic ring. Thus on addition of TF to acrylamide-divinylbenzene mixture, an *in situ* formation of the functional monomer-template complex takes place and the phenolic groups of TF make hydrogen bonds with the amide group of acrylamide. The mixture is mixed with graphite powder so that the composite formed after polymerization becomes conducting. Polymerization occurs on addition of benzoyl peroxide (polymerization initiator) and binding sites with structural and functional groups similar to TF molecules are created. On washing the composite with water-ethanol mixture repeatedly, theaflavins are leached out. Consequently, the surface of the composite remains decorated with molecular cavities having specific selective sites for adsorption of TF. The imprinted polymer undergoes cyclic voltammetry analysis using the target analyte and, in consequence, TF gets adsorbed. The MIP electrode is again regenerated by subsequent elution of TF using ethanol.

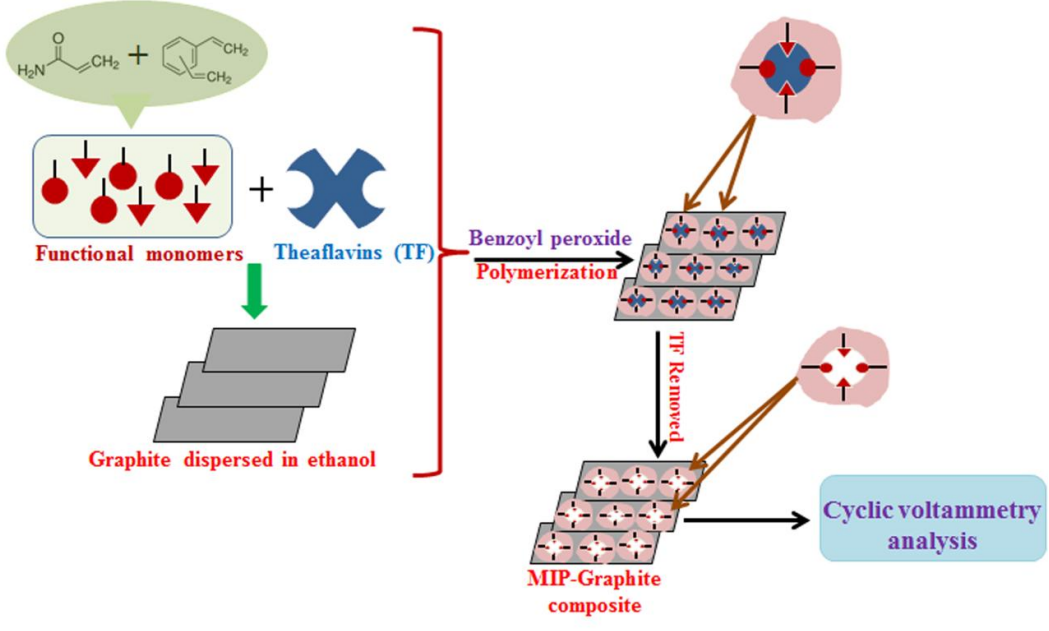

Fig.2.5. Detection principle of TF using MIP technique

Though the present work addresses the detection of total theaflavin using molecular imprinting technique, HPLC analysis of the template molecule has been performed in order to have an insight towards contribution of its fractions. These are detailed in Table 2.3. However, their influences on the analytical performance of the electrode have not been explored in this work.

Table 2.3 Composition of different fractions of theaflavin present in the imprinted template

Sl No.	Fractions of theaflavin	Percentage of composition (%)
1	Simple theaflavin (TF-1)	14.28
2	Theaflavin-3-gallate (TF-2A)	27.39
3	Theaflavin-3'-gallate (TF-2B)	22.69
4	Theaflavin-3-3'-digallate (TF-3)	35.64

On the other hand, in case of MIP-TF2 electrode, though the mechanism of detection is similar as that of MIP-TF1, the most probable reason behind such lower LOD value is due to the presence of polar nitrile groups in acrylonitrile that can effectively bond with the –OH entity of TF. Moreover, the crosslinker EGDMA is responsible for providing mechanical stability to the MIP.

2.4.2. FTIR analysis

Fourier transform infra-red (FTIR) spectroscopy was performed for studying the vibration spectra of the MIP-TF1 sample before and after template removal. The spectra are shown in Fig.2.6 (a) and 2.6 (b), respectively. It is seen from the figures that the peak present at 1633 cm^{-1} in Fig.2.6 (a) due to TF [28] has weakened and is slightly shifted to 1636 cm^{-1} in Fig.2.6 (b). This change in nature of the peaks indicates that TF have been successfully leached out from the polymerized sample. Also, Fig.2.6 (a) and 2.6 (b) depicts the successful polymerization of acrylamide. From the figures, absorption peak in the region of 3430-3450cm^{-1} is due to the $–NH_2$ stretching vibrations of polyacrylamide signifying monomer to polymer transformation. The bands at 2914 cm^{-1} and 2850 cm^{-1} are due to C-H stretching modes of saturated hydrocarbons with secondary and tertiary bonded carbon atoms as $–CH_2$ and CH groups, respectively. The polymerization process can be also witnessed from the bands at 2371 cm^{-1}, 2338 cm^{-1} and 1474 cm^{-1} respectively. These occur due to the –C=N stretching vibrations and $–CH_2$ bonds, respectively [29, 30]. By comparison of Fig.2.6 (a) and

(b), it is observed that all the bands are slightly shifted on removal of TF. This is due to the formation of binding cavities in the imprinted material.

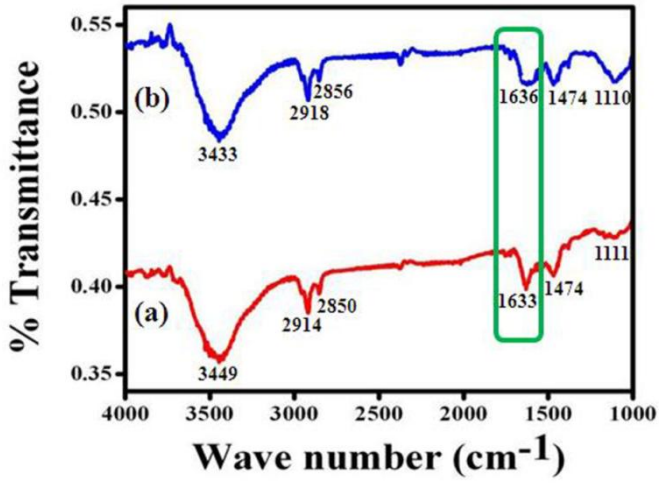

Fig.2.6. FTIR spectra of the MIP sample (a) before and (b) after removal of TF

2.4.3. FESEM analysis

The morphology of the prepared MIP and NIP samples were investigated using field emission scanning electron microscope (FESEM) and the typical images are shown in Fig.2.7 (a) and Fig.2.7 (b), respectively. The structure of NIP is relatively smooth with lesser cavities as compared to that of MIP.

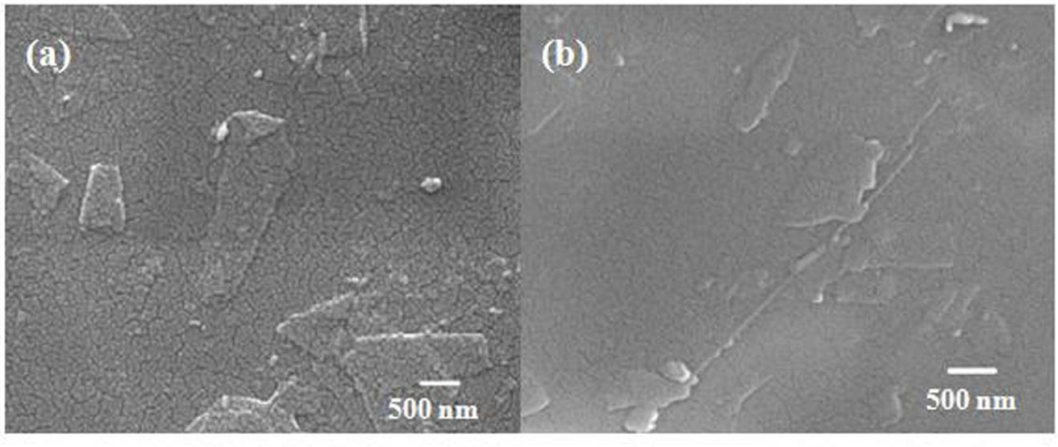

Fig.2.7. FESEM images of (a) MIP and (b) NIP sample

This increase in surface roughness and wrinkled structure of MIP can be attributed to the increased surface area due to accommodation of TF. It mainly occurs due to the presence of binding cavities in the imprinted polymer upon removal of the template molecule. The phenomenon is consistent with the earlier reports on MIP technique [31-33].

2.4.4. Effect of pH and buffer

The responses of the electrodes are extensively affected by the pH of the test solution. Fig.2.8 shows the cyclic voltammogram of the MIP-TF1 electrode on acetate buffer solution of pH values 4, 5, and 6, each containing 1 mM TF. From the figure, it is observed that the peak current intensity increases with the increase of pH from 4 to 5 but decreases when the pH is increased to 6. The highest value of peak current (about 12 µA) was observed for pH 5. TF is very stable within the pH range 4.5-5.5 [34]. The phenolic group of TF gets dissociated thereby losing the hydrogen bonding on increasing the pH. With the rise of pH, simultaneous rise of phenolic anions will increase the solubility of TF in liquid thus prohibiting its adsorption on the surface of solid. Monoanionic TF is very susceptible to oxidation reaction and thus the peak current decreases when the pH is increased to 6. Therefore the highest value of peak current observed for pH 5 corresponds to the small anionic behaviour which is desirable for better redox property. Again, since the application of this imprinted electrode is focussed on the determination of TF in black tea (pH 5), this value of pH is maintained throughout all the experiments.

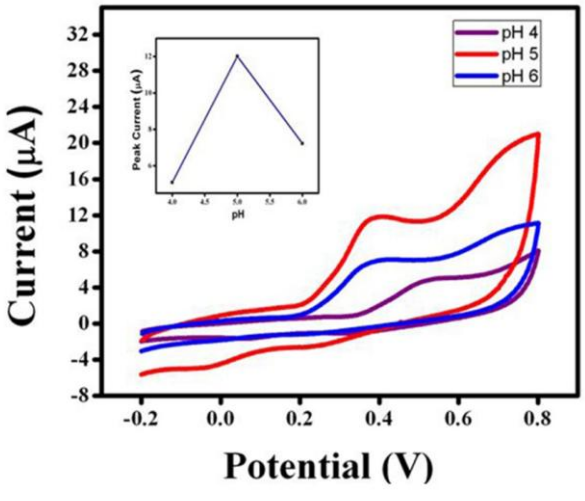

Fig.2.8. CVs obtained for 1 mM TF in acetate buffer of pH values 4, 5 and 6 using MIP-TF1 electrode (inset shows the variation of peak current with pH).

The MIP-TF1 electrode was subjected to acetate buffer, phosphate buffer and citrate buffer solutions, respectively, having pH = 5. The resultant voltammogram is shown in Fig.2.9 (a). It is depicted from the figure that the peak current of the MIP electrode is highest for citrate buffer containing 0.1 mM TF compared to that with the other two buffers under same conditions. The citrate buffer is more effective possibly due to strong association of citrate ion with TF because of its tribasic property which is required during the proton transfer process of the electrochemical reaction.

Fig.2.9 (b) and 2.9 (c) represents the response of MIP-TF1 and NIP electrode in citrate buffer solution with and without the addition of 0.1 mM TF. The electrodes were dipped in the analyte solution for 5 minutes and after that the voltammogram was recorded. As it can be seen from the figures, both the electrodes respond more or less similarly in pure buffer solution whereas, on addition of TF, the peak current of the MIP electrode is higher than that of the NIP electrode. The NIP electrode also shows two distinct reaction steps like MIP electrode, but with inefficient electron transfer due to weak adsorption on the surface of the electrode. The first step (at 0.33 V) appears as a small peak and the second step (at 0.66 V) as a very minor hump. Both the reactions are highly facilitated on the imprinted electrode for which the two steps appears as prominent peaks for oxidation (at 0.16 V and 0.38 V) and reduction (at 0.1 V and 0.31 V), respectively.

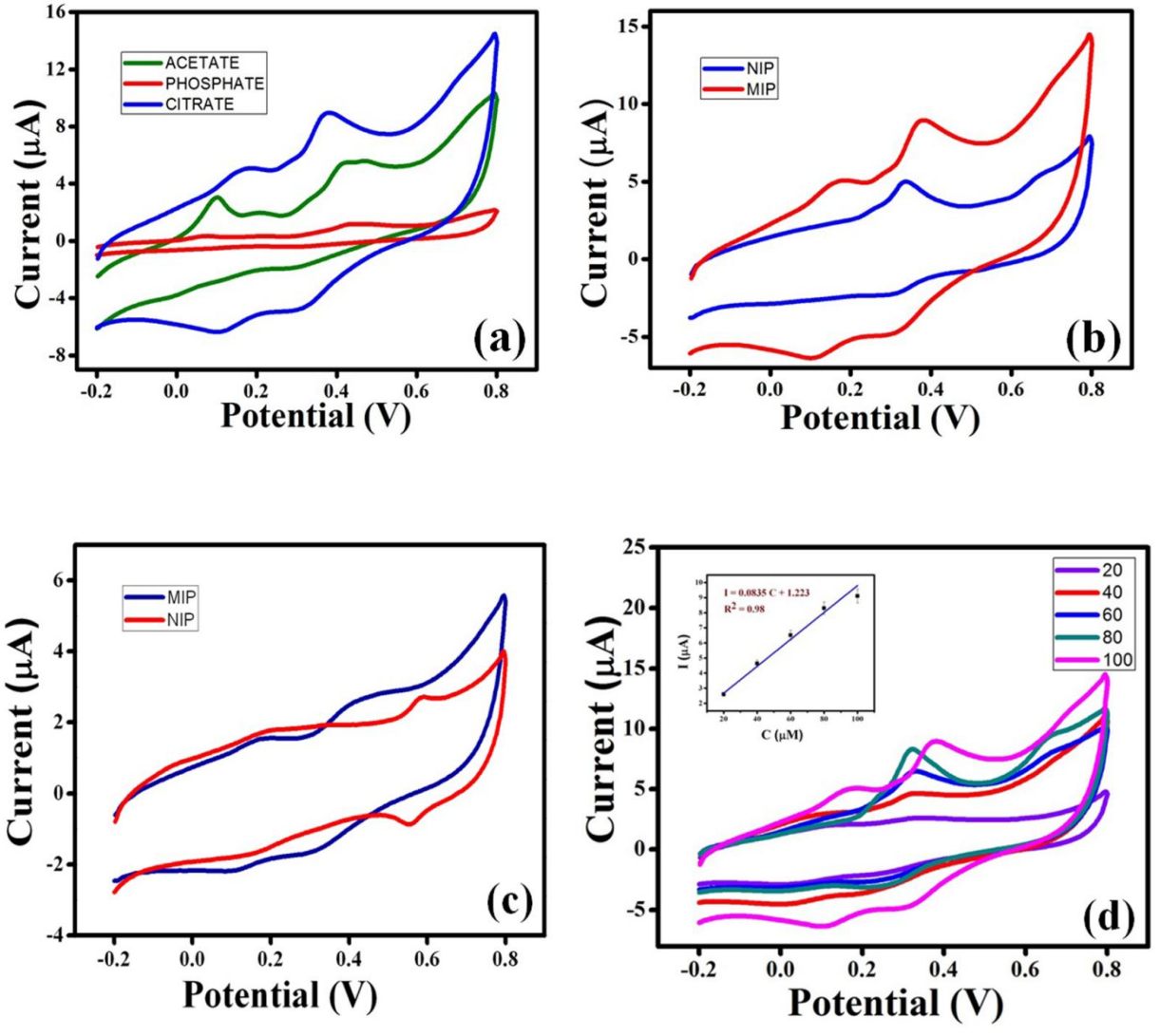

Fig.2.9. (a) CVs obtained using MIP-TF1 electrode for 1 mM TF in acetate, phosphate and citrate buffers; (b) CVs obtained in citrate buffer using MIP and NIP electrode with 1 mM TF; (c) CVs obtained in citrate buffer using MIP and NIP electrode without TF; (d) CVs of blank buffer and 20 µM, 40 µM, 60 µM, 80 µM, 100 µM TF in citrate buffer using MIP electrode (inset shows the variation of peak current with concentration); Scan rate: 0.05 V/s, pH of all buffers: 5

The electrodes were regenerated by washing them in water-ethanol solution for 5 minutes after each experiment. They were further smoothed and subjected to pure buffer solution in order to ensure that no traces of TF remain adsorbed on their surface.

The dependence of the peak current upon different concentrations of TF using both the MIP-TF1 electrode has been studied by means of CV. The experimental results shown in Fig.2.9 (d) delineate that in case of MIP-TF1, the peak current (I) is directly proportional to the

concentration (C) of TF and increases linearly as the concentration is increased from 20 µM to 100 µM. The corresponding regression equation, as obtained from the plot shown in inset of Fig.2.9 (d) is I (µA) = 0.0835C + 1.223 with R^2 = 0.98. The limit of detection (LOD) of TF molecules, based on 3*Sy*/*x*/m (where *Sy*/*x* and m are residual standard deviation of a regression line and the slope of the calibration curve, respectively) [35-37] was calculated as 14 µM.

The cyclic voltammogram obtained using the MIP-TF2 electrode in pure citrate buffer and that in 1 mM TF is depicted in Fig.2.10 (a). It may be observed from the figure that the MIP electrode gives negligible response in pure buffer whereas; the peak current rises to 3.97 µA on subjecting the electrode to 1 mM TF. In a similar manner, on comparison of the performance of the MIP-TF2 and the NIP electrode, it can be seen from Fig.2.10 (b), that the NIP electrode showed a lower current value of 2.76 µA than the MIP electrode. This is mainly due to the presence of various low specific sites on the surface of NIP electrode which hinders the rate of oxidation of TF and as a result, the current is lowered. However, the cavities of MIP, which are similar in orientation to the template molecule, promote the electron transfer by entrapping the template and consequently a rise in peak current takes place.

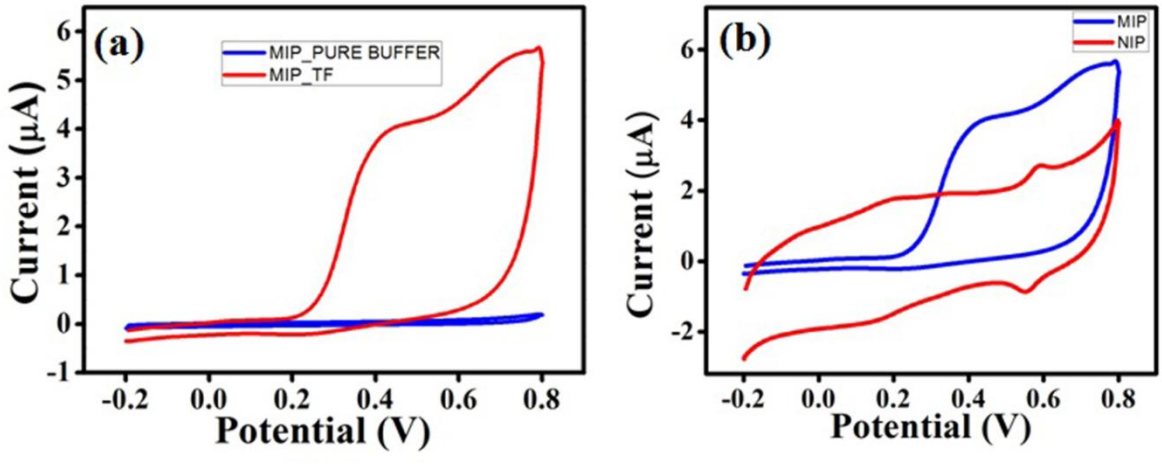

Fig.2.10. CV response curves of (a) the MIP-TF2 electrode in pure buffer and in 1 mM TF; (b) the MIP-TF2 and NIP-TF2 electrodes in 1 mM TF; Buffer: Citrate (pH 5)

On the other hand, DPV has been employed to study the linear characteristics of the MIP-TF2 electrode. Here DPV has been preferred over CV due to its enhanced sensitivity and specificity in quantitative analysis and better signal to background characteristics. Also, DPV yields prominent and well defined peaks at lower levels of concentration as well. The differential pulse voltammogram indicating the dependence of the peak current of the MIP-

TF2 electrode on various concentration of TF has been illustrated in Fig.2.11. From the figure, it can be inferred that a linear relationship exists between the oxidation current (*Ip*) and concentration (*c*) of TF in the range of 8 µM to 50 µM (also shown in Fig.2.11 (b)) having $R^2 = 0.99$. The corresponding regression equation is given in (2.3).

$$Ip = 0.0006c + 0.012 \quad (2.3)$$

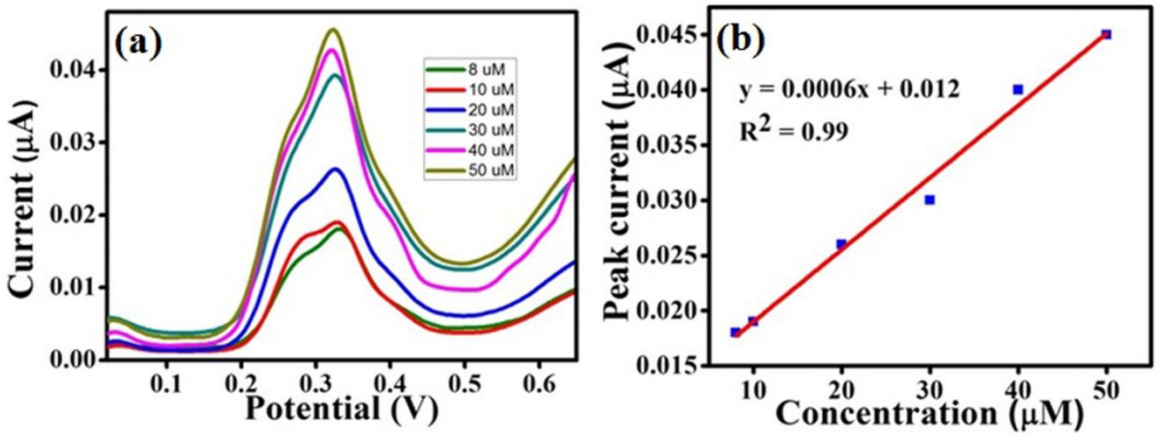

Fig.2.11. (a) DPV of the MIP-TF2 electrode in different concentrations of TF; (b) Linearity plot indicating variation of peak current with different concentrations of TF

It is worth mentioning here, that the TF molecules responded in the concentration value of as low as 50 nM using the proposed electrode. Therefore, the LOD of the MIP-TF2 electrode has been estimated as 50 nM.

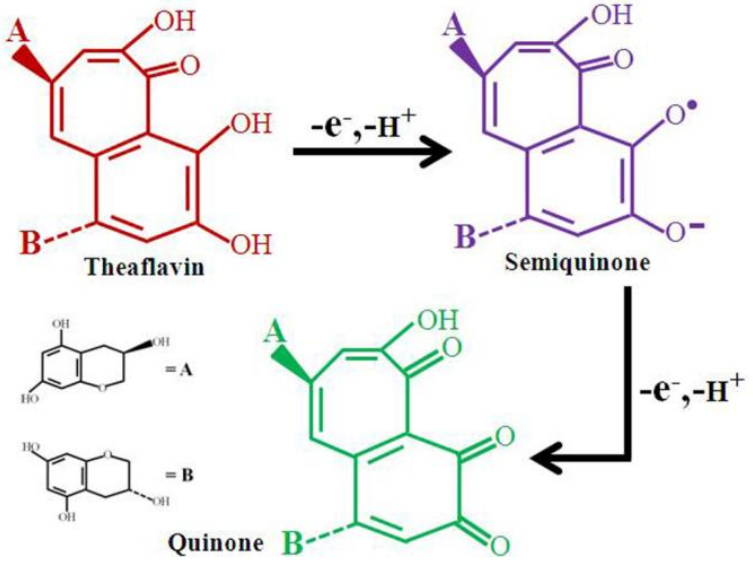

Fig.2.12. Schematic representation of the oxidation of TF

The electrochemical oxidation and reduction of TF as a whole, is a two step process. The corresponding mechanism is illustrated in Fig.2.12. Firstly, TF is converted to semiquinone radical on removal of an electron and a proton. The second step is governed by the subtraction of another electron and a proton leading to the formation of quinone. This type of electrochemical behaviour is revealed by other polyphenols as well [38, 39].

2.4.5. Effect of scan rate

Cyclic voltammetry analysis of 0.1 mM TF using MIP-TF1 electrode on citrate buffer at different scan rates ranging from 0.1 to 0.5 V/s was carried out to determine the electron transfer kinetics of the system. The voltammogram is shown in Fig.2.13 (a). The redox reactions are quasi reversible in nature since the peak current ratios for both the steps are not equal to unity. Moreover, according to the Nernst equation, for a chemically and electrochemically reversible reduction process, the difference between the anodic and cathodic peak potentials known as the peak to peak separation voltage, ΔEp is 57 mV at 25°C and the width at half max on the forward scan of the peak is 59 mV. From the CV response obtained in Fig. 2.13 (a), it may be observed that the average value of ΔEp for both the oxidation and the reduction peaks is greater than 57 mV; thereby indicating that the oxidation and the reduction processes are not reversible in nature.

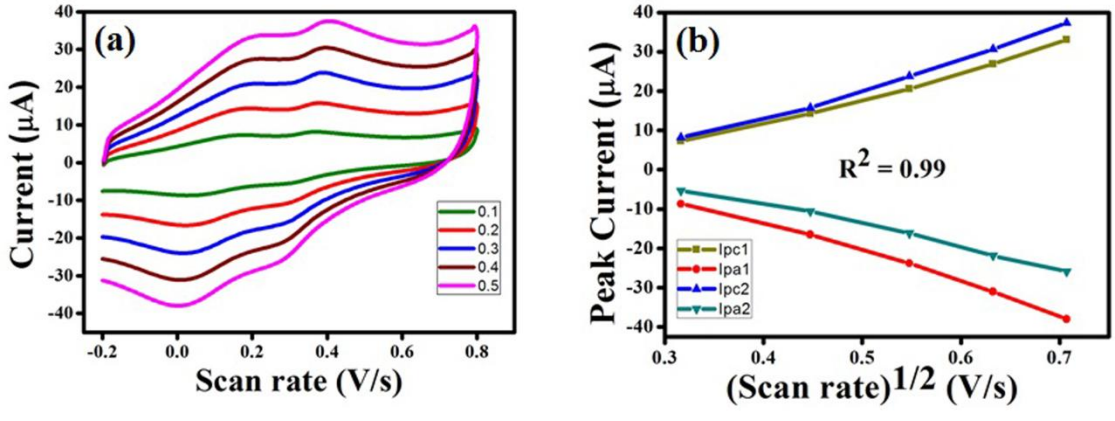

Fig.2.13. (a) CVs of variation of peak current with scan rate (from 0.1 V/s to 0.5 V/s) for MIP-TF1 electrode; (b) Variation of anodic and cathodic peak currents for the first and second redox process with the square root of scan rate; Buffer: Citrate (pH 5).

It is seen that as the scan rate is increased, the cathodic peak potential gradually increases but the anodic peak potential decreases. As a result, the peak potential separation increases along with the increase of scan rate till it reaches 0.4 V/s. After this value, though the peak potential

separation shows a sluggish increase for the first redox process, it drops down in case of the second one. This is due to the slow electron transfer or drop of ohmic potential (IR) [40]. The anodic and the cathodic peak currents (Ipa1, Ipa2 and Ipc1, Ipc2) for both the oxidation and reduction processes respectively, were plotted against square root of the scan rate and the resulting waveform is shown in Fig.2.13 (b). The figure reveals that both the peak currents for the two redox processes increase almost linearly along with the square root of scan rate with $R^2 = 0.99$ thereby indicating that it is a diffusion controlled process [41].

The effects of scan rate have been also investigated in case of the MIP-TF2 electrode. In order to study the reaction kinetics of the system, CV was performed using the electrode in 1 mM TF by varying the scan rate from 0.01 V/s to 0.5 V/s. Fig.2.14 (a) and (b) reveals that the peak current value increased linearly on varying the scan rate (v) from 0.01 V/s to 0.07 V/s thereby indicating it is an adsorption controlled process [42]. Also, from the figures, it can be inferred that the electrochemical reaction is irreversible in nature. The resulting regression equation is shown in (2.4).

$$Ip = 75.20\, v + 0.604 \tag{2.4}$$

The correlation factor as calculated from the calibration curve can be written as $R^2 = 0.99$.

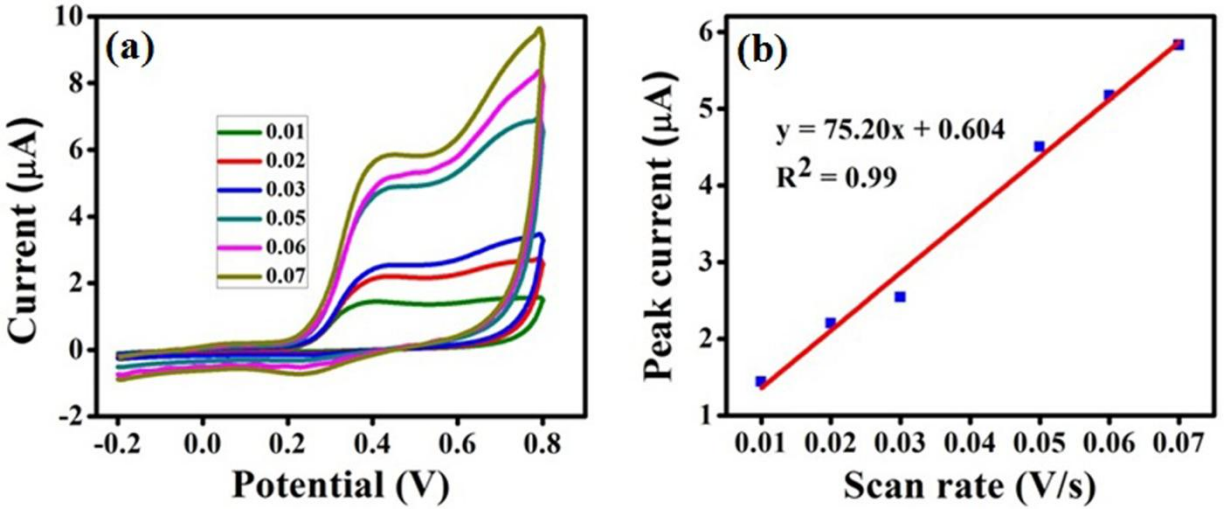

Fig.2.14. (a) CV indicating variation of peak current with different scan rate values using MIP-TF2 electrode; (b) Corresponding linearity plot indicating variation of peak current with scan rate

2.4.6. Selectivity, repeatability and reproducibility of the electrode

To investigate the selectivity of the electrode towards TF, both the electrodes (MIP-TF1 and MIP-TF2) were exposed to similar concentrations of EGCG, CAT and CAF using DPV. The response is presented in the form of a bar plot shown in Fig.2.15.

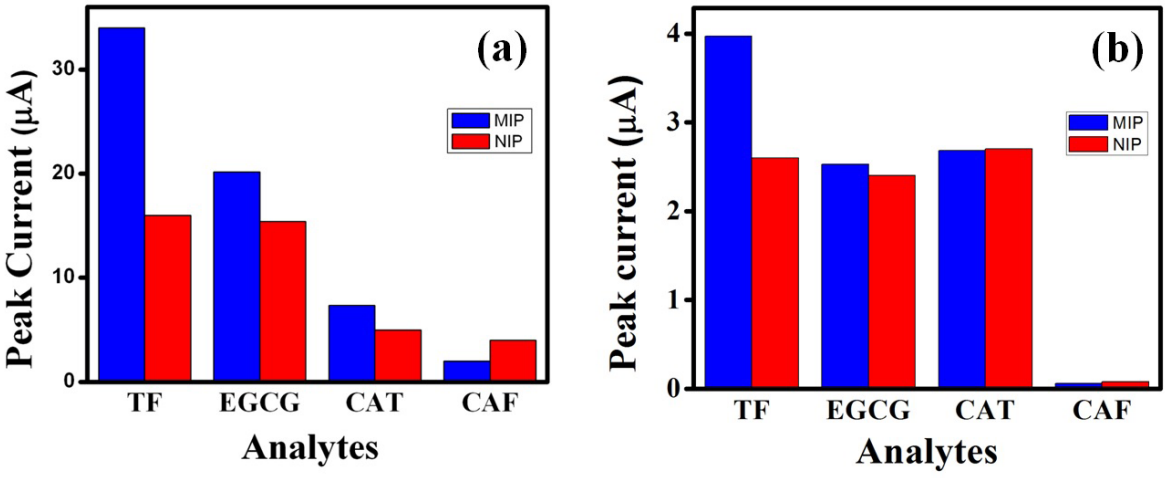

Fig.2.15. Selectivity study of (a) MIP-TF1 and (b) MIP-TF2 electrode in presence of 1 mM TF, 1 mM CAT, 1 mM EGCG and 1 mM CAF; Scan rate: 0.05 V/s, Buffer: Citrate (pH 5)

From the figure, it can be seen that both the MIP-TF1 and MIP-TF2 electrodes show highest affinity for its template molecule, TF. Of the other analytes, though the MIP electrode shows distinct affinity to its structural analogues EGCG and CAT, respectively, the current responses are relatively less.

Moreover, since the proportion of EGCG and CAT is low in black tea [43], these chemicals do not seem to cause interference in the recognition of TF in black tea. The response of the electrode towards CAF is very low and also not prominent.

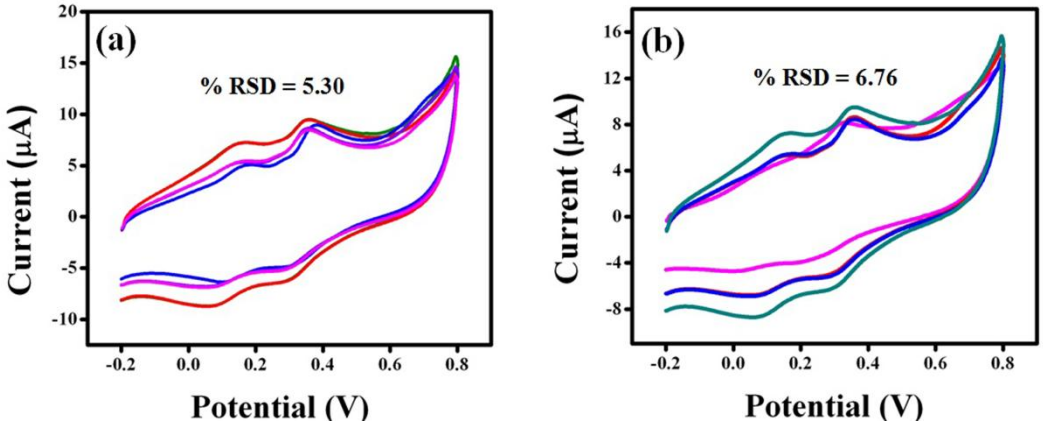

Fig.2.16. (a) CVs obtained for 1 mM TF for five consecutive runs; (b) CVs obtained for 1 mM TF using four MIP-TF1 sensors ; Scan rate: 0.05 V/s, Buffer: Citrate (pH 5).

The repeatability and reproducibility of both the electrodes were studied by cyclic voltammetry. On five repeated applications of the electrode to 0.1 mM of TF under same experimental conditions, it is seen that the signature of the waveform for all the runs are almost identical. Due to repeated exposure of the electrode to TF, the molecule of TF gets adsorbed to the electrode and as a result, the peak current decreases slightly. Nonetheless, the relative standard deviation (RSD) calculated from the repeatability curve is around 5.30% for five measurements using the same MIP-TF1 electrode (shown in Fig.2.16 (a)). The MIP-TF2 electrode was also found repeatable in nature having %RSD as 3.60.

Four electrodes were prepared using the same protocol as described for MIP-TF1 and MIP-TF2 respectively, and cyclic voltammogram were recorded using 0.1 mM TF as analyte in citrate buffer solution. The results show that the electrodes were found to be reproducible having the RSD value of 6.76 % and 6.01 %, respectively. The corresponding CV response curve for MIP-TF1 is depicted in Fig.2.16 (b).

2.4.7. Analysis of black tea samples

In this work, it is intended to measure TF content in black tea (rather than its individual fractions i.e. TF-1, TF-2A, TF-2B or TF-3) and thus the HPLC data were correlated with the total theaflavin content. A typical response curve of a tea sample obtained using the MIP-TF1 and MIP-TF2 electrodes, respectively, is presented in Fig.2.17. Typical oxidation peaks can be visualized from both the figures. Tea is known to be a combination of a large number of polyphenols which includes various fractions of TF as well. Therefore, all the data points obtained from the CV or the DPV were considered for the development of PLS prediction model. The model has been calibrated with the data matrix derived from cyclic voltammetry and the reference estimations of TF from HPLC analysis [44]. The development of the PLS model and the process involved in its training has been depicted in the form of a block diagram in Fig. 2.18. At each fold of LOOCV, the training set was constructed by omitting data set of one of the tea samples and the developed model was tested with the data points from the data set of the omitted tea sample. This procedure is reiterated for all the twelve black tea samples and the number of PLS components were optimized.

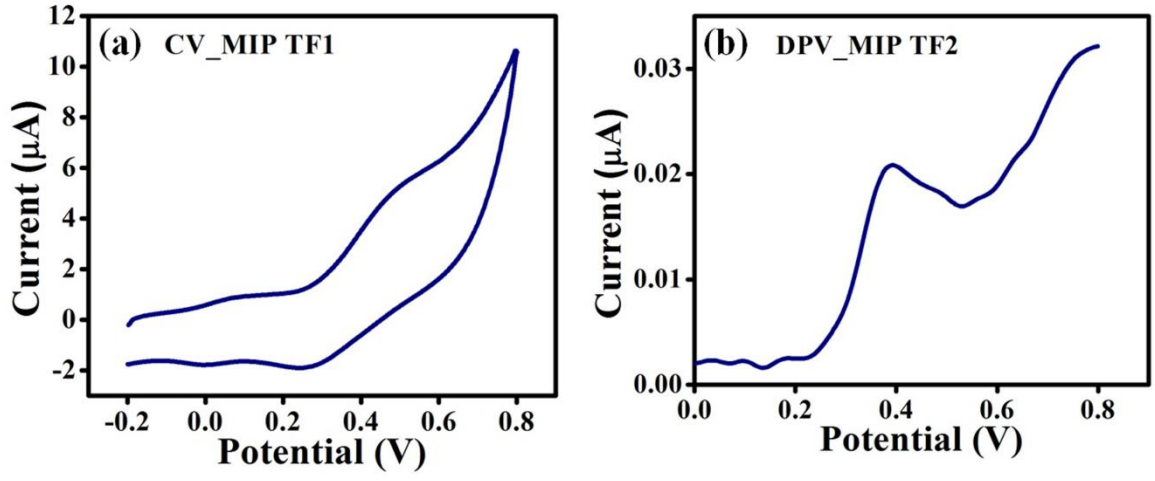

Fig.2.17. Response profile of a black tea sample obtained by means of (a) CV using MIP-TF1 electrode and (b) DPV using MIP-TF2 electrode

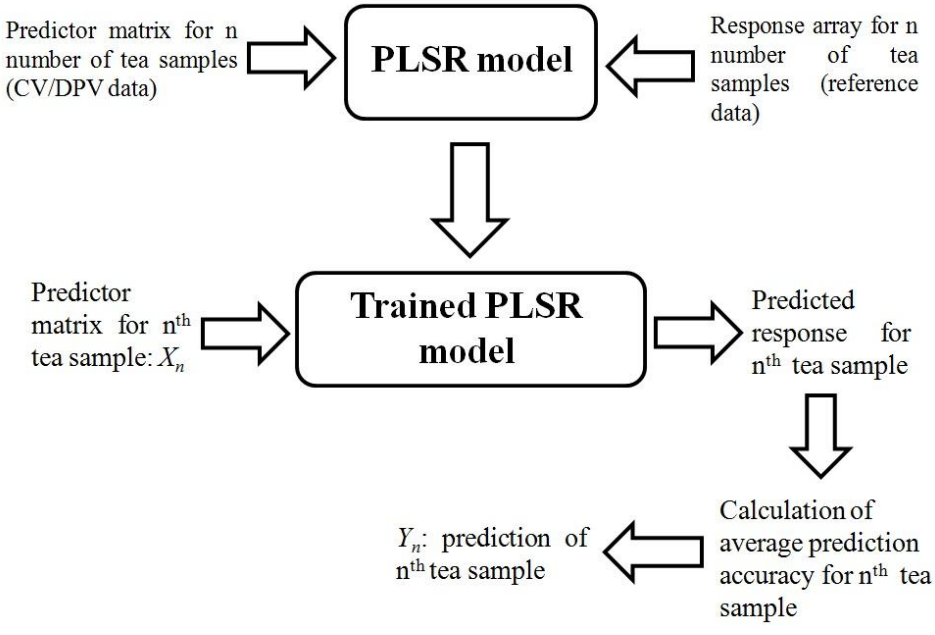

Fig.2.18. Block diagram illustrating the training and testing of PLSR model by means of LOOCV technique

Table 2.4 presents the actual and predicted values of TF along with prediction accuracy using 7 PLS components for MIP-TF1 electrode. Herein, five duplicated readings were obtained from each of the twelve tea samples. Each CV response generated 820 data points for a single run. Therefore the total dataset used for the regression process consisted of 820 x 60 data points. The prediction accuracies of all the samples are greater than 90 % except for two of them which fall between 85 % and 90 %. Four samples have the prediction accuracy of the

order of 99 %, with sample number 7 showing highest accuracy of 99.78 %. Thus the predicted values of TF are found to be in very close agreement with their actual values. An average prediction accuracy of 94 % was obtained for all the tea samples considered.

Similarly, the MIP-TF2 electrode was also subjected to ten different variants of black tea with different amounts of TF in them. The corresponding DPV response profiles were modelled by means of PLS using the principle of LOOCV as explained earlier. In this case, 253 data points were generated by DPV response for a single run and five iterative readings for each of the tea samples were recorded. So the total number of 253 x 50 data points was used for developing the model. Table 2.5 depicts the actual and the predicted values of TF using 6 PLS components. Here, it may be observed that though the prediction accuracy of only one sample is greater than 99 %, but the average prediction accuracy is 94.79 % for all the tea samples. Therefore, MIP-TF2 electrode has been found to predict the TF content in black tea reasonably well.

The results obtained in case of both the electrodes are also presented in the form of a bar plot shown in Fig.2.19.

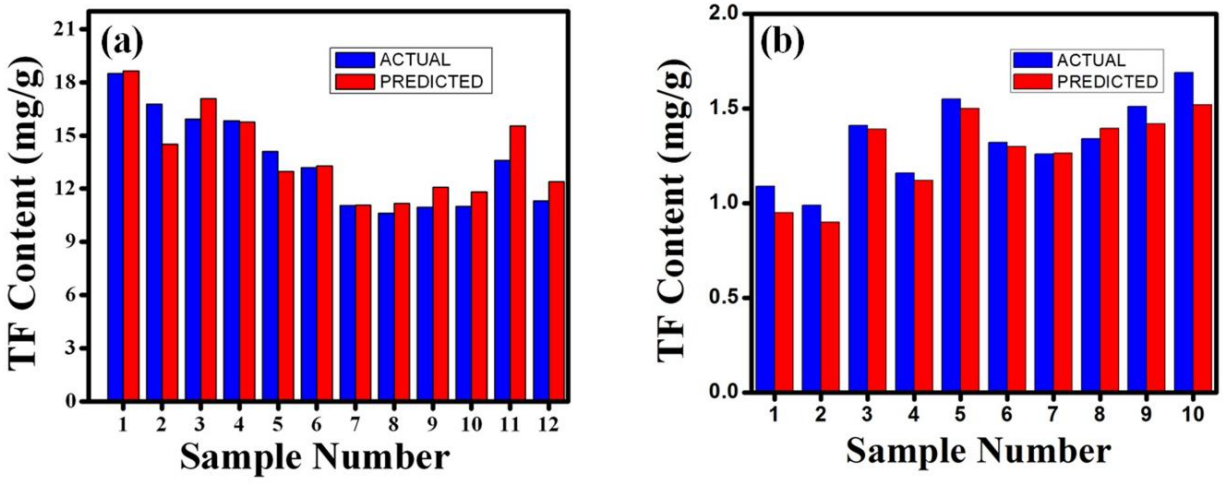

Fig.2.19. Bar plot indicating comparison of actual and predicted concentrations of TF for (a) MIP-TF1 and (b) MIP-TF2 electrode

Table 2.4 Predicted and actual TF concentrations for MIP-TF1 electrode from the LOOCV based PLS model with seven PLS components

Sample No.	Actual TF (mg/g)	Predicted TF (mg/g)	Prediction accuracy (%)
1	18.5	18.644	99.22
2	16.76	14.5	86.57
3	15.93	16.88	94.03
4	15.82	15.76	99.62
5	14.11	12.97	91.93
6	13.19	13.29	99.21
7	11.05	11.07	99.78
8	10.61	11.17	94.66
9	10.95	11.9	91.32
10	11	11.82	92.456
11	13.59	15.45	86.31
12	11.32	12.01	93.9

Table 2.5 Predicted and actual TF concentrations for MIP-TF2 electrode from the LOOCV based PLS model with six PLS components

Sample No.	Actual TF (mg/g)	Predicted TF (mg/g)	Prediction accuracy (%)
1	1.09	0.95	87.16
2	0.99	0.9	90.09
3	1.41	1.39	98.58
4	1.16	1.12	96.55
5	1.55	1.50	96.77
6	1.32	1.3	98.48
7	1.26	1.27	99.60
8	1.34	1.40	95.89
9	1.51	1.42	94.03
10	1.69	1.52	89.94

2.4.8. Comparison of the proposed method with other existing techniques

The proposed method was compared with other existing analytical techniques for the determination of TF. The results are presented in Table 2.6. From the table, it is evident that this is the first approach towards development of an electrode for TF determination. Also, the detection limit of this electrode is very low and is comparable to that of solid phase extraction HPLC technique.

Table 2.6 Comparison of the proposed method with other reported studies

Methodology	LOD (µM)	Linear range (µM)	References
Solid phase extraction, HPLC	20-25 µM	-	[45]
HPLC	0.02 µM	0.88-2.66	[46]
Sephadex LH-20 GLC	-	-	[13]
HSCCC	-	-	[13]
LAPV	-	-	[19]
MLAPV	-	-	[20], [21]
MIP electrode-CV (MIP-TF1)	**14 µM**	**20-100**	**This work**
MIP electrode-DPV (MIP-TF2)	**50 nM**	**8-50**	**This work**

2.5. Conclusion

Detection of theaflavins in black tea is extremely important for the tea producers since these groups of compounds are responsible for the astringent taste of tea and contributes significantly to the complete quality profiling of tea. In this chapter, we have described the development of a low-cost electrode based on molecular imprinted polymer based technique to detect the theaflavins from structurally analogous polyphenols. The objective of this work was also to investigate the effect of monomer and the crosslinker of an MIP on the analytical characteristics of the electrode. Therefore, in this work, two TF sensitive MIP electrodes have been synthesized by using acrylamide and di-vinyl benzene and acrylonitrile and EGDMA, as

the monomer and crosslinker, respectively. The polymer composite is molecularly imprinted with TF. The MIP-TF1 electrode showed a good linear range from 20 to 100 μM having a detection limit of 14 μM. On the other hand, the MIP-TF2 electrode demonstrated a linear range from 8 μM to 50 μM with the corresponding LOD being 50 nM. Both the electrodes (MIP-TF1 and MIP-TF2) also showed good selectivity, repeatability, and reproducibility. Its performance investigated with actual black tea samples was also found to be good when compared with HPLC analysis technique. However, in the present work, the influence of individual fractions of theaflavins have not been considered during the imprinting process of the MIP, as it would make the measurement system more complex with multiple electrodes. This is a first attempt towards the detection of TF using MIP; nevertheless the results presented establish the efficacy of the probe for real time applications in a cost effective manner.

References

[1] M. A. Vermeer, T. P. J. Mulder, H. O. F. Molhuizen, Theaflavins from black tea, especially theaflavin-3-gallate, reduce the incorporation of cholesterol into mixed micelles, J. Agric. Food Chem. 56 (2008) 12031-12036.

[2] V. Preedy, Cancer chemoprevention by black tea polyphenols, in: Tea in health and disease prevention, Academic Press, Elsevier, Oxford, UK, ISBN No. 9780123849373, Pages 1616.

[3] P. O. Owuor, M. Obanda, Clonal variation in the individual theaflavins and their impact on astringency and sensory evaluation, Food Chem. 54 (1995) 273-277.

[4] K. Yoshino, K. Yamazaki, M. Sano, Preventive effects of black tea theaflavins against mouse type IV allergy, J. Sci. Food. Agric. 90 (2010) 1983-1987.

[5] M. Friedman, Overview of antibacterial, antitoxin, antiviral and antifungal activities of tea flavonoids and teas, Mol. Nutr. Food Res. 51 (2007) 116-134.

[6] V. K. Juneja, M. L. Bari, Y. Inatsu, S. Kawamoto, M. Friedman, Thermal destruction of Escherichia coli O157:H7 in sous-vide cooked ground beef as affected by tea leaf and apple skin powders, J. Food Prot. 72 (2009) 860-865.

[7] S. Kaur, P. Greaves, D. N. Cooke, R. Edwards, W. P. Steward, A. J. Gescher, T. H. Marczylo, Breast cancer prevention by green tea catechins and black tea theaflavins in the C3(1) SV40T, t, antigen, transgenic mouse model is accompanied by increased apoptosis and a decrease in oxidative DNA adducts, J. Agric. Food Chem. 55 (2007) 3378-3385.

[8] A. Adhikary, S. Mohanty, L. Lahiry, D. M. S. Hossain, S. Chakraborty, T. Das, Theaflavins retard human breast cancer cell migration by inhibiting NF-*k*B via p53-ROS cross-talk, FEBS Lett. 584 (2010) 7-14.

[9] Y. Hayashino, S. Fukuhara, T. Okamura, T. Tanaka, H. Ueshima, High oolong tea consumption predicts future risk of diabetes among Japanese male workers: a prospective cohort study, Diabet. Med. 28 (2011) 805-810.

[10] D. L. McKay, J. B. Blumberg, The role of tea in human health: an update, J. Am. Coll, Nutr. 21 (2002) 1-13.

[11] C. J. Dufresne, E. R. Farnworth, A review of the latest research findings on the health promotion properties of tea, J. Nutr. Biochem. 12 (2001) 404-421.

[12] P. O. Owuor, M. Obanda, H. E. Nyirenda, N. I. K. Mphangwe, L. P. Wright, Z. Apostolides, The relationship between some chemical parameters and sensory evaluations for plain black tea (*Camelia sinensis*) produced in Kenya and comparison with similar teas from Malawi and South Africa, Food Chem. 97 (2006) 644-653.

[13] Q. Du, H. Jiang, Y. Ito, Separations of theaflavins of black tea. High speed countercurrent chromatography vs. sephadex LH-20 gel column chromatography, J. Liq. Chromatogr. Relat. Technol. 24 (2001) 2363-2369.

[14] P. J. Hilton, Tea, In F.D. Snell & L.S. Ettre (Eds.), Encyclopaedia of industrial chemical analysis, New York:Willey (1973) 455-518.

[15] A. R. Fernando, J. A. Plambeck, Determination of theaflavin in tea liquors using voltammetric methods, Analyst 113 (1988) 479-482.

[16] S. V. Jovanovic, Y. Hara, S. Steenken, M. G. Simic, Antioxidant potential of theaflavins: a pulse radiolysis study, J. Am. Chem. Soc. 119 (1997) 5337-5343.

[17] B. Lee, C. Ong, Comparative analysis of tea catechins and theaflavins by high performance liquid chromatography and capillary electrophoresis, J. Chromatogr. B 881 (2000) 439-447.

[18] V. Roginsky, T. Barsukova, C. F. Hsu, P. A. Kilmartin, Chain-breaking antioxidant activity and cyclic voltammetry characterization of polyphenols in a range of green, oolong and black teas, J. Agric. Food Chem. 51 (2003) 5798-5802.

[19] A. Ghosh, P. Tamuly, N. Bhattacharyya, B. Tudu, N. Gogoi, R. Bandyopadhyay, Estimation of theaflavin content in black tea using electronic tongue, J. Food Eng. 110 (2012) 71-79.

[20] A. Ghosh, T. N. Chatterjee, D. Sing, B. Tudu, P. Tamuly, N. Bhattacharya, R. Bandyopadhyay, Assessment of theaflavin-digallate in black tea by multi-frequency large amplitude pulse voltammetric electronic tongue in: Proceedings Of International Symposium for Electronic nose (ISOEN 2015), June 28 to July 1st, 2015, Dijon, France.

[21] A. Ghosh, T. Chatterjee, P. K. Borah, D. Sing, B. Tudu, P. Tamuly, N. Bhattacharya, R. Bandyopadhyay, Multi-frequency large amplitude pulse voltammetric electronic tongue to assess key compounds imparting the taste of briskness to finished black tea liquor in: ACM International Conference Proceeding series (2015) 252-257.

[22] P. K. Kundu, M. Kundu, The e-tongue based classification and authentication of mineral water samples using cross-correlation based PCA and Sammon's non-linear mapping, J. Chemometrics 27 (2013) 379-393.

[23] I. Campos, R. Bataller, R. Armero, J. M. Gandia, J. Soto, R. M. Máñez, L. G. Sánchez, Monitoring the grape ripeness using a voltammetric electronic tongue, Food Res. Int. 54 (2013) 1369-1375.

[24] K. Karim, F. Breton, R. Rouillon, E. V. Piletska, A. Guerreiro, I. Chianella, S. A. Piletsky, How to find effective functional monomers for effective molecularly imprinted polymers?, Adv. Drug Deliv. Rev. 57 (2005) 1795-1808.

[25] Henry N. Po, N. M. Senozan, The Henderson-Hasselbalch Equation: Its history and limitations, J. Chem. Educ. 78 (2001) 1499-1503.

[26] S. Wold, M. Sjostrom, L. Eriksson, PLS-regression: a basic tool of chemometrics, Chemom. Intell. Lab. Syst. 58 (2001) 109-130.

[27] S. D. Jong, SIMPLS: an alternative approach to partial least square regression, Chemom. Intell. Lab. Syst. 18 (1993) 251-263.

[28] M. O. Coinceanainn, C. Astill, S. Schumm, Potentiometric, FTIR and NMR studies of the complexation of metals with theaflavins, Dalton Trans. 0 (2003) 801-807.

[29] K. Varaprasad, Y. M. Mohan, S. Ravindra, N. N. Reddy, K. Vimala, K. Monika, B. Sreedhar, K. M. Raju, Hydrogel-silver nanoparticles composites: A new generation of microbials, J. Appl. Polym. Sci. 115 (2010) 1199-1207.

[30] E. Kolek, P. Šimko, P. Simon, A. Gatial, Confirmation of polymerisation effects of sodium chloride and its additives on acrylamide by infrared spectrometry, J. Food Nutr. Res. 46 (2007) 39-44.

[31] F. Bates, M. D. Valle, Voltammetric sensor for theophylline using sol-gel immobilized molecular imprinted polymer particles, Microchim. Acta 182 (2015) 933-942.

[32] X. Shi, A. Wu, G. Qu, R. Li, D. Zhang, Development and characterisation of molecularly imprinted polymers based on methacrylic acid for selective recognition of drugs, Biomaterials 28 (2007) 3741-3749.

[33] O. Brüggemann, Catalytically active polymers obtained by molecular imprinting and their application in chemical reaction engineering, Biomol. Eng. 18 (2001) 1-7.

[34] A. Robertson, The chemistry and biochemistry of black tea production-the non-volatiles, in: K.C. Willson, M.N. Clifford (Eds.), Tea cultivation to consumption, Springer Netherlands, 1992, pp. 555-601.

[35] D. Nie, D. Jiang, D. Zhang, Y. Liang, Y. Xue, T. Zhou, L. Jin, G. Shi, Two-dimensional molecular imprinting approach for the electrochemical detection of trinitrotoluene, Sens. Actuator B Chem. 156 (2011) 43-49.

[36] M. M. Farid, L. Goudini, F. Piri, A. Zamani, F. Saadati, Molecular imprinting method for fabricating novel glucose sensor: Polyvinyl acetate electrode reinforced by MnO_2/CuO loaded on graphene oxide nanoparticles, Food Chem. 194 (2016) 61-67.

[37] R. Ismail, H. Y. Lee, N. A. Mahyudin, F. A. Bakar, Linearity study on detection and quantification limits for the determination of avermectins using linear regression, J. Food Drug Anal. 22 (2014) 407-412.

[38] P. Janeiro, A. M. O. Brett, Catechin electrochemical oxidation mechanisms, Anal. Chim. Acta 518 (2004) 109-115.

[39] K. Fan, X. Luo, J. Ping, W. Tang, J. Wu, Y. Ying, Q. Zhou, Sensitive determination of (-)-epigallocatechin gallate in tea infusion using a novel ionic liquid carbon paste electrode, J. Agric. Food Chem. 60 (2012) 6333-6340.

[40] Md. M. Hasan, Md. E. Hossain, M. A. Mamun, M. Q. Ehsan, Study of redox behaviour of Cd (II) and interaction of Cd (II) with proline in the aqueous medium using cyclic voltammetry, J. Saudi Chem. Soc. 16 (2012) 145-151.

[41] A. Salimi, C. E. Banks, R. G. Compton, Abrasive immobilization of carbon nanotubes on a basal plane pyrolytic graphite electrode: application to the detection of epinephrine, Analyst 129 (2004) 225-228.

[42] A. Radi, A. Khafagy, A. El-shobaky, H. El-mezayen, Anodic voltammetric determination of gemifloxacin using screen printed carbon electrode, J. Pharm. Anal. 3 (2013) 132-136.

[43] http://inhumanexperiment.blogspot.in/2009/01/caffeine-and-polyphenol-contents-of.html, Caffeine and polyphenol contents of green tea, black tea, oolong tea & pu-erh tea, January 19, (2009).

[44] S. Sabhapondit, P. Bhattacharyya, L.P. Bhuyan, M. Hazarika, B.C. Goswami, Optimisation of withered leaf moisture during the manufacture of black tea based upon theaflavin fractions, Int. J. Food Sci. Tech. 49 (2014) 205-209.

[45] M. Nishimura, K. Ishiyama, A. Watanabe, S. Kawano, T. Miyase, M. Sano, Determination of theaflavins including methylated theaflavins in black tealeaves by solid-phase extraction and HPLC analysis, J. Agric. Food Chem. 55 (2007) 7252–7257.

[46] A. Rana, H.P. Singh, A rapid HPLC-DAD method for analysis of theaflavins using C_{12} as stationary phase, J. Liq. Chromatogr. Relat. Technol. 35 (2012) 2272–2279.

Chapter 3

Molecular imprinted polymer based electrode for sensing catechin (+C) in green tea

In this chapter, development of an MIP based sensor is presented for the selective detection of catechin (+C) in green tea. The electrode has been synthesized using the co-polymer of acrylonitrile and EGDMA and was subsequently imprinted with catechin. The sample was studied in detail using FTIR and FESEM, respectively. The electrochemical studies using cyclic voltammetry and differential pulse voltammetry revealed a linear range of 5-100 µM along with an LOD of 37 nM. The analytical characteristics of the electrode have been studied in detail and the response profile as obtained from the green tea samples were compared with that of the HPLC data. Good prediction accuracy has been obtained and the results were in excellent union with each other.

List of sections

Content of this chapter is based on the following publication:

T. Nandy Chatterjee et al., Molecular imprinted polymer based electrode for sensing catechin (+C) in green tea, IEEE Sens. J. 18 (2018) 2236-2244.

Chapter 3

Molecular imprinted polymer based electrode for sensing catechin (+C) in green tea

3.1. Introduction

The recognition of taste attributing agents of tea is extremely important as they have a considerable impact on its export worthiness and commercialization. Green tea leaves are the unfermented leaves generated from the young shoots of the plant *Camelia sinensis* [1]. During its processing, freshly harvested leaves are steamed to prevent fermentation unlike black tea, thereby yielding a dry, stable product [2]. This shorter processing time accounts for their lighter flavour. The intake of green tea is highly advantageous to human health owing to the presence of a number of biologically active polyphenolic compounds called flavonoids [3]. Flavanols, being the member of most diversely available flavonoids, constitutes of two aromatic rings (A and B) linked through three carbon atoms forming an oxygenated heterocyclic ring (C). They are known to possess antioxidant properties due to the presence of the aromatic OH groups [4]. Catechins or flavanol-3-ol is a group of compound comprising around 70% of total polyphenols present in tea leaves. The important catechins present in green tea are epigallocatechin (EGC), epigallocatechin gallate (EGCG), epicatechin gallate (ECG), epicatechin (EC), +catechin (+C) and gallo catechin (GC) [5]. The structure of catechin (+C) is shown in Fig.3.1. It possesses two different pharmacophores containing the catechol group in ring B and the resorcinol group in ring A. Also, a hydroxyl group is present at position 3 in ring C [6]. Catechin is of immense medicinal value due to its anti-viral [7], anti-allergic, anti-inflammatory [8], anti-carcinogenic [9], and anti-diabetic [10] properties. It also acts as a strong inhibitor of neurodegenerative disorders [11], chelating redox transition metal ions [12] and restrains platelet adhesion. These health benefits of catechin can be accredited to their redox characteristics and free radical scavenging abilities. It permits continuous neutralization of the adverse effects of free radicals by reducing their number [13]. Therefore, a simple, efficient and cost effective detection of catechin is highly imperative for the tea and the pharmaceutical industries.

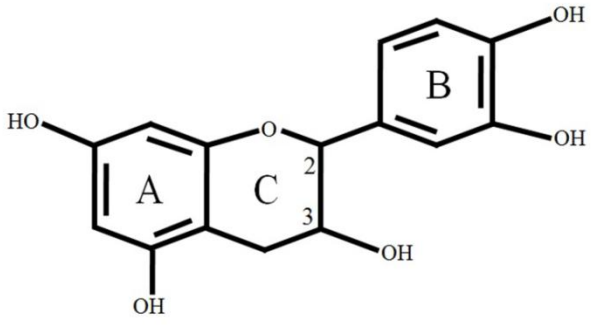

Fig.3.1. Chemical structure of catechin (+C)

Here also a number of analytical methods have been reported for the detection and quantification of catechin. These include HPLC [14], spectrophotometry, mass spectroscopy [15], flow column electrolysis [16], flurorescence analysis [17] and chemiluminescence [18]. Though by means of these techniques the results generated are of high precision and accuracy, but they are time consuming, expensive and require skilled operational experts. Moreover, it is not possible to adapt such techniques by small scale industries located at remote places. Electrochemical detection has been practised as an alternative to these approaches in the recent era, due to their simplicity, fast response time, good sensitivity and selectivity. Ezhil Vilian et al., developed a catechin sensor by modification of the GCE using MnO_2/carbon nanotubes decorated with the nanocomposite of Pt nanoparticles [19]. Also, Manasa et al., employed electrochemical detection of catechin by means of poly (methylene blue) modified carbon paste electrode [4]. Pang et al., used nitrogen doped graphene modified CPE as an electrochemical probe for the determination of catechin [20].

The objective of the work presented in this chapter is to develop a low cost, reusable and simple sensor for detection of catechin (+C) in green tea samples by combining the principle of electrochemistry and molecular imprinted polymer (MIP) technique. The novelty of the proposed methodology is that the preparation process is inexpensive; electrodes are easy to fabricate and have a reasonable sensitivity towards its target analyte. The basic strategy followed for the synthesis and electrochemical studies of the MIP-CAT electrode can be witnessed from Fig.2.2 (a) and (b) respectively, depicted in Chapter 2. In this work, acrylonitrile has been selected as the monomer for the construction of the polymer backbone due to its highly polar nitrile group, which is also capable of making hydrogen bonds with the template molecule (i.e. catechin). Moreover, acrylonitrile is also capable of enhancing the mechanical strength of the graphite based composite due to its high physical interaction with the guest graphite particles. The synthesized MIP electrode yielded a linear range in the order of 5 µM – 100 µM with detection limit as low as 37 nM. Finally a PLSR model has been

developed and trained with the HPLC data to predict the content of catechin in green tea samples using leave one out cross validation (LOOCV) procedure. The electrode demonstrated an acceptable performance with a prediction accuracy of about 92 %.

3.2. Experimental process

3.2.1. Chemical reagents

Acrylonitrile, ethylene glycol dimethacrylate (EGDMA), catechin hydrate, epigallocatechin gallate (EGCG), caffeine (CAF), ascorbic acid (AA) and commercial graphite powder (99 %) were procured from Sigma Aldrich. Paraffin oil and ethanol were obtained from Merck. Benzoyl peroxide was supplied by Sisco Research Laboratories Pvt. Ltd. All the reagents used in the experiment were of analytical grade and used without further purification. The entire experimentation and rinsing of the electrodes were performed using Millipore water (Resistance = 18 MΩ).

3.2.2. Synthesis of the MIP and the NIP

Firstly, 0.95 g of commercial graphite powder was dispersed in 15 ml ethanol for 3 h by ultrasonication. Then 0.05 g of acrylonitrile and 0.05 g of catechin hydrate was added to the dispersed solution under constant stirring. After 2 h, 400 µl of EGDMA and 1 mg of benzoyl peroxide (polymerization initiator) were added to the mixture and it was left to stir for another 2 h in pure N_2 atmosphere. Then the mixture was heated in a water bath for 1h in order to undergo polymerization. The resultant polymerized powder sample was dried and collected. This preparation condition was optimized for best sensitivity.

For the preparation of the MIP, the dried polymerized sample was repeatedly washed in the mixture of 100 ml ethanol and water (70:30) till no traces of the template i.e. catechin was found in it. The complete removal of catechin was evidenced by UV-vis spectroscopy in the scanning range of 200 nm - 450 nm. The NIP sample was synthesized using the same methodology; except that catechin was not added during its preparation.

3.2.3. Preparation of the electrodes

The MIP and the NIP electrodes were prepared by the addition of paraffin oil to 0.25 g of the respective powders, in order to make a fine paste. After that the paste was put in to glass capillary tubes of inner diameter 2.5 mm respectively, and pressed with a steel rod. Pt-wire was connected from the backside of the tubes in order to build the electrical contacts. The surface of the electrodes were polished with Al_2O_3 slurry, smoothed and rinsed carefully with

double distilled water prior to each electrochemical measurement. The procedure of the preparation of the electrode and the instrumentation used to perform all the measurements are depicted in Fig.2.3 and Fig.2.4 in Chapter 2, respectively.

3.2.4. Preparation of the buffer solutions

Here in this work phosphate buffer and acetate buffer in the pH range from 5 to 7 and pH 5, respectively has been used. Additionally, phthalate buffer of pH value 5 has also been used to study the response of the sensing material. The procedures for preparing phosphate buffer and acetate buffer have been discussed in the previous chapter (*Section 2.2.4*). In order to prepare phthalate buffer of pH value 5, firstly, 10.21 gm of potassium hydrogen phthalate was taken in 1000 ml of double distilled water. Then appropriate amount of 0.1 M standardized NaOH was added to the beaker containing potassium hydrogen phthalate and the remaining volume was adjusted using water. The pH of the phthalate buffer, so obtained, was verified to 5 followed by preservation of the buffer in a volumetric flask.

3.2.5. Preparation of the stock analyte solution

1 mM CAT solution was prepared by mixing 0.029 gm of CAT in 20 ml water. The remaining volume of the flask was made up by water after the analyte got dissolved fully.

3.2.6. Preparation of the green tea liquor for real sample analysis

For the preparation of green tea, all the steps were kept identical as mentioned in the previous chapter (*Section 2.2.6*), except that the infusion time was reduced to 5 minutes. Differential pulse voltammetry was used to obtain the response of rest of the electrodes. Consequently, five duplicated response profiles were obtained from each of the samples using the respective MIP electrodes.

3.3. Results and discussions

3.3.1. Proposed mechanism of detection

The graphical representation involving the detection of catechin using the MIP technique is illustrated in Fig.3.2. Catechin consists of functional OH groups attached to its resorcinol-A and catechol-B moieties, respectively. Acrylonitrile, on the other hand, possesses polar nitrile groups that can effectively form physical bonding with the catechin molecule. On addition of the crosslinker EGDMA to the mixture containing graphite and acrylonitrile loaded with the

template molecule, a pre-polymerization complex is formed. The polymerization reaction proceeds with the addition of the initiator, benzoyl peroxide thereby resulting in to polyacrylonitrile-graphite composite. On extraction of catechin from the polymerized sample, binding cavities complementary in shape and size to that of the template molecule are generated. As a result, when the electrode is subjected to catechin using voltammetry, rebinding of the template molecule takes place in the vacant spaces and a sharp rise in peak current is observed. This mainly occurs due to the adsorption of the target analyte on the surface of the electrode. The surface of the electrode is again regenerated by washing it with water.

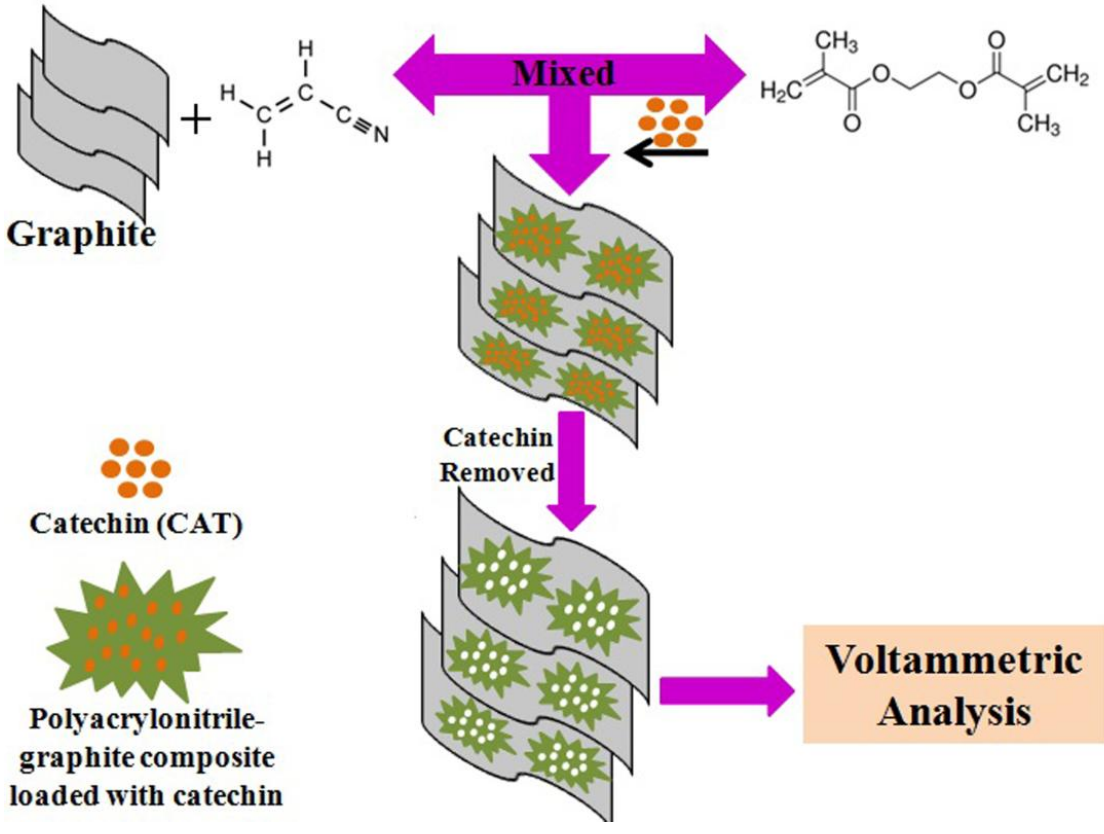

Fig.3.2. Proposed mechanism of detection of catechin using the MIP electrode

3.3.2. FTIR analysis

Fourier transform infra-red (FTIR) spectroscopy was performed in order to ascertain the formation of the polymer and the subsequent removal of catechin during the imprinting process. The spectrum of the sample before and after removal of catechin, respectively, is shown in Fig.3.3.

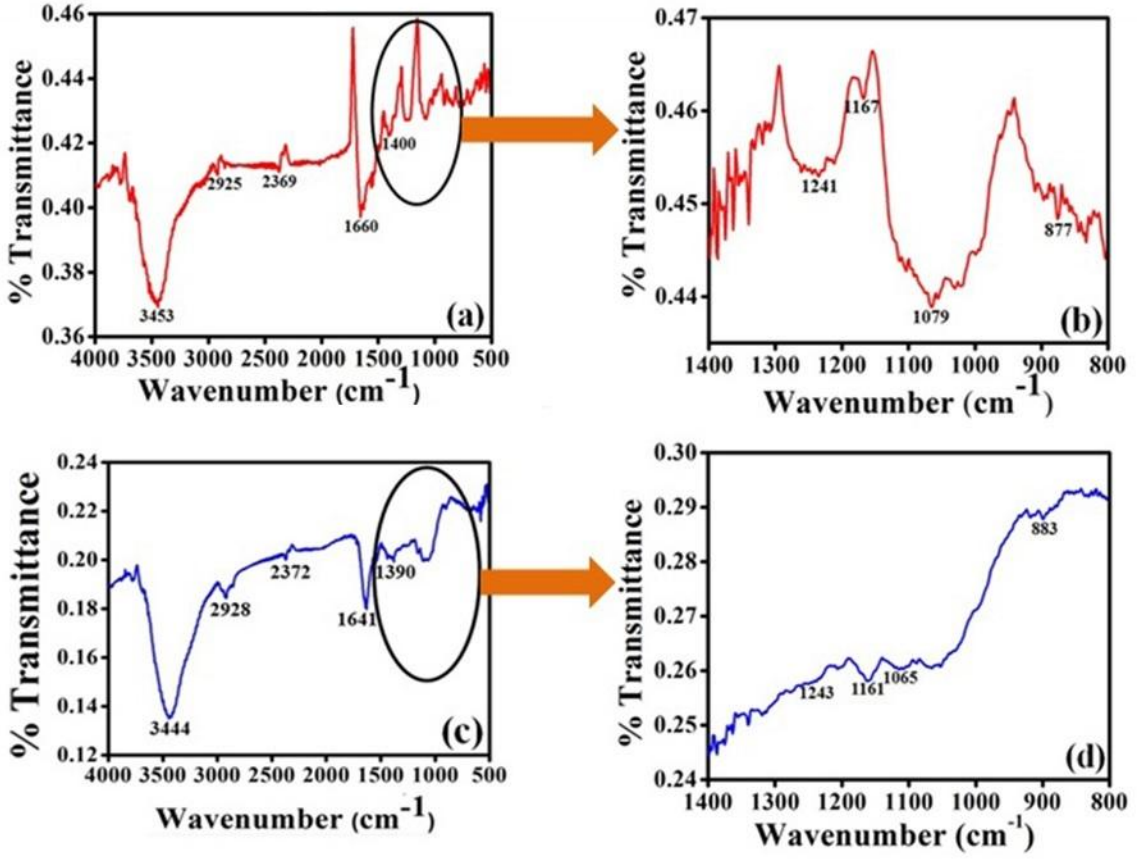

Fig.3.3. Comparison of FTIR spectra: spectrum of (a) polyacrylonitrile-graphite nanocomposite before removal of catechin; (b) zoomed part for catechin before removal; (c) polyacrylonitrile-graphite nanocomposite after removal of catechin; (d) zoomed part for catechin after removal

In Fig.3.3 (a), the stretching vibration of O−H group was detected at 3453 cm^{-1}. A typical signature of polyacrylonitrile can be recognized due to the presence of bands at 2925 cm^{-1} and 2857 cm^{-1}, corresponding to the stretching and bending vibrations of methylene ($-CH_2$) group [21], respectively. Also, the vibrations of strong intramolecular bounded C=O bond, free and bounded C=C and C=N bond in the region between 1550-1650 cm^{-1}, C−N bond at 1017 cm^{-1} indicates the formation of polyacrylonitrile. The similar features have been observed in Fig.3.3 (c) as well, which represents the FTIR spectra of the sample after removal of catechin. The distinct bands at 1400 cm^{-1}, 1241 cm^{-1}, 1167 cm^{-1} and 877 cm^{-1} due to

catechin [22], shown in Fig.3.3 (b) somewhat got broadened and disappeared upon its extraction (shown in Fig.3.3 (d)), thereby signifying its successful removal from the polymerized sample. Moreover, from Fig.3.3 (a) and 3.3 (c), it may be noted that all the vibrational bands are slightly shifted. This small change in the spectra may be due to high concentration of analyte molecules on the surface of cavities, which is produced as a result of solvent leaching.

3.3.3. Morphological characterization using FESEM

The surface morphology of the MIP and the NIP sample obtained from FESEM analyses are depicted in Fig.3.4 (a) and 3.4 (b), respectively. It is observed from the figure that the surface of the MIP sample is rough and wrinkled in nature as compared to that of the NIP. This is mainly due to the formation of binding cavities as a result of elution of catechin from the MIP sample.

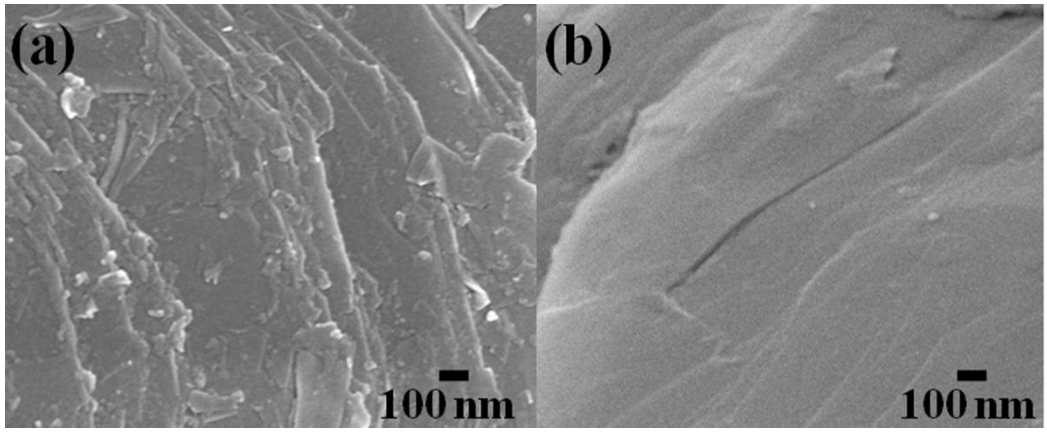

Fig.3.4. FESEM images of the (a) MIP and the (b) NIP sample

The NIP sample on the other hand; underwent no such procedure and thus as a result, have relatively smoother surface. This trend is pertinent to other MIP and NIP samples reported in the literature as well [23-25].

3.3.4. Effect of pH value and buffer

The pH of the buffer solution plays a pivotal role in determining the analytical characteristics of a sensor. Cyclic voltammogram was obtained using the MIP electrode dipped in 1 mM catechin in the presence of phosphate buffer solution (PBS) of three different pH values, viz., 5, 6 and 7. From the response profile shown in Fig.3.5, it is evident that highest peak current (18.10 μA) is obtained for the pH value of 5.

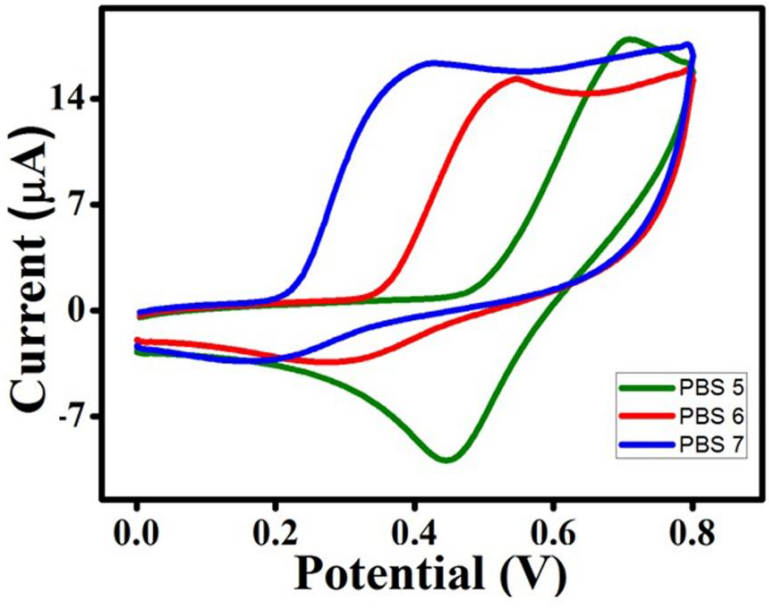

Fig.3.5. CV of 1 mM catechin in phosphate buffer solution of pH values 5-7

Further, in order to optimize the suitable buffer for electrochemical reactions of catechin, the MIP electrode was subjected to 1 mM of catechin in three different buffers, viz., acetate buffer, phosphate buffer and phthalate buffer respectively, each of pH 5. The corresponding cyclic voltammogram is shown in Fig.3.6 (a). It is observed from the figure that the peak current of the MIP electrode is highest for phthalate buffer. This is probably due to the presence of aromatic ring in phthalate molecule, which is reasonably adsorbed on the surface of polar polyacrylonitrile by forming hydrogen bonded complex with catechin. Based on the results obtained, all the subsequent measurements were performed using phthalate buffer of pH 5.

Fig.3.6 (b) and 3.6 (c) depicts the response of MIP and NIP electrode, in pure buffer and in presence of 1 mM catechin, respectively. Both the electrodes responded more or less similarly in pure buffer solution. The minor humps present at the response curves for the electrodes are due to the presence of non-specific or low specific sites on the electrode surface.

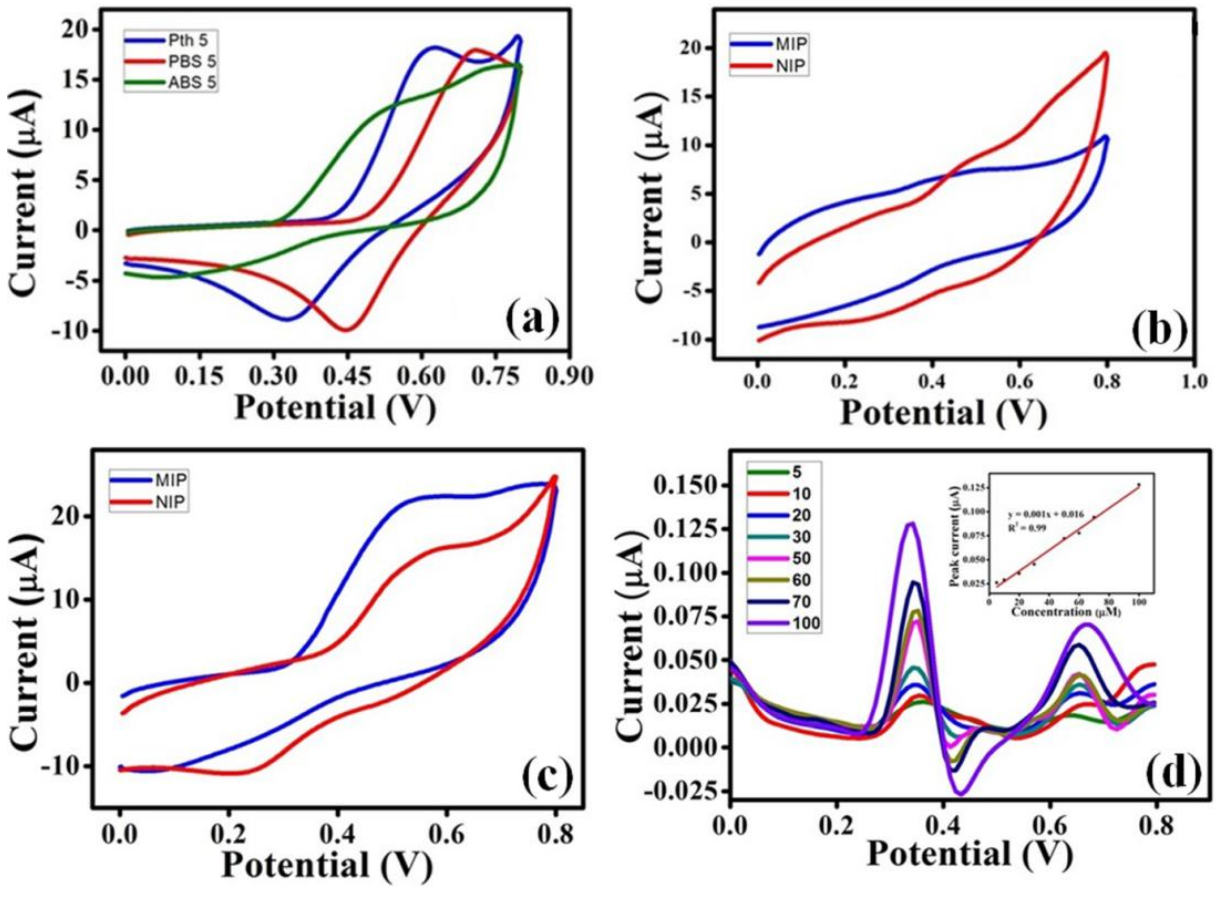

Fig.3.6. (a) CV obtained for 1 mM catechin in phthalate, phosphate and acetate buffer solutions; CV response of the MIP and the NIP electrode in phthalate buffer (b) without the addition of catechin and (c) in presence of 1 mM catechin; (d) DPV response indicating the concentration variation of catechin in phthalate buffer using the MIP electrode (inset shows the variation of peak current with concentration); pH of all buffers: 5

But with the addition of catechin to the buffer, the current intensity increased sharply in case of the MIP electrode and a prominent peak at 0.52 V became visible. The NIP electrode, on the other hand, showed a peak with lower current intensity at 0.59 V. After each electrochemical measurement, the electrode was dipped in ethanol-water mixture (70:30) and new surface was regenerated. Cyclic voltammogram of the MIP electrode in pure buffer was further obtained to ensure that no residues of catechin remain adsorbed on the electrode's surface.

Differential pulse voltammetry (DPV) technique has been used in order to study the analytical performance of the MIP electrode. For this electrochemical measurement, the different parameters of DPV are optimized. The potential window was chosen between 0.0 V to 0.8 V. The step potential, modulation amplitude and modulation time was maintained at

0.01 V, 0.005 V and 0.2 s, respectively. The scan rate was kept fixed at 0.025 V/s. Fig.3.6 (d) delineates that the peak current rises linearly on increasing the concentration range from 5 µM to 100 µM. The calibration curve obtained from the response profile is linear in nature having the regression equation as shown in equation (3.1):

$$I_p = 0.001c + 0.016 \quad (3.1)$$

with $R^2 = 0.99$. The limit of detection (LOD) of catechin was calculated as 37 nM based on 3*Sy*/*x*/*m*. Here, *Sy*/*x* and *m* are the standard deviation of the regression line and slope of the calibration curve, respectively [26, 27]. Like most other polyphenols [28, 29], the electrochemical oxidation of catechin also involves a two step process. Firstly, catechin gets converted to the semiquinone radical by releasing an electron and a proton. In the second step, another electron and a proton are discharged thereby resulting in to the formation of quinone (as shown in Fig.3.7). This phenomenon is in consistence with the previous reports [6, 36]. The appearance of two distinct peaks in the DPV shown in Fig.3.6 (d) is probably due to the two step oxidation mechanism as exhibited by the catechin molecule.

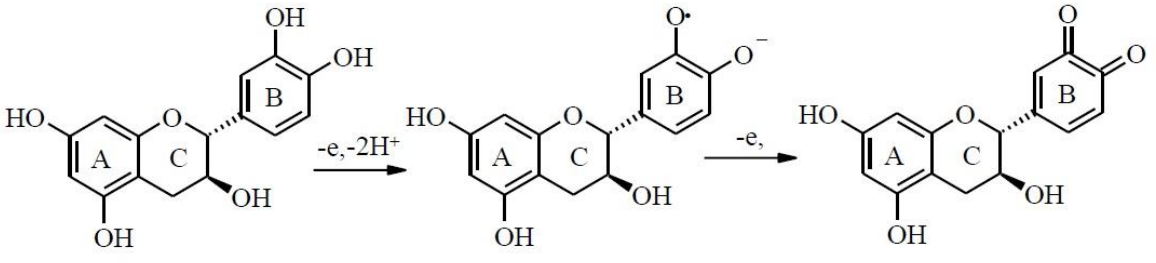

Fig.3.7. Electrochemical oxidation mechanism of catechin

3.3.5. Effect of scan rate

The effect of scan rate was investigated for having an insight to the electrochemical mechanisms involved and the kinetics of the reaction system. Fig.3.8 (a) depicts the cyclic voltammogram of 1 mM catechin in phthalate buffer using the MIP electrode by varying the scan rate from 20 to 400 mV/s. It can be seen from the figure that the redox reaction is quasi reversible in nature as I_p/I_c is not equal to unity.

From the figure, it is also evident that both the anodic and the cathodic peak currents increases linearly along with the square root of the scan rate thereby indicating that the electrochemical oxidation and reduction of catechin is an adsorption controlled process [31], being also guided by the hydrogen bonding with the phthalate ion. The correlation coefficient

value obtained from the calibration curve shown in Fig.3.8 (b) is R^2= 0.99 for the oxidation and the reduction process, respectively.

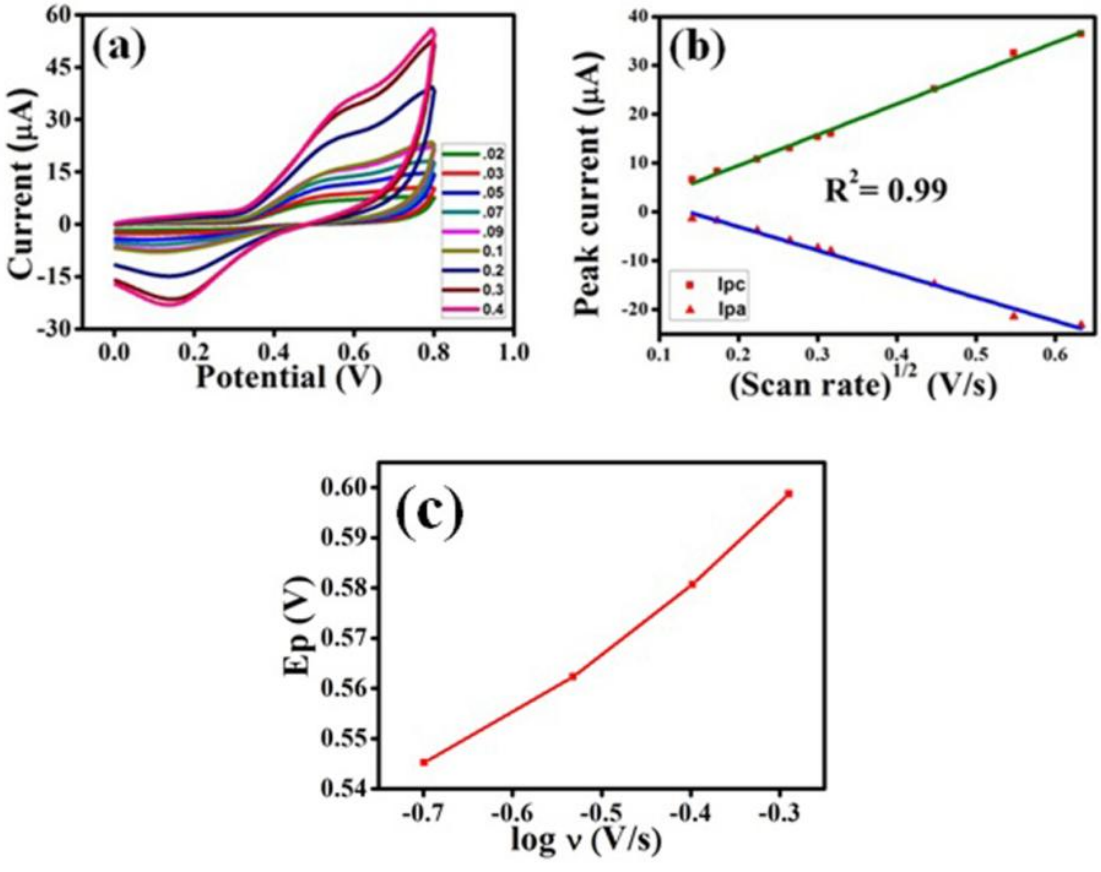

Fig.3.8. (a) CV indicating the variation of peak current with scan rate (0.02 to 0.4 V/s); (b) Variation of the anodic and cathodic current with the square root of scan rate; (c) Variation of peak potential (Ep) with the logarithm of scan rate (log v)

The number of electrons transferred during the oxidation reaction and the adsorbed amount of catechin on the surface of the MIP electrode has been calculated by means of Randles-Sevcik equation as shown in eq. (3.2).

$$I_p = \frac{nFQv}{4RT} = \frac{n^2F^2Av\Gamma_c}{4RT} \quad (3.2)$$

here, n is the number of electrons transferred, F is the Faraday's constant, A is the area of the electrode, Γ_c is the surface concentration of catechin, Q is the quantity of charge consumed during the oxidation reaction and v is the scan rate [32]. Based on the equations, the value of n and Γ_c, obtained for the oxidation reaction are 2.13 and 8.45 x 10^{-10} mole cm^{-2}, respectively. The number of electrons transferred calculated highly agrees with the appearance of the two oxidation peaks of catechin discussed in the previous section. Therefore, experimental and analytical results are well correlated with each other in this work.

Further, Laviron's equation [33, 34] has been employed to determine the heterogeneous rate constant (k_s) of the reaction system. Depending on the relationship between oxidation potential (Ep) and logarithm of scan rate (log v) [35], a calibration curve is constructed (shown in Fig.3.8 (c)). It is observed from the figure that the relationship between these two parameters is linear in nature (shown in eq. (3.3)).

$$E_p = 0.130 \log v + 0.634 \tag{3.3}$$

with R^2 = 0.99. The electron transfer coefficient (α) has been estimated to be 0.78 from the value of the slope of the curve. This value of α agrees well with the literature [4]. Laviron's equation can be expressed as in eq. (3.4):

$$\log k_s = \alpha \log (1 - \alpha) + (1 - \alpha) \log \alpha - \log (RT/nF\, v) - nF\Delta E_p\, \alpha(1 - \alpha)/2.3RT \tag{3.4}$$

The value of k_s calculated from the above equation is 0.21 s^{-1}. A comparison of the values of α and k_s for the detection of catechin using other electrodes is summarized in Table 3.1. It can be inferred from the table, that the value of k_s is much higher or is comparable to the reported methods [36]. Therefore, considering the above results, the synthesized MIP electrode is expected to aid the electron transfer kinetics thereby enhancing the electrochemical oxidation of catechin.

Table 3.1 Comparison of the electron transfer kinetics of the proposed electrode with the reported works

Electrodes	**Electron transfer co-efficient (α)**	**Heterogeneous rate constant (k_s)**	**References**
Pt electrode	0.43 ± 0.05	(2.88 ± 0.05) x 10^{-4} s^{-1}	[36]
PMB/CPE	0.7	1.2 s^{-1}	[4]
MIP electrode	**0.78**	**0.21 s^{-1}**	**This work**

3.3.6. Selectivity, repeatability, stability and reproducibility of the MIP Electrode

The selectivity of the MIP sensor was examined in presence of other important constituents of green tea viz., epigallocatechin gallate (EGCG), ascorbic acid (AA) and caffeine (CAF). The results are presented in the form of a bar plot shown in Fig.3.9. The MIP electrode delivered an enhanced peak current towards its target analyte (i.e. catechin) than the other

three analogues. The response of the NIP electrode, on the other hand, was more or less similar for all the three compounds.

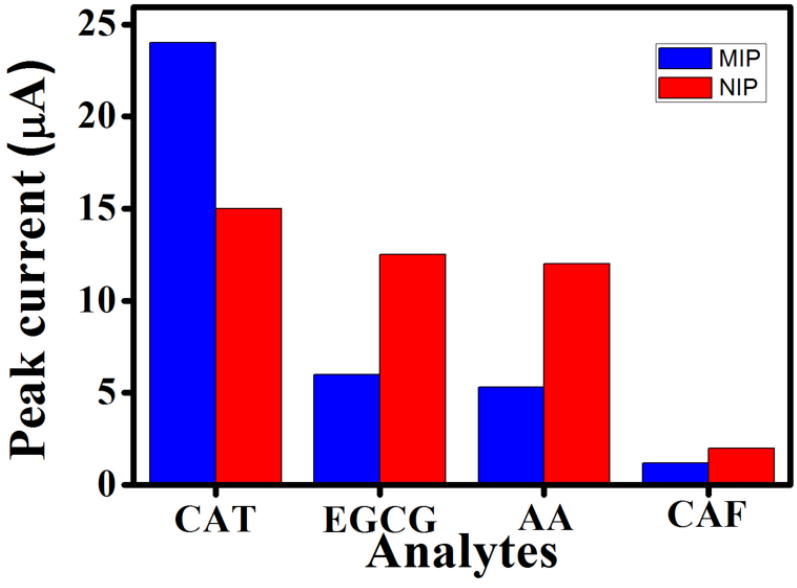

Fig.3.9. Bar plot indicating the selectivity of the MIP electrode towards 1 mM CAT, EGCG, AA and CAF; Buffer: phthalate, pH: 5, scan rate: 0.05 V/s

The reusability of the proposed MIP electrode has been studied by analyzing its stability and repeatability characteristics. Five successive electrochemical determination of 1mM catechin in phthalate buffer solution was employed using the same MIP electrode. The relative standard deviation (RSD) calculated from the voltammogram (shown in Fig.3.10 (a)), was found to be 4.14 %, thereby indicating a good repeatability. The MIP electrode was also subjected to cyclic voltammetry in the presence of 1 mM catechin solution in an interval of seven days under ambient conditions. The response profile was again obtained after three months under similar experimental conditions. The corresponding peak current values are depicted in the form of a pie chart shown in Fig.3.10 (b). It may be observed from the figure, that the sensitivity of the electrode decreased to a nominal value of 0.85 % after a month. However, after three months, the performance of the electrode declined to 5.49 %. Therefore, it can be ascertained that the sensor is extensively reusable and can be used with a minimum drift in current.

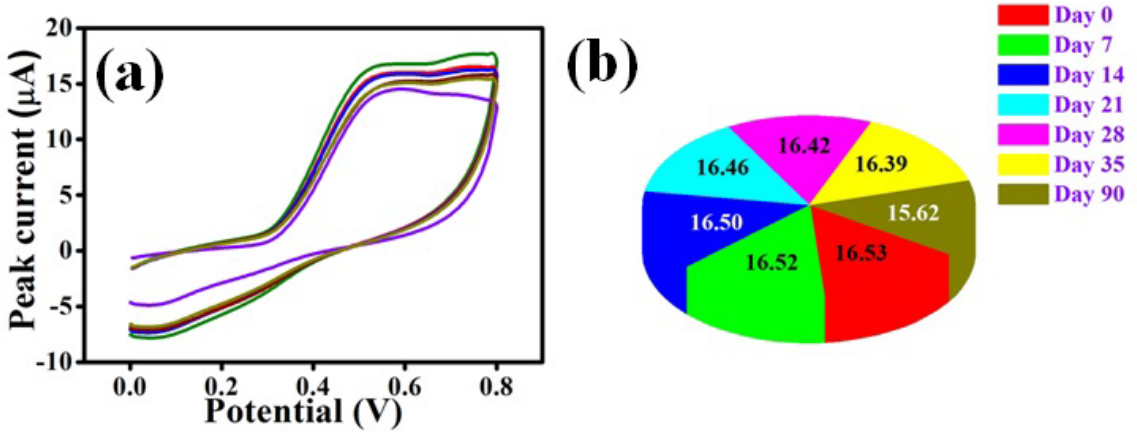

Fig.3.10. Reusability of the MIP electrode in terms of (a) repeatability and (b) stability

The reproducibility of the proposed electrode was analyzed by means of cyclic voltammetry. Four different MIP electrodes were synthesized using the same technique and they were subjected to 1 mM catechin in phthalate buffer solution. The electrodes demonstrated a reasonable reproducibility with the %RSD value of 5.95.

3.3.7. Quantification of catechin in green tea samples using the MIP electrode

The synthesized MIP electrode was employed to quantify the amount of catechin present in green tea samples to examine its real time applications. DPV response profile of a typical tea sample is given in Fig.3.11.

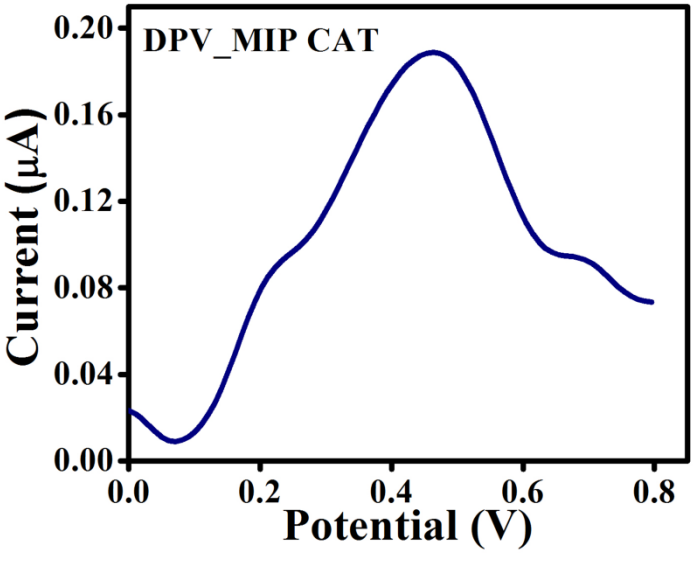

Fig.3.11. DPV response of a typical green tea sample obtained using MIP-CAT electrode

The catechin content in twelve green tea samples was predicted by developing a PLS model using MATLAB Version 10. The model was calibrated with the voltammogram and the reference HPLC data. LOOCV technique was employed for testing the performance of the model [37].

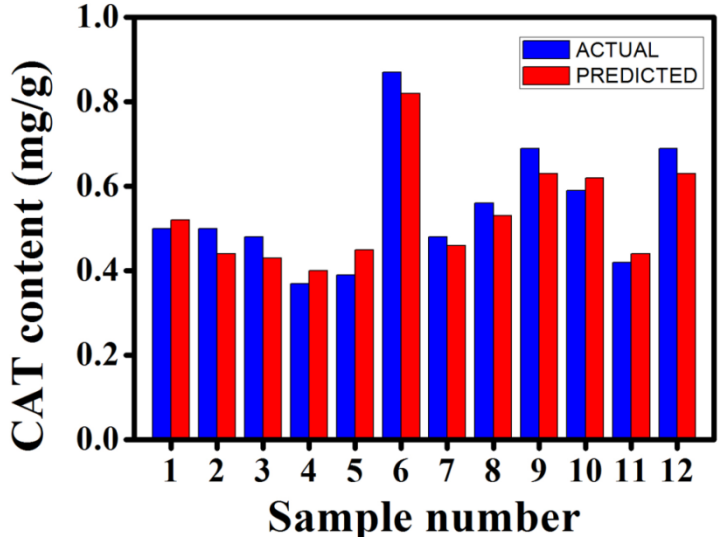

Fig.3.12. Bar plot indicating the actual and predicted values of catechin

During the onset of cross validation, the training data set was constructed by eliminating the data points of a particular tea sample and the model was tested using that omitted dataset. This methodology was iterated for all the samples and the respective prediction accuracies were calculated. It is interesting to note, that when the number of components of the developed model was kept to seven, a fair agreement between the root mean square error of cross validation (RMSECV) and correlation factor (CF) was observed thereby yielding highest prediction accuracy. The actual concentration of catechin, mean predicted concentration and the prediction accuracy of all the green tea samples used for the experiment are elucidated in Table 3.2. It is seen from the table, that the prediction accuracy of nine samples are considerably high, being greater than 90%, and the accuracy level of only three of them falls between 84 % to 90 %. The comparison of the actual and predicted concentration of catechin are also presented in the form of a bar plot shown in Fig.3.12. The actual and the predicted values are found to be in good union and the average prediction accuracy for all the samples was calculated to be about 92 %. Therefore, the results indicate the satisfactory performance of the electrode for qualitative and quantitative estimation of catechin in green tea.

Table 3.2 Actual and predicted catechin (+C) content from the LOOCV based PLS model with seven PLS components

Sample no.	Actual catechin (mg/g)	Predicted catechin (mg/g)	Prediction accuracy (%)
1	0.50	0.52	96.00
2	0.50	0.44	88.00
3	0.48	0.43	89.58
4	0.37	0.40	91.89
5	0.39	0.45	84.62
6	0.87	0.82	94.25
7	0.48	0.46	95.83
8	0.56	0.53	94.64
9	0.69	0.63	91.30
10	0.59	0.62	94.91
11	0.42	0.44	95.24
12	0.69	0.64	92.75

3.3.8. Comparison of the proposed method with existing techniques

The viability and the analytical characteristics of the proposed method for the detection of catechin (+C) have been compared with that of the reported techniques. The results are shown in Table 3.3. It is well evident from the table that the MIP electrode is capable of yielding a detection limit almost comparable to some of the electrodes and many times better than the other ones. Moreover, in this work, it has been intended to develop a low cost and reusable electrode for sensing catechin in green tea samples. This can serve as a cost effective alternative to the tea industries. From our limited literature survey, it has been found that normally, the amount of catechin present in green tea ranges from 0.09 to 6.10 mg/g of dry weight [38], being of the order of µM. Therefore, the proposed electrode (detection limit: 37 nM) can effectively detect catechin in green tea samples.

Table 3.3 Comparison of the proposed method with the reported techniques

Methodology	LOD (nM)	Linear range (µM)	References
Osteryoung-square wave anodic voltammetry (OSWAV) using HP-β-CD based sensor	0.12	0.001 – 7.2	[39]
Differential pulse cathodic votlammetry (DPCV) using HP-β-CD based sensor	0.30	0.002 – 4.2	[39]
DPV using poly(methylene)blue modified carbon paste electrode	4.9	1 – 1000	[4]
DPV using poly-aspartic acid film based sensor	72	0.25 – 30	[40]
DPV using multiwalled carbon nanotube paste electrode	17	0.10 – 2.69	[41]
Square wave voltammetry (SWV) using nickel (II) complex and thiol on gold electrode	826	3.31 – 25.3	[42]
CV using ($Ru(bpy)_3^{3+}$) modified BDD	121	0.3268 – 0.1591	[43]
DPV using MIP electrode	**37**	**5 – 100**	**This work**

3.4. Conclusion

Catechin is an essential antioxidant and imparts medicinal values to green tea, thus having a siginificant impact on human health. We have described in this chapter the synthesis, characterizations and the electrochemical characteristics of the sensor. The novelty of this work is that here we have employed the principle of MIP in order to detect the amount of catechin present in green tea. Among a host of other methodologies, MIP technology has been preferred for sensing of catechin as it is relatively simple, inexpensive and results in a highly sensitive electrode. Here a reusable electrode has been prepared by imprinting catechin in a nanocomposite consisting of graphite along with a co-polymer of polyacrylonitrile and EGDMA. The structural and morphological characterization of the

material has been performed using FTIR and FESEM. Moreover, the analytical characteristics of the electrode were studied and it was found to be repeatable, stable, reproducible and also capable of sensing catechin effectively among other structural analogues. It offered a linear range from 5 µM – 100 µM and a LOD of 37 nM (S/N). Though the detection limit obtained is higher than some of the electrodes mentioned in the reported works, but the proportion of catechin present in green tea enables its efficient detection using the synthesized electrode. Further, the MIP electrode has been used successfully to quantify the amount of catechin present in green tea samples and the results were highly agreeable having a prediction accuracy of about 92 % with that of the HPLC data.

References

[1] M. W. L. Koo, C. H. Cho, Pharmacological effects of green tea on the gastrointestinal system, Eur. J. Pharmacol. 500 (2004) 177–185.

[2] N. Khan, H. Mukhtar, Tea polyphenols for health promotion, Life Sci. 81 (2007) 519-533.

[3] Y. M. Juang, H. J. Chien, C. J. Chen, C. C. Lai, Graphene flakes enhance the detection of TiO_2-enriched catechins by SALDI-MS after microwave-assisted enrichment, Talanta 153 (2016) 347–352.

[4] G. Manasa, R. J. Mascarenhas, A. K. Satpati, O. J. D'Souza, A. Dhason, Facile preparation of poly(methylene blue) modified carbon paste electrode for the detection and quantification of catechin, Mater. Sci. Eng. C 73 (2017) 552–561.

[5] S. Sabhapondit, T. Karak, L. P. Bhuyan, B. C. Goswami, M. Hazarika, Diversity of catechin in northeast indian tea cultivars, Sci. World J. 2012 (2012) Art. no. 485193.

[6] P. Janeiro, A. M. O. Brett, Catechin electrochemical oxidation mechanisms, Anal. Chim. Acta 518 (2004) 109–115.

[7] C. Lakenbrink, S. Lapczynski, B. Maiwald, U. H. Engelhardt, Flavonoids and other polyphenols in consumer brews of tea and other caffeinated beverages, J. Agri. Food Chem. 48 (2000) 2848–2852.

[8] V. K. Ananingsih, A. Sharma, W. Zhou, Green tea catechins during food processing and storage: A review on stability and detection, Food Res. Int. 50 (2013) 469–479.

[9] N. T. Zaveri, Green tea and its polyphenolic catechins: Medicinal uses in cancer and noncancer applications, Life Sci. 78 (2006) 2073–2080.

[10] P. V. A. Babu, K. E. Sabitha, P. Srinivasan, C. S. Shyamaladevi, Green tea attenuates diabetes induced Maillard-type fluorescence and collagen cross-linking in the heart of streptozotocin diabetic rats, Pharamacol. Res. 55 (2007) 433–440.

[11] R. P. Singh, S. Sharad, S. Kapur, Free radicals and oxidative stress in neurodegenerative diseases: Relevance of dietary antioxidants, J. Indian Acad. Clin. Med. 5 (2014) 218–225.

[12] S. J. S. Flora, Structural, chemical and biological aspects of antioxidants for strategies against metal and metalloid exposure, Oxidative Med. Cellular Longevity 2 (2009) 191–206.

[13] J. V. Higdon, B. Frei, Tea catechins and polyphenols: Health effects, metabolism, and antioxidant functions, Critical Rev. Food Sci. Nutrition 43 (2003) 89–143.

[14] S. Carando, P. Teissedre, J. Cabanis, Comparison of (+)- catechin determination in human plasma by high-performance liquid chromatography with two types of detection: Fluorescence and ultraviolet, J. Chromatogr. B Biomed. Sci. Appl., 707 (1998) 195–201.

[15] P. Miketova, K. H. Schram, J. Whitney, M. Li, R. Huang, E. Kerns, S. Valcic, B. N. Timmermann, R. Rourick, S. Klohr, Tandem mass spectrometry studies of green tea catechins. Identification of three minor components in the polyphenolic extract of green tea, J. Mass Spectrom. 35 (2000) 860–869.

[16] H. Hotta, S. Nagano, M. Ueda, Y. Tsujino, J. Koyama, T. Osakai, Higher radical scavenging activities of polyphenolic antioxidants can be ascribed to chemical reactions following their oxidation, Biochim. Biophys. Acta-Gen. Subjects 1572 (2002) 123–132.

[17] H. Sereshti, S. Samadi, S. Asgari, M. Karimi, Preparation and application of magnetic graphene oxide coated with a modified chitosan pH-sensitive hydrogel: An efficient biocompatible adsorbent for catechin, RSC Adv. 5 (2015) 9396–9404.

[18] J. M. Lee, M. M. Karim, S. H. Lee, Determination of catechin in aqueous solution by chemiluminescence method, J. Fluorescence 15 (2005) 735–739.

[19] A. T. E. Vilian, R. Madhu, S. Chen, V. Veeramani, M. Sivakumar, Y. S. Huh, Y. Han, Facile synthesis of MnO_2/carbon nanotubes decorated with a nanocomposite of Pt nanoparticles as a new platform for the electrochemical detection of catechin in red wine and green tea samples, J. Mater. Chem. B 3 (2015) 6285–6292.

[20] J. Pang, X. Wu, A. Li, X. Liu, M. Li, Detection of catechin in chinese green teas at N-doped carbon-modified electrode, Ionics 23 (2017) 1889–1895.

[21] H. Wu, D. H. Bremner, H. Li, Q. Shi, J. Wu, R. Xiao, L. Zhu, A novel multifunctional biomedical material based on polyacrylonitrile: Preparation and characterization, Mater. Sci. Eng. C 62 (2016) 702–709.

[22] Y. M. Chen, T. M. Tsao, C. C. Liu, P. M. Huang, M. K. Wang, Polymerization of catechin catalyzed by Mn-, Fe- and Al-oxides, Colloids Surf. B 81 (2010) 217–223.

[23] S. Yang, Y. Wang, M. Xu, M. He, M. Zhang, D. Ran, X. Jia, Synthesis of modified chitosan-based molecularly imprinted polymers for adsorptive protein separation, Anal. Methods 5 (2013) 5471–547.

[24] X. Shi, A. Wu, G. Qu, R. Li, D. Zhang, Development and characterisation of molecularly imprinted polymers based on methacrylic acid for selective recognition of drugs, Biomaterials 28 (2007) 3741–3749.

[25] R. Cohen, Y. Mazuz, M. Tikhonov, C. N. Sukenik, Carboxylic acid decorated self-assembled monolayer films: New acid synthesis chemistry and reaction chemistry including bridged diacyl peroxide preparation, Langmuir 31(2015) 3049–3058.

[26] M. M. Farid, L. Goudini, F. Piri, A. Zamani, F. Saadati, Molecular imprinting method for fabricating novel glucose sensor: Polyvinyl acetate electrode reinforced by MnO_2/CuO loaded on graphene oxide nanoparticles, Food Chem. 194 (2016) 61–67.

[27] D. A. Armbruster, T. Pry, Limit of blank, limit of detection and limit of quantitation, Clin. Biochem. Rev. 29 (2008) S49–S52.

[28] K. Fan, X. Luo, J. Ping, W. Tang, J. Wu, Y. Ying, Q. Zhou, Sensitive determination of (-)-epigallocatechin gallate in tea infusion using a novel ionic liquid carbon paste electrode, J. Agri. Food Chem. 60 (2012) 6333–6340.

[29] L. P. Souza, F. Calegari, A. J. G. Zarbin, L. H. Marcolino-Júnior, M. F. Bergamini, Voltammetric determination of the antioxidant capacity in wine samples using a carbon nanotube modified electrode, J. Agri. Food Chem. 59 (2011) 7620–7625.

[30] D. Sarkar, S. Das, A. Pramanik, A solution spectroscopy study of tea polyphenol and cellulose: Effect of surfactants, RSC Adv. 4 (2014) 36196–36205.

[31] R. N. Goyal, S. Bishnoi, H. Chasta, M. A. Aziz, M. Oyama, Effect of surface modification of indium tin oxide by nanoparticles on the electrochemical determination of tryptophan, Talanta 85 (2011) 2626–2631.

[32] K. Huang, D. Niu, J. Sun, C. Han, Z. Wu, Y. Li, X. Xiong, Novel electrochemical sensor based on functionalized graphene for simultaneous determination of adenine and guanine in DNA, Colloids Surf. B Biointerfaces 82 (2011) 543–549.

[33] E. Laviron, General expression of the linear potential sweep voltammogram in the case of diffusionless electrochemical systems, J. Electroanal. Chem. Interfacial Electrochem. 101 (1979) 19–28.

[34] E. Laviron, Adsorption, autoinhibition and autocatalysis in polarography and in linear potential sweep voltammetry, J. Electroanal. Chem. Interfacial Electrochem. 52 (1974) 355–393.

[35] Y. Fan, K. Huang, D. Niu, C. Yang, Q. Jing, TiO_2- graphene nanocomposite for electrochemical sensing of adenine and guanine, Electrochim. Acta 56 (2011) 4685–4690.

[36] A. Masek, E. Chrzescijanska, M. Zaborski, Electrochemical properties of catechin in non-aqueous media, Int. J. Electrochem. Sci. 10 (2015) 2504–2514.

[37] S. Wold, M. Sjöström, L. Eriksson, PLS-regression: A basic tool of chemometrics, Chemometrics Intell. Lab. Syst. 58 (2001) 109–130.

[38] J. Burana-Osot, W. Yanpaisan, Catechins and caffeine contents of green tea commercialized in Thailand, J. Pharm. Biomed. Sci 22 (2012) 1–7.

[39] D. A. El-Hady, Selective and sensitive hydroxypropyl-betacyclodextrin based sensor for simple monitoring of (+)-catechin in some commercial drinks and biological fluids, Anal. Chim. Acta 593 (2007) 178–187.

[40] X. Wang, J. Li, Y. Fan, Fast detection of catechin in tea beverage using a poly-aspartic acid film based sensor, Microchim. Acta 169 (2010) 173–179.

[41] S. Masoum, M. Behpour, F. Azimi, M. H. Motaghedifard, Potentiality of chemometric approaches for the determination of (+)-catechin in green tea leaves at the surface of multiwalled carbon nanotube paste electrode, Sens. Actuators B Chem. 193 (2014) 582–591.

[42] S. K. Moccelini, S. C. Fernandes, T. P. de Camargo, A. Neves, I. C. Vieira, Self-assembled monolayer of nickel(II) complex and thiol on gold electrode for the determination of catechin, Talanta 78 (2009) 1063–1068.

[43] J. Wu, H. Wang, L. Fu, Z. Chen, J. Jiang, G. Shen, R. Yu, Detection of catechin based on its electrochemical autoxidation, Talanta 65 (2005) 511–517.

Chapter 4

Development of a nickel hydroxide nanopetal decorated molecular imprinted polymer based electrode for sensitive detection of epigallocatechin-3-gallate in green tea

This chapter reports the application of nickel hydroxide nanopetal decorated molecular imprinted polymer-graphite nanocomposite for efficient and selective detection of epigallocatechin-3-gallate (EGCG) in green tea. The diffraction patterns, structural variations and morphology of the samples were determined using XRD, FTIR, UV-vis spectroscopy and FESEM, respectively. The voltammetric results showed that the MIP-$Ni(OH)_2$ electrode demonstrated a considerable improvement in the detection of EGCG than the unmodified counterparts. The electrode exhibited a linear range from 10 µM to 100 µM and the corresponding detection limit is 7 nM (S/N=3). All the analytical characteristics of the electrode have been investigated detail and also the response in the green tea samples were found to be well correlated with the HPLC data.

List of sections

Content of this chapter is based on the following publications:

1. *T. Nandy Chatterjee et al., Development of a nickel hydroxide nanopetal decorated molecular imprinted polymer based electrode for sensitive detection of epigallocatechin-3-gallate in green tea, Sens. Actuators B Chem., 283 (2019) 69-78.*

2. *D. Das et al., Discrimination of green tea using an epigallocatechin-3-gallate (EGCG) sensitive molecular imprinted polymer (MIP) based electrode, Carbon-Science and Technology, 2018.*

Chapter 4

Development of a nickel hydroxide nanopetal decorated molecular imprinted polymer based electrode for sensitive detection of epigallocatechin-3-gallate in green tea

4.1. Introduction

It is known that the presence of polyphenols in green tea, which are rich in antioxidants, is referred as the 'Nutraceuticals of Modern Life' [1]. Catechins, belonging to the flavonoid group of polyphenols are in particular, the main quality parameter of green tea. It has four derivatives based on their structural variations namely, epicatechin (EC), epigallocatechin (EGC), epicatechin gallate (ECG) and epigallocatechin-3-gallate (EGCG). The most abundant and powerful form of catechin is EGCG, an ester of epigallocatechin and gallic acid [2, 3]. EGCG accounts for about 10 % of the extract in dry weight [4] and 50–80 % i.e. 200–300 mg in a brewed cup of green tea [5]. The structure of EGCG is shown in Fig.4.1.

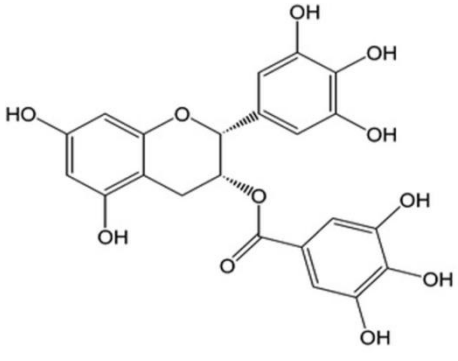

Fig.4.1. Chemical structure of EGCG

EGCG can act as a possible restorative agent for preventing neurodegenerative [6], inflammatory diseases [7], mainly due to their antioxidant, radical scavenging, metal chelating, anti-carcinogenic, and anti-apoptotic [8, 9] properties. The radical scavenging and metal chelating characteristics of EGCG is accredited to the presence of an ortho-trihydroxyl group in the B ring and the attachment of the galloyl moiety in its structure [10, 11]. Further, extensive research on EGCG have brought into light their ability to promote healthy ageing by improving the functional alterations that occur in a naturally ageing brain, their ability to suppress cognitive dysfunction [12], increase the learning ability [13] and reduce oxidative

damage in the brain [14]. Considering such potentials, development of a cost effective and reusable sensor for the detection of EGCG will be highly beneficial for the tea industries and the health sectors.

A number of sophisticated instrumental methods, such as high performance liquid chromatography (HPLC) [15-18], spectroscopic and spectrophotometric methods [19] have been employed for the determination of EGCG. Besides being costly, such techniques are tedious and demands highly skilled personnel. Electrochemical detection of EGCG, being comparatively much less expensive and a less time consuming process, have been practiced by few researchers as an alternative to the high-end ones [20]. But the working electrode used for the purpose is non-specific and thus unable for selective determination of EGCG.

In the previous chapters, MIP strategy has been already implemented for the detection of total theaflavins and catechin in black tea and green tea, respectively. Also, in regard to the detection of EGCG, there are very few literature reports which indicates the use of electropolymerized poly(*o*-phenylenedamine) [21] and β-cyclodextrin [22] for the preparation of MIPs thereby enabling determination of EGCG. However, it may be noted that the sensitivity of a MIP sensor is mainly dependant on the number of effective imprint sites available on the sensor surface [23]. Therefore, as compared to the electrodes having planar surfaces, modification of the MIP electrodes with nanostructured materials can result into high surface/volume ratio significantly enhancing the number of imprinted sites vacant for binding. In this pursuit, a number of reports are available concerning the preparation of electrodes using nanomaterial modified MIPs [24-27]. It is expected that with the advent of nanotechnology, nanostructured metal oxides/hydroxides, tailored to a desirable morphology accompanied by the MIP technique can serve as an alternate source of a cost effective and reusable sensor.

In this chapter, we describe the development of an EGCG sensor, where the MIP electrode has been prepared and further modified with nanostructured metal oxide/hydroxide nanoparticles using a simple solution route. The methodology followed for the synthesis and electrochemical studies of the MIP-EGCG electrode can be witnessed from Fig.2.2 (a) and (b) respectively, depicted in Chapter 2. The MIP was synthesized by the co polymerization of acrylonitrile along with EGDMA and was homogeneously mixed with the nanoparticles (CuO, TiO_2, $Ni(OH)_2$), thereby resulting in to MIP-CuO, MIP-TiO_2 and MIP-$Ni(OH)_2$ electrode. It has been observed from the CV results that the MIP-$Ni(OH)_2$ electrode

responded most profoundly towards EGCG than the other modified electrodes. Consequently, the electrochemical characteristics of the MIP-$Ni(OH)_2$ electrode towards EGCG has been detailed in this chapter. The analytical characteristic of the electrode has been vividly studied and it delivered a considerable wide linear range along with good selectivity, repeatability, reproducibility and stability characteristics. Further, the amount of EGCG in green tea samples were quantified using the proposed electrode and the results were found to be in an excellent union with the standard HPLC data when correlated by means of a partial least square regression (PLSR) model.

4.2. Experimental process

4.2.1. Chemical reagents

Commercial graphite powder (99%), acrylonitrile, cetylpyridinium chloride, ethylene glycol dimethacrylate (EGDMA), epigallocatechin gallate (EGCG), catechin hydrate (CAT), epicatechin gallate (ECG) and ascorbic acid (AA) were obtained from Sigma Aldrich, India. Benzoyl peroxide was purchased from Sisco Research Laboratories Pvt. Ltd, India. Nickel chloride hexahydrate ($NiCl_2.6H_2O$), sodium hydroxide (NaOH), copper chloride ($CuCl_2$), hydrofluoric acid, ammonium hydroxide, ethanol and paraffin oil were acquired from Merck & Co, India, respectively. All the reagents used in the experiment were of analytical grade and used as received. In all stages of the experiment and electrode preparation, Millipore water (Resistance 18 MΩ), obtained from Milli-Q water purification system was used.

4.2.2. Synthesis of nickel hydroxide ($Ni(OH)_2$) nanoparticles

Nickel hydroxide ($Ni(OH)_2$) nanopetals were synthesized in our laboratory based on a protocol as described in literature [28]. In a typical experiment, 6 g of $NiCl_2.6H_2O$ was dissolved in 250 ml of water followed by constant stirring for 30 minutes at 50˚C. Further, 4 g of NaOH pellets were dissolved in 20 ml of water and then added drop wise to the previous solution until its pH value approached 8. The solution was then filtered using a mixture of ethanol and water (60:40) thereby drying it at 80 °C for 4 hours. The material so obtained, was further calcined at 200°C in air for an hour to obtain the crystalline $Ni(OH)_2$ nanoparticles.

4.2.3. Synthesis of copper oxide (CuO) nanoparticles

Porous copper oxide nanoparticles have been synthesized by sol gel method. For the process, 10 gm of copper chloride ($CuCl_2$) is dissolved in 500 ml ethanol through rapid stirring for 10 minutes. Further, cetylpyridinium chloride is added to this solution followed by continuous stirring for 30 mins. The pH of the solution was monitored by adding 1 N sodium hydroxide (NaOH) solution dropwise till it became~ 8-9. After reaching the desired value of pH, a green colour precipitation is obtained. The precipitate is filtered and washed repeatedly with ethanol followed by drying in an oven for 1 hour at 50 °C. The dried sample was calcined at 400 °C for 3 hours in air after which a black colour copper oxide (CuO) powder is obtained.

4.2.4. Synthesis of titanium oxide (TiO_2) nanoparticles

Titanium dioxide nanoparticles have been synthesized by taking 10 gm of titanium dioxide in 50 ml of hydrofluoric acid followed by addition of 10 ml of polyethylene glycol. The resulting solution is stirred well in a magnetic stirrer. After that 40 ml of ammonium hydroxide is added cautiously until a white precipitation observed. The resultant precipitate is filtered and washed with distilled water followed by drying. The white precipitation is then heat treated in air for 3 hours at 500 °C in air, thereby yielding a yellowish powder.

4.2.5. Synthesis of molecular imprinted polymer (MIP) and non-imprinted polymer(NIP)

The MIP sample was prepared using an already optimized protocol discussed in Chapter 3. Firstly, 0.95 g of commercial graphite powder was dispersed in 15 ml of ethanol for 2 hours. Then 0.05 g of acrylonitrile and 0.02 g of EGCG were added to the dispersed solution under constant stirring. After 2 hours, 1 mg of benzoyl peroxide (polymerization initiator) and 400 µL of EGDMA were added to the same solution and it was stirred constantly for 2 hours in pure N_2 atmosphere. The mixture was then heated in a water bath for 1 hour for polymerization to take place. The final product, i.e., the polymerized powder, was then collected and dried.

For the preparation of the MIP, the template (here EGCG) was extracted from the polymerized powdered sample by washing it with a mixture of acetone and water (80:20) repeatedly until no traces of EGCG were found. The complete removal of EGCG was confirmed by UV-vis spectroscopy in the scanning range of 200-800 nm. The NIP sample was prepared in the same way except that EGCG was not added during its preparation.

4.2.6. Preparation of the electrodes using metal oxide/hydroxide modified MIP and NIP samples

For the preparation of the electrodes, previously synthesized nanoparticles of CuO, TiO_2 and $Ni(OH)_2$ were added to both the MIP and the NIP samples keeping the ratio to 1:4. Then 0.3 g of the respective powders was made into fine paste with the addition of paraffin oil. The paste was then poured into fine capillary glass tubes of inner diameter 2.5 mm. The electrical contacts of the electrode were made by connecting a Pt wire to the backside of the tubes. The surface of the electrodes were polished with Al_2O_3 slurry, smoothed and rinsed carefully with Millipore water before each electrochemical measurement. The methodology related to the preparation of the electrode and the corresponding measurement setup employed in our laboratory has been illustrated in Fig.2.3 and Fig.2.4 in Chapter 2, respectively.

4.3. Results and discussions

4.3.1. XRD analysis of the prepared nanoparticles

The powder X-ray diffraction pattern of the prepared $Ni(OH)_2$, CuO and TiO_2 samples are depicted in Fig.4.2, respectively.

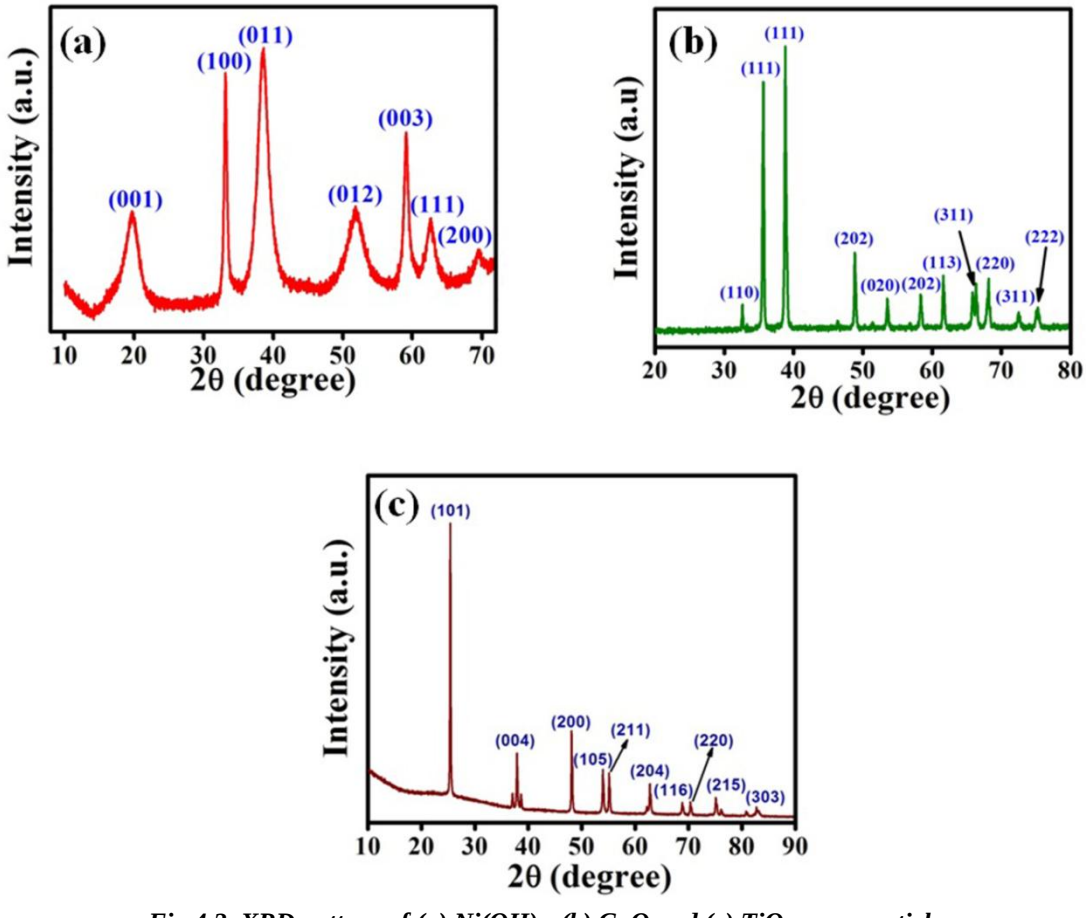

Fig.4.2. XRD pattern of (a) $Ni(OH)_2$, (b) CuO and (c) TiO_2 nanoparticles

Fig.4.2 (a) reveals well defined spectra distinctive of $Ni(OH)_2$ as correlated from JCPDS No. 74-2075. Diffraction peaks obtained at 19.69°, 33.27°, 38.65°, 51.988°, 59.14°, 62.74°, 69.92°, respectively, can be attributed to the (001), (100), (011), (012), (003), (111) and (200) planes of the hexagonal $Ni(OH)_2$.

The formation of CuO was confirmed from JCPDS No. 80-1916, where diffraction peaks were obtained at 32.47°, 35.49°, 38.68°, 38.89°, 46.19°, 48.65°, 53.40°, 61.45°, 66.1°, 68°, 72.32° and 75.12°, respectively. These can be assigned to the (110), (111), (202), (020), (113), (311) and (222) planes and the structure of CuO is monoclinic in nature. Similarly, the formation of anatase TiO_2 as shown in Fig.4.2 (c) can be witnessed from the diffraction peaks present at 25.45°, 36.93°, 37.98°, 47.99°, 54.06°, 55.25°, 62.63°, 68.95°, 70.28°, 75.30°, 80.71° and 82.81°, respectively (JCPDS No. 84-1286). The corresponding (hkl) planes are (101), (103), (004), (200), (105), (211), (204), (116), (220), (215), (008) and (303), respectively. The absence of any other peaks in the XRD spectra of the samples shown in Fig.4.2 also indicates that the corresponding $Ni(OH)_2$, CuO and TiO_2 so formed, consists of no impure phases.

The average crystallite size of the samples were calculated using the Debye-Scherer method [29] considering the diffraction pattern of the most intense peaks and it was found to be (11.39 ± 6.31) nm, (41.6 ± 7.70) nm and (38.6 ± 9.86) nm for $Ni(OH)_2$, CuO and TiO_2, respectively.

4.3.2. FTIR and UV-vis spectroscopic analysis

The FTIR spectra of the $Ni(OH)_2$ modified MIP sample was carried out and the results are depicted in Fig.4.3 (a). The figure reveals the presence of bands at 3432 cm^{-1}, due to the –OH stretching of water. The spectra present in the region of 2852 cm^{-1}, 2921 cm^{-1}, 1436 cm^{-1} and 1074 cm^{-1}, respectively, can be attributed to the formation of polyacrylonitrile [30]. The stretching and bending vibrations of methylene group is witnessed at bands centered at 2921 cm^{-1} and 1436 cm^{-1}, respectively [31]. Moreover, the band at 1647 cm^{-1} corresponding to the C-N bond unveils the typical signature of polyacrylonitrile. Additionally, it may also be noted from the figure that at 598 cm^{-1}, there is a spectrum due to the Ni-O-H stretching vibrations [32]. Therefore, the FTIR spectra strongly justifies the formation of the polyacrylonitrile-graphite nanocomposite modified by $Ni(OH)_2$ nanoparticles.

An UV-vis absorption spectroscopy has been performed with the samples before (BRT) and after (ART) removal of EGCG, respectively. The absorption spectra are shown in Fig.4.3 (b). It may be observed from the figure that the absorption peak of EGCG at 277 nm [33] disappeared completely upon its extraction during the formation of MIP. This confirms that the template molecule was removed successfully from the MIP sample.

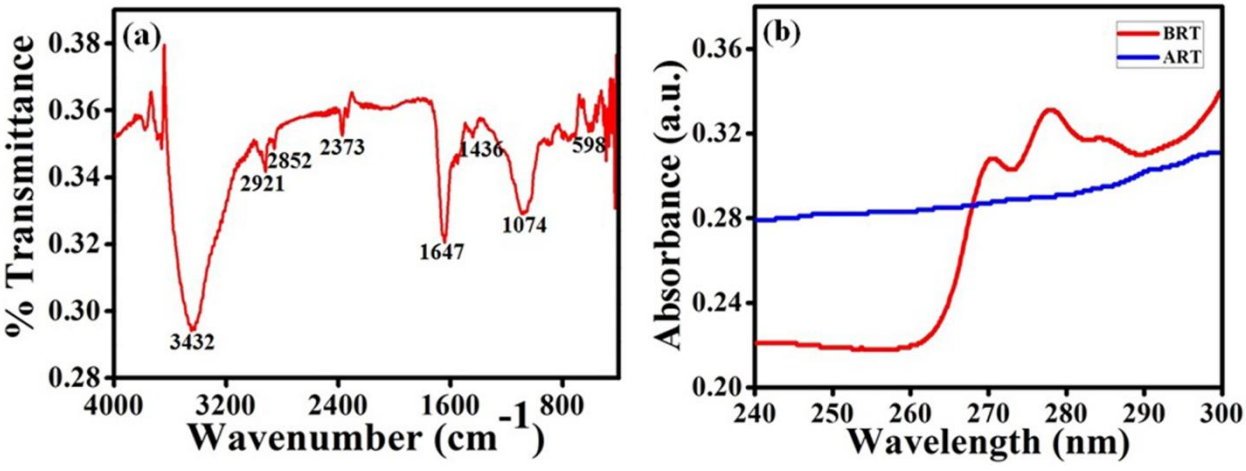

Fig.4.3. (a) FTIR spectra of the MIP sample; (b) UV-vis spectra of the sample before (BRT) and after (ART) removal of EGCG

4.3.3. Morphological studies using FESEM

The field emission scanning electron microscopy (FESEM) images as shown in Fig.4.4 (a) and (b) reveal the morphologies of $Ni(OH)_2$ in different magnification ranges. The images depict nanoflower like structure of $Ni(OH)_2$ of thickness (12 ± 3) nm with its petals interweaved together. Additionally, Fig.4.4 (c) and (d) shows the FESEM images of the MIP and the NIP sample, respectively. It may be observed from the figure that the surface of the MIP sample is rough and rugged; whereas, the NIP sample is comparatively smoother in nature.

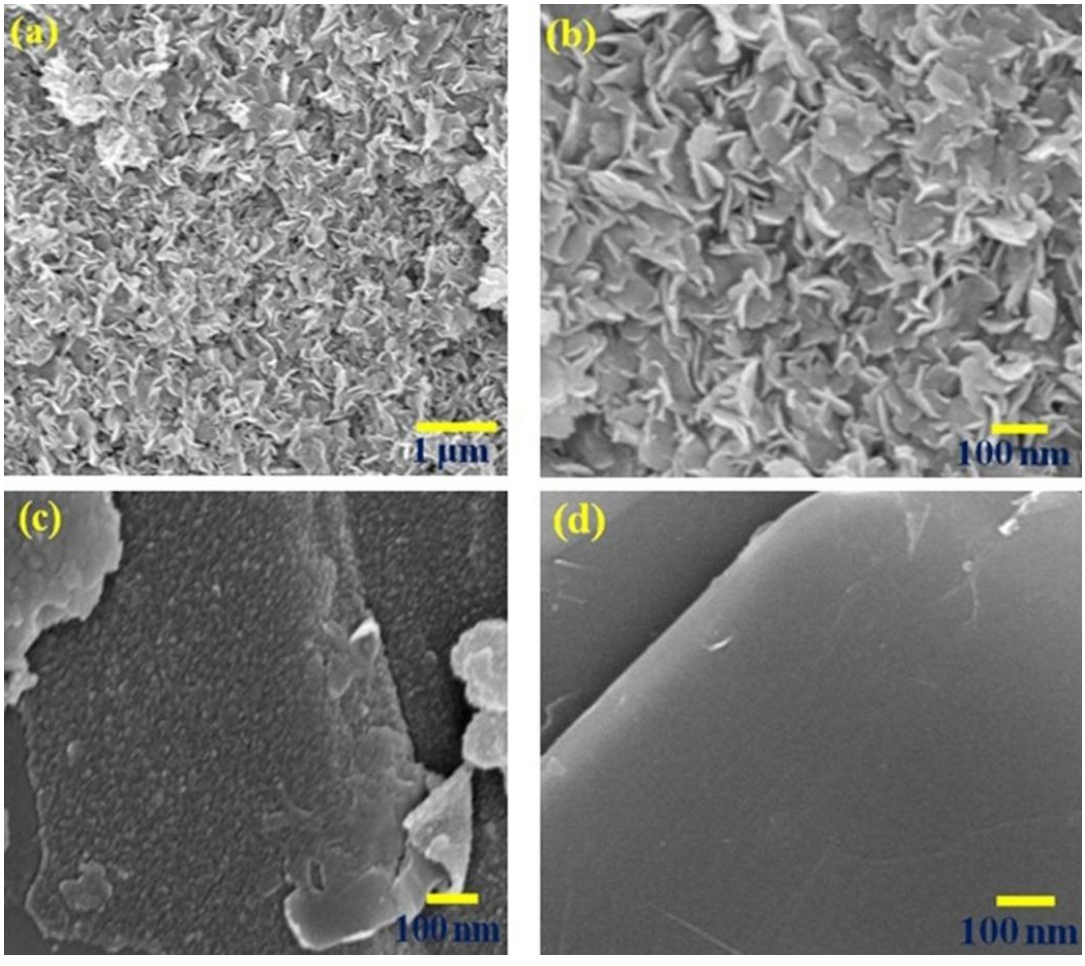

Fig.4.4. (a) and (b) FESEM images of $Ni(OH)_2$ sample at different magnifications; FESEM images of (c)MIP sample and (d) NIP sample

4.3.4. Optimization of the experimental conditions

The electrochemical characteristics of all the synthesized metal oxide/hydroxide nanoparticle modified MIP electrodes were compared in presence of 1mM EGCG for selecting the best electrode among the four in terms of detection of EGCG. The corresponding CV is depicted in Fig.4.5.

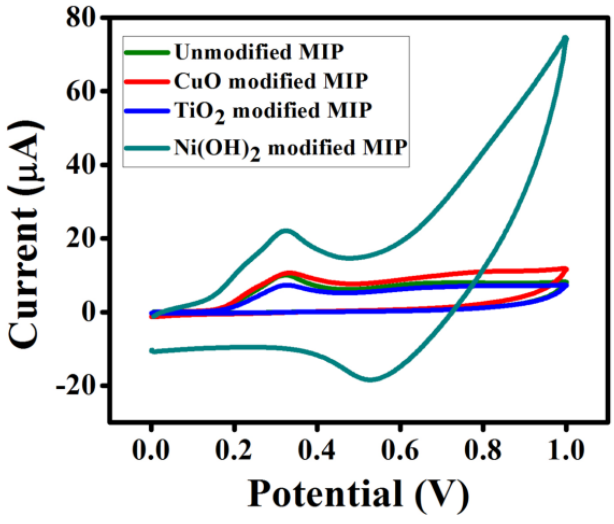

Fig.4.5. Comparative CV containing the response profile of unmodified MIP, CuO modified MIP, TiO_2 modified MIP and $Ni(OH)_2$ modified MIP electrodes in presence of 1 mM EGCG

Table 4.1 Comparison of the peak currents of the metal oxide/hydroxide nanoparticle modified MIP electrodes

Sl. No.	Electrodes	Peak current (µA)
1	TiO_2 modified MIP	7.76
2	CuO modified MIP	11.07
3	**$Ni(OH)_2$ modified MIP**	**22.46**
4	Unmodified MIP	10.23

Table 4.1 presents the peak current values obtained for each of the working electrodes from the CV response profile. It may be noted from the figure and the table that $Ni(OH)_2$ modified MIP electrode showed the highest peak current (22.46 µA) than the other electrodes, when exposed to the similar concentration of EGCG. Thus the further electrochemical measurements were carried out using $Ni(OH)_2$ modified MIP electrode in this chapter.

The electrochemical characteristics of an electrode are highly affected by the pH value of the test solution. Therefore, in order to investigate the influence of pH on the modified MIP sensor, cyclic voltammetry tests were carried out in 1 mM EGCG using phosphate buffer solution (PBS) of pH values 5, 6 and 7, respectively. The response curves are shown in Fig.4.6 (a). It may be observed from the figure that in case of PBS 6, the electrode offered sharp response having a peak current of 23.47 µA, much prominent and higher than that of the other pH values. Hence, PBS 6 is chosen to be the test solution for the entire experiment.

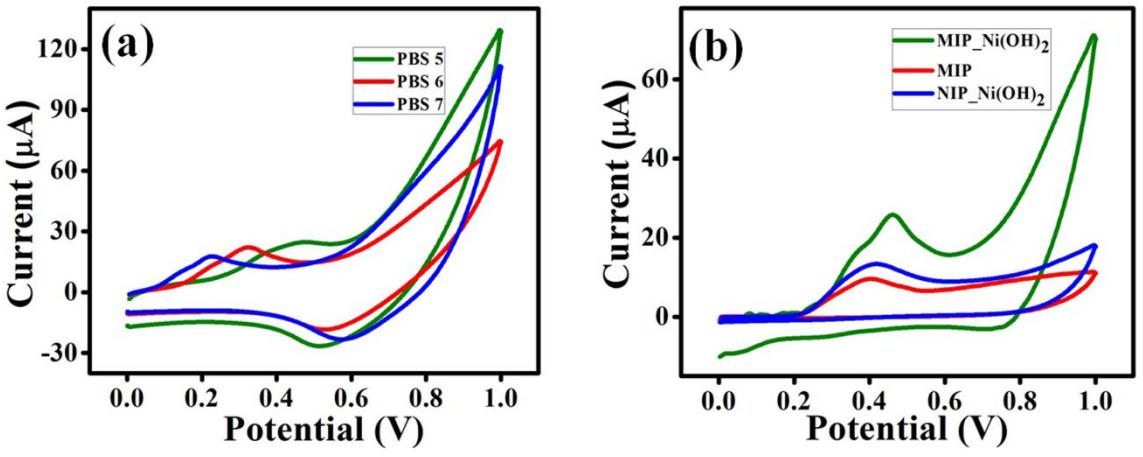

Fig.4.6. CV of 1 mM EGCG in (a) PBS 5, PBS 6 and PBS 7; (b) using MIP_Ni(OH)$_2$, NIP_Ni(OH)$_2$ and unmodified MIP electrode.

Further, in order to study the performance of the $Ni(OH)_2$ modified MIP electrode over the unmodified one, cyclic voltammogram were obtained using both the electrodes in 1 mM EGCG solution. After each electrochemical measurement, electrodes were washed in a mixture of acetone and water and the surface were regenerated. The corresponding response profile, as shown in Fig.4.6 (b) reveals that the MIP-$Ni(OH)_2$ electrode showed a considerable rise in peak current at 0.46 V than that offered by the unmodified MIP electrode. Also, it can be seen from the figure that though the NIP-$Ni(OH)_2$ electrode responded adequately to the target analyte at the potential value of 0.42 V, the corresponding peak current is relatively lower than that of the MIP-$Ni(OH)_2$ electrode.

The sharp increment in the peak current, as revealed by the MIP-$Ni(OH)_2$ electrode, is mainly due to the high surface area and high surface to volume ratio of the $Ni(OH)_2$ nanopetals.They are believed to promote high electron transfer in the active sites as created due to the removal of EGCG from the polymer composite. However, in case of the unmodified MIP sample, the rate of electron transfer is hindered to a considerable extent and thus it depicts a comparatively lower peak current. On the other hand, the NIP-$Ni(OH)_2$ electrode was found to offer reduced response inspite of the existence of $Ni(OH)_2$ nanoparticles. This is mainly due to the presence of low specific or non specific sites on the electrode surface.

4.3.5. Concentration variation and linearity

Differential pulse voltammetry (DPV) measurements were conducted to study the dependence of current profile of the electrode on the concentration of the analyte solution. As documented earlier, the potential range of the DPV experiments was kept between 0.0 V to

0.8 V. The step potential, modulation amplitude and modulation time was maintained at 0.01 V, 0.005 V and 0.2 s, respectively. The scan rate and the interval time were kept fixed at 0.025 V/s and 0.4 s, respectively.

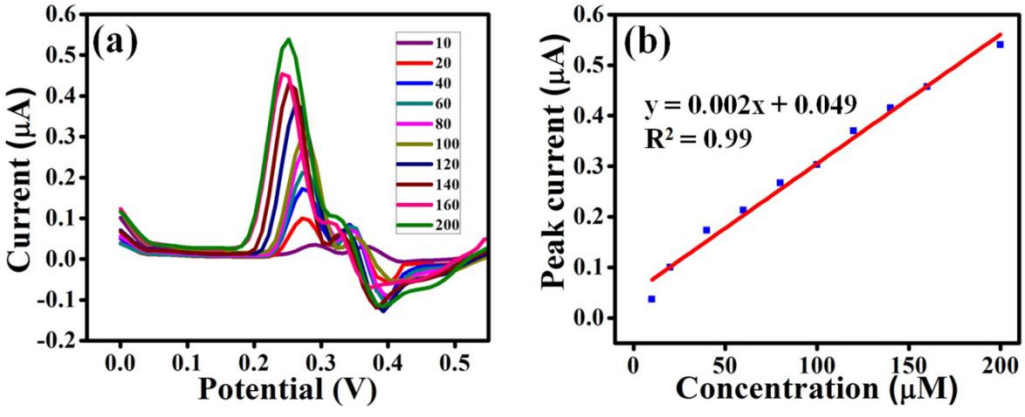

Fig.4.7. (a) DPV showing the concentration variation; b) Linearity plot of concentration variation

Fig.4.7 (a) shows that with the increase in the concentration (*c*) of EGCG, the corresponding oxidation peak current (*Ip*) increases, thereby having a linear relationship in the concentration range from 10 µM to 200 µM. The calibration curve, as shown in Fig.4.7 (b) can be represented in the form of the following equation (4.1)

$$Ip = 0.002c + 0.049 \quad (4.1)$$

where the square of the correlation coefficient (R) has been calculated as R^2= 0.99. The proposed MIP-Ni(OH)$_2$ exhibited limit of detection (LOD) value of 7 nM as calculated from 3*Sy/x/m* [34]. Here *Sy/x* and *m* are the standard deviation of the regression line and slope of the calibration curve, respectively.

4.3.6. Effect of scan rate

To study the electrochemical behavior of synthesized electrode and the kinetics involved in the reaction, the scan rate was varied, keeping the concentration of the test solution fixed. The MIP-Ni(OH)$_2$ electrode was subjected to CV in 1mM EGCG by varying the scan rate from 0.005 V/s to 0.09 V/s (shown in Fig.4.8 (a)). It is obvious from the figure that the electrochemical reaction is irreversible in nature. Also, it can be inferred from Fig.4.8 (b), the peak current (*Ip*) of the test solution increases linearly along with that of the scan rate (*v*), thereby indicating that the oxidation of EGCG is an adsorption controlled process [35]. The corresponding linear regression equation can be expressed as in equation (4.2).

$$Ip = 221.3\,v + 7.344 \quad (4.2)$$

The correlation coefficient of the calibration curve has been calculated as R^2= 0.99.

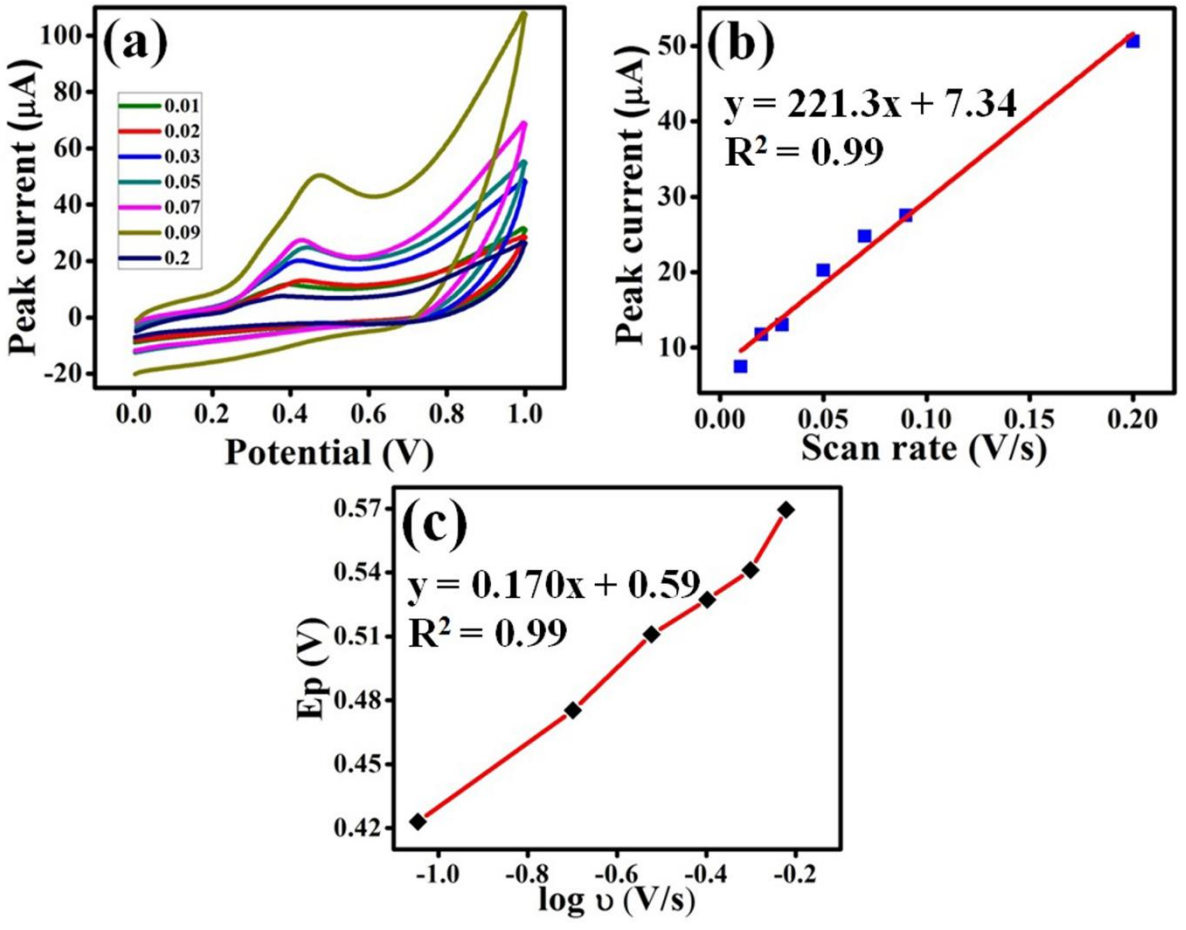

Fig.4.8. (a) CV indicating the variation of scan rate; (b) Variation of peak current with the scan rate; (c) Variation of peak potential with the logarithm of scan rate

In this work, for the first time, the kinetics of the reaction system involved in the oxidation of EGCG has been studied in detail. The number of electrons transferred as well as the surface concentration of the EGCG has been calculated using equation (4.3) [36],

$$Ip = \frac{nFQv}{4RT} = \frac{n^2F^2Av\Gamma_c}{4RT} \quad (4.3)$$

where, n, F, A, Γ_c, Q, R and T are the number of electrons transferred, Faraday's constant, area of the electrode, surface concentration, quantity of charge consumed during the oxidation process, gas constant and absolute temperature, respectively. The value of n and Γ_c calculated from equation (4.3) are 2.29 and 2.22 x 10^{-9} mole cm^{-2}, respectively. Fig.4.8 (c) depicts the relationship between oxidation potential (E_p) and logarithm of the scan rate (log ν). The value of E_p shifts in the positive direction and also increases linearly along with log ν. The regression equation of the calibration curve is given in equation (4.4) with R^2= 0.99.

$$E_p = 0.170 \log v + 0.598 \quad (4.4)$$

The electron transfer coefficient (α) was calculated as 0.85 from the slope of the calibration curve of Eq. (4.4). The heterogeneous rate constant (k_s) of the oxidation reaction has been calculated as 0.16 s^{-1} using the well known Laviron's equation [37, 38] expressed in equation (4.5).

$$\log k_s = \alpha \log (1 - \alpha) + (1 - \alpha) \log \alpha - \log (RT/nF\,v) - nF\Delta E_p\, \alpha(1 - \alpha)/2.3RT \qquad (4.5)$$

Therefore, from the above deductions, it can be concluded that the proposed electrode exhibits a two electron-two proton transfer process and it also promotes the electron transfer by a reasonable amount.

4.3.7. Analytical characteristics of the electrode

The analytical properties of the synthesized electrode have been studied in terms of its selectivity, stability, repeatability and reproducibility characteristics.

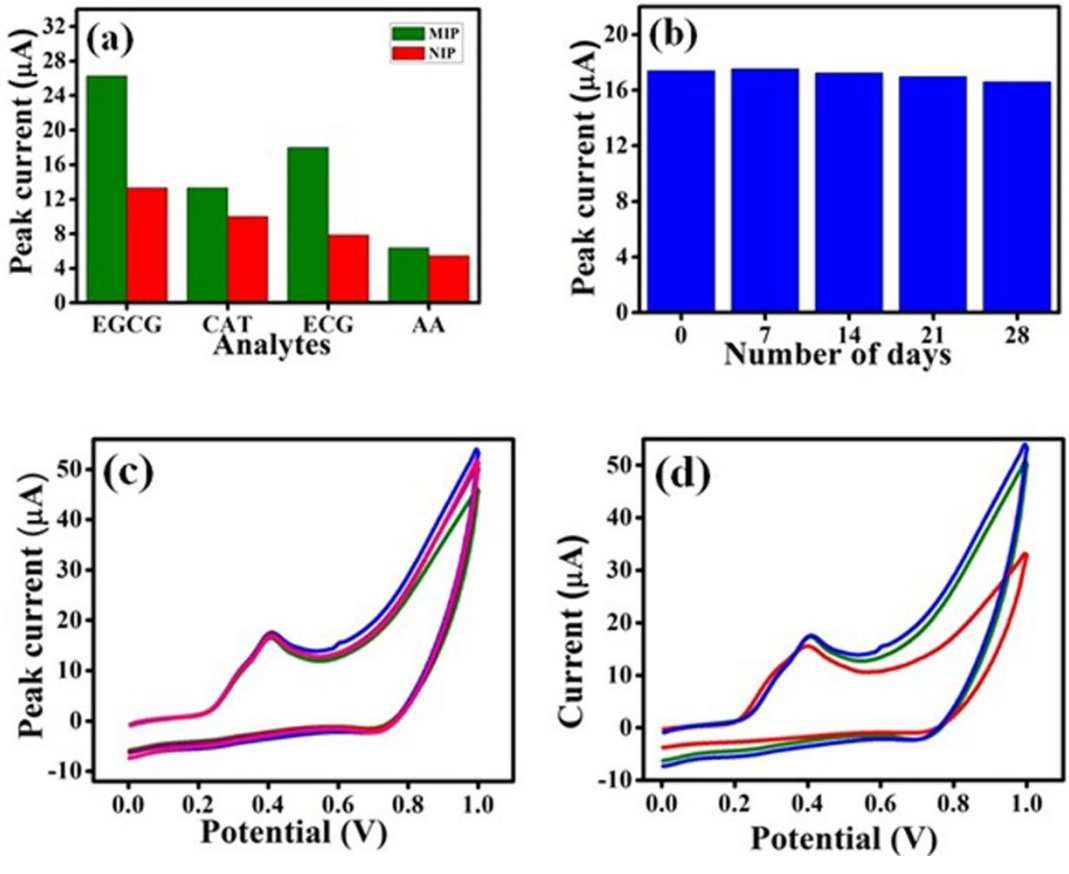

Fig.4.9. Analytical characteristics of the electrode showing (a) selectivity; (b) stability; (c) repeatability and (d) reproducibility

The MIP-$Ni(OH)_2$ electrode, along with EGCG, was subjected to some of the important chemical constituents of green tea for example, structural analogous compounds such as catechin (CAT), ECG and also in AA. All test solutions were prepared in the same concentration of 1 mM. The MIP-$Ni(OH)_2$ and the NIP-$Ni(OH)_2$ were dipped into these solutions and the corresponding response profile was recorded (shown in Fig.4.9 (a)).

From the figure, we can easily conclude that the MIP sensor shows highest affinity for its probe molecule when compared to its analogues. For ascorbic acid, both the MIP and NIP electrodes give the lowest oxidation peak currents as expected.

To evaluate the long-term stability of the modified electrode, it was stored at room temperature in air for 7 days. Then, the modified electrode was tested again in the same test solution of 1 mM EGCG in PBS buffer after every 7 days. The results shown in Fig.4.9 (b) revealed that there was no significant change in the peak currents. All these results indicate that the MIP-$Ni(OH)_2$ has good stability, which make it attractive for the fabrication of a new electrochemical sensor and also indicates that the imprinted electrode can be used for a relatively long time to detect EGCG.

In view of studying the repeatability of the electrode, the MIP-$Ni(OH)_2$ electrode was employed to obtain five successive responses of 1 mM EGCG solution. The corresponding voltammogram, as shown in Fig.4.9 (c), indicates that the responses curves are almost identical to each other, indicating an excellent repeatability. The relative standard deviation (RSD) calculated from the waveform, accounted to be 2.17 %.

The reproducibility of the electrode was studied by preparing three different sensors using the same protocol. Cyclic voltammogram were obtained using all the electrodes in 1 mM EGCG solution. As can be inferred from Fig.4.9 (d), the change in peak current corresponding to a fixed concentration of analyte is minimum having RSD value of 6.45%. Therefore, the electrode is reproducible in nature and can yield repeatable results.

4.3.8. Analysis of green tea samples

The MIP-$Ni(OH)_2$ electrode synthesized in the present work, was subjected to fifteen green tea samples inorder to measure the amount of EGCG present in them. DPV response of a typical tea sample is presented in Fig.4.10.

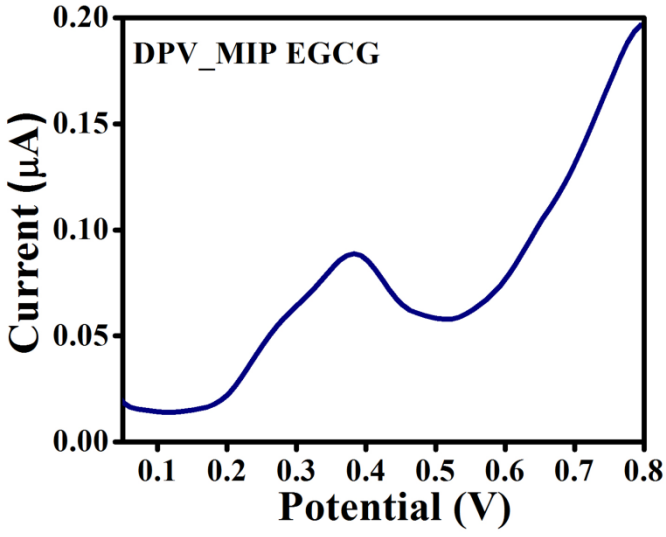

Fig.4.10. DPV response of a green tea sample obtained using the MIP-EGCG electrode

Here also the total EGCG content in the units of mg/g green tea samples were predicted by means of a partial least square regression (PLSR) model using MATLAB Version 14 [39]. Herein, leave one out cross validation (LOOCV) technique has been employed where the training set was constructed by eliminating dataset of a sample randomly, and the model was tested using the excluded data set. The predicted value of EGCG along with its actual value (from HPLC data) and the corresponding prediction accuracy are detailed in Table 4.2. The number of components of the model was kept to four thereby considering the root mean square error of cross validation (RMSECV) and the correlation factor (CF) values, which were 0.85 and 0.08, respectively. It is interesting to note that the prediction accuracies of ten samples (67 % of the total set) are greater than 90 % and three of them have an accuracy of over 99 %. The average prediction accuracy has been calculated as 93.85 %. Therefore, the prediction results suggest that performance of the electrode is reasonably good for the quantification of EGCG in real samples.

Table 4.2 Actual and predicted EGCG content from the LOOCV based PLS model

Sample No.	Actual EGCG (mg/g)	Predicted EGCG (mg/g)	Prediction accuracy (%)
1	8.7	8.75	99.39
2	8.1	8.25	98.05
3	10.65	10.65	99.96

Sample No.	Actual EGCG (mg/g)	Predicted EGCG (mg/g)	Prediction accuracy (%)
4	11.53	10.61	92.07
5	12	10.79	89.93
6	12.49	11.07	88.67
7	8.13	9.63	81.51
8	9.63	10.92	86.58
9	10.53	10.76	97.78
10	10.38	10.83	95.66
11	11.64	11.31	97.19
12	10.05	9.30	97.32
13	11.58	11.04	95.35
14	10	11.12	88.71
15	11.33	11.38	99.55

4.3.9. Comparison of the proposed technique with the reported methods

There are very few reports in connection with the electrochemical detection of EGCG. Table 4.3 compares the results obtained by such methods with the proposed mechanism of detection described in this chapter. It may be observed from the table that the methodology described here yielded a very wide linear range and also the limit of detection is lowest among the other ones, which includes some works on MIP as well.

Table 4.3 Comparison of the proposed technique with that of the reported works

Electrode's material	Principle of detection	LOD (nM)	Linear range (μM)	References
Glassy carbon electrode	-	65.9	0.1-1	[20]
Glassy carbon electrode modified with poly(*o*-phenylenediamine) film	MIP	160	0.5-100	[21]
β-cyclodextrin and graphene oxide modified glassy carbon electrode	MIP	8.78	0.03-10	[22]

Electrode's material	Principle of detection	LOD (nM)	Linear range (µM)	References
$Ni(OH)_2$ modified polyacrylonitrile-graphite nanocomposite electrode	**MIP**	**7**	**10-200**	**This work**

4.4. Conclusion

The astringency and bitterness to a lower degree is mainly due to the EGCG content present in green tea. It is the most powerful antioxidant present in green tea having several health benefits. In the research work presented in this chapter, we describe the development of a highly sensitive and selective electrochemical sensor modified with $Ni(OH)_2$ nanopetals for the detection of EGCG based on molecular imprinted polymer technology. The thin $Ni(OH)_2$ nanopetals, in combination with the selective MIP reduces the electron diffusion distance and allows surface dependent Faradaic reactions to occur. The experimental results demonstrated that the MIP electrode modified with $Ni(OH)_2$ offered better electrochemical response than the unmodified MIP. Under optimized experimental conditions, the response of the imprinted electrode was linear in the concentration range from 10µM to 100µM with a detection limit as low as 7 nM. The obtained value of LOD is sufficiently lower than the amount of EGCG (approx. 0.016 M) present in green tea. The electrode also demonstrated a sensible selectivity along with good repeatability and reproducibility. Additionally, this sensor has been applied successfully to detect EGCG in the real green tea samples, as revealed by the PLSR model. Therefore, the proposed methodology can be understood as a simple, easily deployable and cost effective technique for the efficient quantitative determination of EGCG in the remote tea industries.

References

[1] Green tea polyphenols; nutraceuticals of modern life, Ed. By Lekh R. Juneja, Mahendra P. Kapoor, Tsutomu Okubo and Theertham P. Rao, CRC press, 2013.

[2] T. Nakazato, K. Ito, Y. Ikeda, M. Kizaki, Green tea component, catechin, induces apoptosis of human malignant B cells via production of reactive oxygen species, Clin. Cancer Res. 11 (2005) 6040–6049.

[3] J. D. Lambert, R. J. Elias, The antioxidant and pro-oxidant activities of green tea polyphenols: A role in cancer prevention, Arch. Biochem. Biophys. 501 (2010) 65–72.

[4] N. A. Singh, A. K. A. Mandal, Z. A. Khan, Potential neuroprotective properties of epigallocatechin-3-gallate (EGCG), Nutr J. 15 (2016) 1-17.

[5] N. Khan, F. Afaq, M. Saleem, N. Ahmad, H. Mukhtar, Targeting Multiple Signaling Pathways by Green Tea Polyphenol (-) Epigallocatechin-3-Gallate, Cancer Res. 66 (2006) 2500-2505.

[6] S. Mandel, O. Weinreb, T. Amit, M. B. Youdim, Cell signaling pathways in the neuroprotective actions of the green tea polyphenol (-)-epigallocatechin-3-gallate: implications for neurodegenerative diseases, J. Neurochem. 88 (2004) 1555-1569.

[7] R. Singh, N. Akhtar, T. M. Haqqi, Green tea polyphenol epigallocatechin-3-gallate: inflammation and arthritis, Life Sci. 86 (2010) 907–918.

[8] H. Fujiki, S. Yoshizawa, T. Horiuchi, M. Suganuma, J. Yatsunami, S. Nishiwaki, S. Okabe, R. N. Matsushnima, T. Okuda, T. Sugimura, Anticarcinogenic effects of (-)-epigallocatechin gallate, Prev. Med. 21 (1992) 503-509.

[9] G. Nie, C. Jin, Y. Cao, S. Shen, B. Zhao, Distinct effects of tea catechins on 6-hydroxydopamine-induced apoptosis in PC12 cells, BArch BiochemBiophys. 397 (2002) 84–90.

[10] F. Nanjo, K. Goto, R. Seto, M. Suzuki, M. Sakai, Y. Hara, Scavenging effects of tea catechins and their derivatives on 1,1- diphenyl-2-picrylhydrazyl radical, Free. Radic. Biol. Med. 21 (1996) 895–902.

[11] C. Hu, D. D. Kitts, Evaluation of antioxidant activity of epigallocatechin gallate in biphasic model systems *in vitro*, Mol. Cell. Biochem. 218 (2001) 147-155.

[12] K. Unno, F. Takabayashi, T. Kishido, N. Oku, Suppressive effect of green tea catechins on morphologic and functional regression of the brain in aged mice with accelerated senescence (SAMP10), Exp. Gerontol. 39 (2004) 1027-1034.

[13] K. Unno, F. Takabayashi, H. Yoshida, D. Choba, R. Fukutomi, N. Kikunaga, T. Kishido, N. Oku, M. Hoshino, Daily consumption of green tea catechin delays memory regression in aged mice, Biogerontology 8 (2007) 89–95.

[14] S. Schaffer, H. Asseburg, S. Kuntz, W. E. Muller, G.P. Eckert, Effects of polyphenols on brain ageing and Alzheimer's disease: Focus on mitochondria, Mol. Neurobiol. 46 (2012) 161–178.

[15] M. S. EI- Shahawi, A. Hamza, S. O. Bahaffi, A. A. AI- Sibaai, T. N. Abduljabbar, Analysis of some selected catechins and caffeine in green tea by high performance liquid chromatography, Food Chem. 134 (2012) 2268-2275.

[16] J. F. Fangueiro, A. Parra, A. M. Silva, M. A. Egea, E. B. Souto, M. L. Garcia, M. L. Calpena, Validation of high performance liquid chromatography method for the stabilization of epigallocatechin gallate, Int. J. Pharm. 475 (2014) 181-190.

[17] S. Misaka, K. Kawabe, S. Onoue, J. P. Werba, M. Girolli, J. Kimura, H. Watanabe, S. Yamada, Development of rapid and simultaneous quantitative method for green tea catechins on the bioanalytical study using UPLC/ ESI-MS, Biomed Chromatogr. 27 (2013) 1-6.

[18] S. Khokhar, D. Venema, P. C. H. Hollman, M. Dekker, W. Jongen, A RP-HPLC method for the determination of tea catechins, Cancer Lett. 114 (1997) 171-172.

[19] Y. M. Ibrahim, A. Musa, I. A. Yakasai, Spectrophotometric method for determination of catechins in green tea and herbal formulations, Niger. J Pharm. Sci. 16 (2017) 25-30.

[20] I. Novak, M. Šeruga, Š. K. Lovrić, Electrochemical characterization of epigallocatechin gallate using square wave voltammetry, Electroanalysis 21 (2009) 1019-1025.

[21] Y. Duan, X. Luo, Y. Qin, H. Zhang, G. Sun, X. Sun, Determination of epigallocatechin-3-gallate with a high-efficiency electrochemical sensor based on a molecularly imprinted poly(*o*-phenylenediamine) film, J. Appl. Polym. Sci. 129 (2013) 2882-2890.

[22] Y. Liu, L. Zhu, Y. Hu, X. Peng, J. Du, A novel electrochemical sensor based on a molecularly imprinted polymer for the determination of epigallocatechin gallate, Food Chem. 221 (2017) 1128-1134.

[23] M. A. Beluomini, J. L. da Silva, G. G. Sedenho, N. R. Stradiotto, D-mannitol sensor based on molecularly imprinted polymer on electrode modified with reduced graphene oxide decorated with gold nanoparticles, Talanta 165 (2017) 231-239.

[24] X. Tan, Q. Hu, J. Wu, X. Li, P. Li, H. Yu, X. Li, F. Lei, Electrochemical sensor based on molecularly imprinted polymer reduced graphene oxide and gold nanoparticles modified electrode for detection of carbofuran, Sens Actuators B Chem. 220 (2015) 216-221.

[25] H. Rao, M. Chen, H. Ge, Z. Lu, X. Liu, P. Zou, X. Wang, H. He, X. Zeng, Y. Wang, A novel electrochemical sensor based on Au@PANI composites film modified glassy carbon electrode binding molecular imprinting technique for the determination of melamine, Biosens. Bioelect. 87 (2017) 1029-1035.

[26] L. Wang, L. Miao, H. Yang, J. Yu, Y. Xie, L. Xu, Y. Song, A novel nanoenzyme based on Fe_3O_4 nanoparticles@thionine-imprinted polydopamine for electrochemical biosensing, Sens. Actuators B Chem. 253 (2017) 108-114.

[27] J. Huang, X. Zhang, S. Liu, Q. Lin, X. He, X. Xing, W. Lian, D. Tang, Development of molecularly imprinted electrochemical sensor with titanium oxide and gold nanomaterials enhanced technique for determination of 4-nonylphenol, Sens Actuators B Chem. 152 (2011) 292-298.

[28] A. Rahdar, M. Aliahmad, Y. Azizi, NiO Nanoparticles: Synthesis and Characterization, J. Nanostruct. 5 (2015) 145- 151.

[29] B. D. Cullity and S. R. Stock, Elements of X-ray diffraction, Addison-Wesley, Boston, MA, USA, 2001.

[30] F. Nacimiento, R. Alcántara, J. R. González, J. L. Tirado, Electrodeposited polyacrylonitrile and cobalt-tin composite thin film on titanium substrate, J. Electrochem. Soc. 159 (2012) A1028-A1033.

[31] H. Wu, D. H. Bremner, H. Li, Q. Shi, J. Wu, R. Xiao, L. Zhu, A novel multifunctional biomedical material based on polyacrylonitrile: Preparation and characterization, Mater. Sci. Eng. C 62 (2016) 702-709.

[32] D. P. Dubal, V. J. Fulari, C. D. Lokhande, Effect of morphology on supercapacitive properties of chemically grown β-$Ni(OH)_2$ thin films, Microporous Mesoporous Mater. 151 (2012) 511-516.

[33] X. Zheng, A. Chen, T. Hoshi, J. Anzai, G. Li, Electrochemical studies of (−)-epigallocatechin gallate and its interaction with DNA, Anal. Bioanal. Chem. 386 (2006) 1913-1919.

[34] D. A. Armbruster, T. Pry, Limit of blank, limit of detection and limit of quantitation, Clin. Biochem. Rev. 29 (2008) S49–S52.

[35] İ. H. Taşdemir, M. A. Akay, N. Erk, E. Kiliç, Voltammetric behavior of Telmisartan and cathodic adsorptive stripping voltammetric method for its assay in pharmaceutical dosage forms and biological fluids, Electroanalysis 22 (2010) 2101-2109.

[36] K. Huang, D. Niu, J. Sun, C. Han, Z. Wu, Y. Li, X. Xiong, Novel electrochemical sensor based on functionalized graphene for simultaneous determination of adenine and guaninein DNA, Colloids Surf. B 82 (2011) 543–549.

[37] E. Laviron, General expression of the linear potential sweep voltammogram in the case of diffusionless electrochemical systems, J. Electroanal.Chem. Interfacial Electrochem. 101 (1979) 19–28.

[38] E. Laviron, Adsorption, autoinhibition and autocatalysis in polarography and in linear potential sweep voltammetry, J. Electroanal.Chem. Interfacial Electrochem. 52 (1974) 355–393.

[39] S. Wold, M. Sjöström, L. Eriksson, PLS-regression: A basic tool of chemometrics, Chemometrics Intell. Lab. Syst. 58 (2001) 109–130.

Chapter 5

Conclusions and future scopes

The major findings of the thesis work are summarised here in the concluding chapter. A comparative study is presented indicating the performance of the electrode towards the respective analytes. The chapter is further devoted on to the recommendations and possible future scopes of this work that can be implemented in order to develop a customized electronic tongue using tea specific sensors.

List of sections

Chapter 5

Conclusions and future scopes

5.1. Introduction

To start with, the present thesis opens up a new paradigm for the qualitative estimation of tea in terms of its taste contributing agents. Presently, there are mainly two types of quality evaluation methodology practised by the tea industries. The first one is the empanelment of tea tasters' where a group of human panellists taste and grade the tea in score matrix of 1-10 depending upon its different attributes. The second method is the installation of analytical instruments which can accurately estimate the different biochemical parameters present in tea and in turn evaluate its quality. But the high price of these instruments limits their use in industries located in the remote areas. The third strategy, E-tongue, is somewhat an improvising version of the first one, where an array of sensors is employed by means of electronic circuitry so that it can mimic the human sense of taste. Thus, by means of this technique, it is possible to remove the human inconsistencies and subjectivity, as a result of which, the response patterns or the qualitative judgements are reproducible in nature.

Despite of being objective and less costly than the analytical instruments, the major disadvantage of an E-tongue is the use of non-specific or low specific sensing elements. In an E-tongue, the overall response pattern obtained from an array of noble metal electrodes are processed by means of suitable pattern recognition algorithms so as to provide the qualitative information of tea. This set of electrodes can also be used to estimate the quality of other liquid samples as well. Therefore, the chemical information of the different analytes present in tea and their contribution cannot be assessed by this technique. Moreover, due to the usage of a large number of noble metal electrodes as sensing elements, E-tongue becomes little expensive.

To circumvent the above limitations of an E-tongue and in quest of sensors having high affinity and sensitivity, a possible method of preparation of the sensing elements have been proposed in this thesis. The principle envisages the use of molecular imprinted polymer based method where imprinted cavities similar in orientation and shape of the target molecule are created within a polymer matrix. As a result, when the electrode is getting exposed to that

particular analyte, its sensitivity increases and a response profile is generated. This methodology can be helpful for the tea industries due to the following advantages [1-3]:

a) The overall cost of the instrument where the electrodes will be designed by MIP technique will be far lower than the recently used E-tongue. This is because; the precursors involved in an MIP based method are less costly as compared to noble metal electrodes.
b) The preparation of the electrodes using this process is extremely simple and easy to replicate.
c) The MIP technique involves the use of individual constituent of a substance as the target analyte during the preparation of the electrodes. Therefore, certain information regarding the reaction kinetics of the system, the redox properties of the biochemical ingredients can be easily obtained using this method.

Considering the above advantages of the MIP technique, it has been aimed in this thesis work to explore the opportunities of development of sensors corresponding to the important taste attributing agent of tea. Three target analytes, namely, theaflavin, catechin and epigallocatechin-3-gallate have been selected here and used to design the specific sensors. Theaflavin has a special significance in regard to black tea, as it is highly responsible for its astringency and also contribute to the bright orange-red color of black tea. Catechin and epigallocatechin-3-gallate, on the otherhand, are the equally important polyphenols present in green tea. They are also responsible for the astringency and antioxidant nature of green tea. The summary of the findings in this present thesis has been illustrated in the following section.

5.2. Summary of findings

The major findings that have been witnessed during the process of development of electrodes are outlined as follows:

a) TF sensitive electrodes have been synthesized by means of MIP technique and also the effect of monomer and the crosslinker on the development of a sensor has been elucidated. Herein, TF sensor has been prepared by means of two types of monomers and crosslinkers. These are namely, acrylamide and divinyl benzene [1] and also acrylonitrile and EGDMA, respectively. It has been observed from the performance of the sensors, that the one fabricated using acrylonitrile and EGDMA yielded a lower

detection limit as compared to the previous one. The electrochemical characteristics of both the sensors have been detailed in this chapter and a possible reason behind the superior performance of the second sensor has been cited. Both the sensors were exposed to black tea liquor and their ability of quantification and discrimination has been validated using supervised algorithms. This is presented in Chapter 2 of this thesis.

b) A catechin specific sensor has been fabricated using acrylonitrile and EGDMA, as the monomer and the crosslinker, respectively. The selection of the monomer and the crosslinker has been optimized based on the response gathered from the previous chapter. Here also, the electrochemical characterizations have been studied in detail using CV and DPV techniques. Moreover, the effect of scan rate and the reaction kinetics of the system have been discussed here in detail. The sensor was subjected to green tea samples and the corresponding response profiles were found to be well matched with the standard HPLC data [2]. Chapter 3 of this thesis presents the detailed synthesis, characterizations and testing of this sensor.

c) Metal oxide/hydroxide nanoparticles have been incorporated into the polymer matrix in order to enhance the selectivity of MIP. In pursuit of these, an EGCG sensitive electrode has been prepared by homogeneously mixing the MIP (synthesized by acrylonitrile and EGDMA as the monomer and crosslinker, respectively) with the metal oxide/hydroxide nanoparticles [3, 4]. The performance of the system using different nanoparticles have been studied and optimized. Further, the electrochemical properties of EGCG were also assessed, and the synthesized electrode was subjected to different green tea samples for analyzing its performance related to real time applications [3]. This is detailed in Chapter 4 of the thesis.

The analytical characteristics of all the electrodes synthesized in this work for the detection of TF, CAT and EGCG, respectively has been summarized in the following Table 5.1.

Table 5.1 Summary of findings in the proposed work

Sl. No.	Target compound	Electrode	Precursors	Linear range	LOD	Repeatability (% RSD)	Reproducibility (% RSD)	References
1	Theaflavin	MIP-TF1	a) Monomer: Acrylamide b) Crosslinker: DVB	20-100 µM	14 µM	5.30	6.76	[1]

Sl. No.	Target compound	Electrode	Precursors	Linear range	LOD	Repeatability (% RSD)	Reproducibility (% RSD)	References
2	Theaflavin	MIP-TF2	a) Monomer: Acrylonitrile b) Crosslinker: EGDMA	8-50 µM	50 nM	3.60	6.01	-
3	Catechin	MIP-CAT	a) Monomer: Acrylonitrile b) Crosslinker: EGDMA	5-100 µM	37 nM	4.14	5.95	[2]
4	Epigallocatech-in-3-gallate	MIP-EGCG	a) Monomer: Acrylonitrile b) Crosslinker: EGDMA c) Modifier: $Ni(OH)_2$ nanoparticl-es	10-100 µM	7 nM	2.17	6.45	[3]

It may be observed from the table that there is a clear improvement in the response characteristics of the electrode due to the selection of the respective precursors. For example, the MIP-TF2 electrode, prepared using acrylonitrile and EGDMA, yielded a better LOD than that of MIP-TF1 electrode, synthesized using acrylamide and DVB. The MIP-CAT electrode synthesized using the similar monomers as that in MIP-TF2, also resulted in an LOD of as low as 37 nM. Further, an enhanced sensitivity has been obtained on modifying the MIP based electrode for EGCG with metal oxide NPs. Moreover, in terms of repeatability, it may also be noticed that the NP modified MIP electrode is far more repeatable in nature than the other ones.

Though the above works involved the design and development of low cost, reusable and specific sensors, but it may be observed from the chapters, that the surface of the electrodes were washed thoroughly and needed to be regenerated prior to each measurement. This in turn lowers the life of an electrode as the material gets exhausted easily. Therefore, these limitations of the above prepared sensors should be mitigated so as to make them worthy for the commercial sectors.

5.3. Recommendations

The proposed thesis work in its present form can be recommended for the following applications in the tea industry.

a) Tea industries can use the MIP-TF electrode to estimate the quality of black tea liquor and as a result decide its commercial viability in terms of cost and export worthiness.

b) The MIP-TF electrodes can also be implemented to study the fermentation characteristics of tea.

c) Green tea is particularly popular due to its therapeutic benefits. The MIP-CAT and MIP-EGCG electrode can be implemented to study the antioxidant characteristics of green tea.

d) Apart from the tea industries, the proposed electrodes in this dissertation can also be recommended for use in the health industries as all of the analytes used here possesses several health beneficiary attributes.

5.4. Future scopes of research

There are several areas in which the proposed methodology discussed in the previous sections can undergo improvement. These are listed as follows:

a) As discussed previously, the sensors should be made more commercially viable for implementation in the tea industries. It may be done using disposable sensors or sensors made using screen printed electrodes. By employing such types of methodologies, the problem of regenerating the surface every time the electrode is exposed to target analyte, may be dissolved. Moreover, those sensors will also be able to yield a greater level of precision.

b) All the sensors described herein, were tested using a limited number of tea samples supplied by Tocklai Tea Research Institute, Jorhat, Assam, India. In order to prepare a sensor that can be implemented in the industry level it must be trained with datasets corresponding to different types of tea samples from different tea gardens. Therefore, there is a need to evaluate the performance of the sensors when it is exposed to different genres of tea corresponding to different tea gardens. Further, the electrodes should also be exposed to different variants of tea (green, black, oolong, etc.) inorder to procure a wide range of samples for the performance validation of the electrodes.

c) In this thesis, though suitable protocols are described for the fabrication of the sensors, but only PLS technique have been used to evaluate them in terms of quantification of tea constituents and discrimination of different variants of tea. Consequently, there is a need for the application of different pattern recognition algorithms and various classification models in order to efficiently extract the

information content of the electrodes. Moreover, different algorithms should also be compared in terms of their figure of merit or qualitative index such that a prototype of an instrument containing suitable model parameters can be designed.

d) In this thesis, only sensors specific to TF, CAT and EGCG has been fabricated. In order to have a complete insight to the quality of tea liquor, sensors specific to other taste contributing agents need to be designed. This will enable to have a complete notion regarding the taste of tea.

e) This thesis is mainly focused on the taste contributing agents of tea. It has been also felt that if specific sensors can be designed for perceiving the tea aroma and brightness of tea liquor, a combinatorial approach consisting of E-tongue, E-nose and E-vision, respectively, can be pursued for performing the overall quality analysis of tea.

f) In this thesis, the MIP based sensors have been designed with a view to replace the noble metal based E-tongue for more objective analysis of tea. Thus an important future scope lies on the fabrication of tea specific sensors so as to generate a customized E-tongue that can be used explicitly in the tea industries.

g) Along with the development of the customized sensors as mentioned earlier, suitable techniques can be developed in future such that the measurement can be procured using a portable data acquisition system without the requirement of any personal computer.

h) Moreover, since the MIP technique yields highly selective sensors, this technology can be implemented for the development of sensors for other agricultural applications as well. The sensors prepared using this technique may quantify the important constituents of medicinal plants and also can be used in fisheries to determine the wellness of the aquatic environment.

The above mentioned future scopes and areas of further researches enable the idea of a visionary tea specific E-tongue that can be designed for the objective qualitative estimation of tea. According to the concept, there will be an array of electrodes, each of them being specific to a particular chemical constituent of tea. The customized E-tongue will process the

overall information obtained from the specific electrodes using suitable modelling techniques and will generate values for that particular taste constituent of tea. Moreover, the output of the E-tongue can also be processed by means of a smart phone system on IOS/Android platforms such that by installing an appropriate application, one can easily assess the quality of tea. This can be visualized in terms of the following thematic diagram as shown in Fig.5.1.

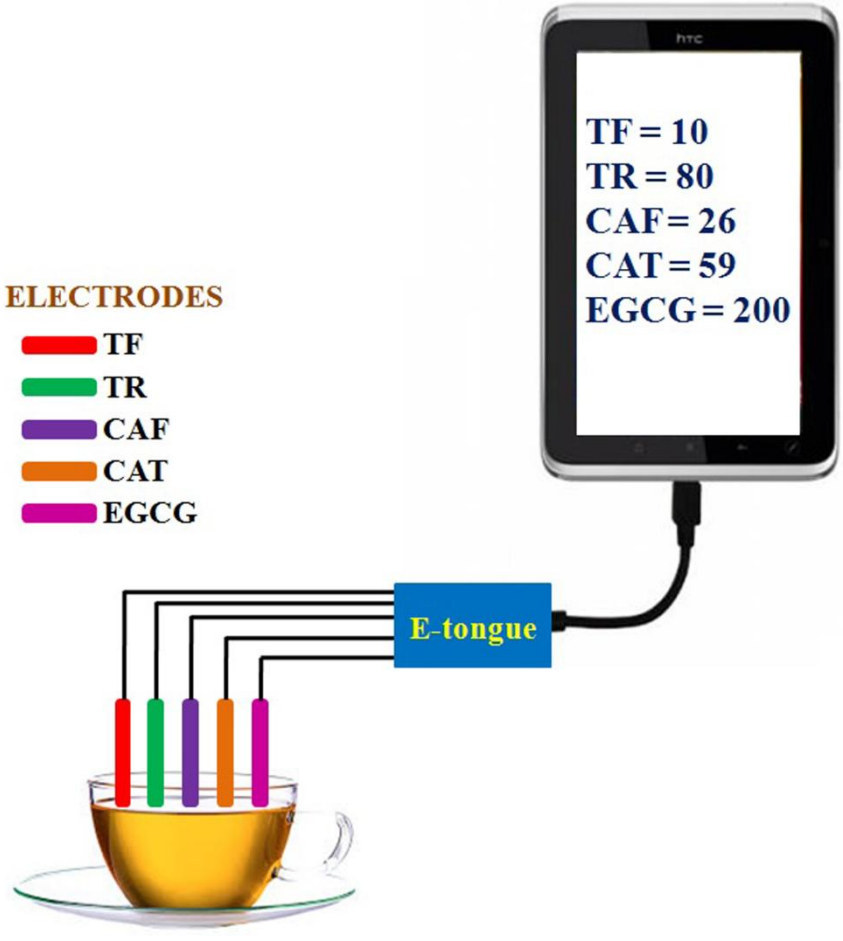

Fig.5.1. Proposed thematic diagram of the smart phone based customized E-tongue

5.5. Conclusion

The proposed methodology of MIP based sensor fabrication for the qualitative estimation of tea liquor is only an initial step towards the development of a customised E-tongue. Though the presented research is in its nascent stage of development, but there is no denying the fact that it can pave a way for more objective analysis of tea. As the health benefits of these constituents are also quite evident, a continuous effort towards this direction can lead to the development of a very promising instrument that can not only be used by the tea manufactures but can also be employed by the pharmaceutical sectors as well.

References

[1] T. N. Chatterjee, R. B. Roy, B. Tudu, P. Pramanik, H. Deka, P. Tamuly, R. Bandyopadhyay, Detection of theaflavins in black tea using a molecular imprinted polyacrylamide-graphite nanocomposite electrode, Sens. Actuators B Chem. 246 (2017) 840-847.

[2] T. N. Chatterjee, D. Das, R. B. Roy, B. Tudu, S. Sabhapondit, P. Tamuly, P. Pramanik, R. Bandyopadhyay, Molecular imprinted polymer based electrode for sensing catechin (+C) in green tea, IEEE Sens. J. 18 (2018) 2236-2244.

[3] T. N. Chatterjee, D. Das, R. B. Roy, B. Tudu, A. K. Hazarika, S. Sabhapondit, P. Tamuly, R. Bandyopadhyay, Development of a nickel hydroxide nanopetal decorated molecular imprinted polymer based electrode for sensitive detection of epigallocatechin-3-gallate in green tea, Sens. Actuators B Chem., 283 (2019) 69-78.

[4] D. Das, T. N. Chatterjee, R. B. Roy, B. Tudu, S. Sabhapondit, A. K. Hazarika, P. Pramanik, R. Bandyopadhyay, Discrimination of green tea using an epigallocatechin-3-gallate (EGCG) sensitive molecular imprinted polymer (MIP) based electrode, Carbon-Science and Technology, 2018.